The peripheral airways in Asthma: assessment of clinical significance and response to targeted therapy

Claire Frances O'Sullivan

Newcastle University, UK

in affiliation with

Monash University and Alfred Health, Melbourne

Supervisors

Newcastle University

Professor Chris Ward

Dr Graham Burns

Monash University

Professor Bruce Thompson

Thesis submitted for the degree of Doctor of Philosophy

June 2023

Abstract

There is a growing body of evidence highlighting the role of peripheral airway dysfunction in asthma. This thesis presents two studies using multi-breath nitrogen washout and oscillometry, that assess ventilation heterogeneity, respiratory impedance, and airway closure, to examine the role of peripheral airway function in asthma.

The first study assessed the relationship between peripheral airway function and acute exacerbations with 3 groups; subjects with stable asthma, subjects who were prone to exacerbations based on history, and subjects who had experienced a recent exacerbation of asthma. Results showed elevated acinar ventilation heterogeneity and dynamic airway closure in the exacerbation prone group, whereas subjects within one month of exacerbation had peripheral airway function similar to the stable group. These findings implicate peripheral airway dysfunction in the mechanisms behind asthma exacerbations.

In addition to physiological techniques, the second study used ventilation MR imaging techniques (Specific Ventilation Imaging, SVI, and Phase-REsolved FUnctional Lung imaging, PREFUL) to assess spatial ventilation to evaluate the efficacy of small (2.6µm) and large (6.2µm) particle short-acting bronchodilator. Overall, the small particle bronchodilator led to improvements in more physiological parameters compared to large particle bronchodilator. Reversal of airway dysfunction was reflected in reduction in spatial ventilation heterogeneity from SVI, in response to small particle bronchodilator. However, quantitative PREFUL parameters failed to detect a superiority of small particle bronchodilator. Subjects who showed a physiological response on spirometry or oscillometry displayed a greater reversal of airflow limitation and reduction in airway closure, with the small particle bronchodilator. This demonstrated that particle size of inhaled bronchodilator is an important determinant of response and suggests the potential benefit of targeting small airways in individuals with peripheral dysfunction.

This work highlights the utility of sophisticated physiological assessments in clinical practice and asthma research, with the potential to enable asthma management tailored to individual patient characteristics.

Acknowledgements

I could not have completed this PhD without the support of many colleagues, friends and family, to whom I will be forever grateful. Firstly, the opportunity to undertake this research was made possible thanks to Professor Bruce Thompson and Professor Chris Ward, whose mutual enthusiasm for initiating and supporting research projects and academic growth, led to this internationally collaborative PhD. I am grateful for their instrumental roles at the beginning and continued support throughout. Thank you also to Dr Graham Burns, for his valuable clinical perspective and encouragement. To Professor Pete Thelwall and Dr Ian Forrest who formed my progression panel, I extend my gratitude for their expert guidance, and advice which helped steer this work toward completion.

I am deeply grateful to Professor Kim Prisk for his invaluable and patient teaching and supervision, particularly in the area of MRI. I would like to express special thanks to Dr Kris Nilsen for his assistance with coding and overall encouragement throughout the process. Together – Kim, Kris and Bruce provided unquantifiable support, helpful insights, stimulating discussion, expertise, and much needed laughter during the challenging time of pandemic research.

From the lung function department at the Alfred Hospital I have received immense support. I am grateful to Brigitte Borg and Pam Matsas for their assistance in overcoming many obstacles. I thank the respiratory scientists, for their role in recruiting study participants as well as their camaraderie.

I would like to also thank: Louise Mitchell and Richard McIntyre, Monash Biomedical Imaging, for their assistance in the booking and completion demanding scanning sessions; Dr Beau Pontre and Prof. David Dubowitz, Centre for Advanced MRI, University of Auckland, New Zealand, for hosting studies to allow comparison of MR scan protocols; Professor Jim Fink, Aerogen Ltd. for his help in procuring equipment pivotal in study completion; and Professor Jen Vogel-Claussen and Dr. Andreas Voskrebenzev, The

Institute for Diagnostic and Interventional Radiology, Hannover, for the analysis of PREFUL datasets.

Finally, I would like to share my heart felt appreciation for my friends, family and housemates who have been there throughout the ups and downs of this research.

Table of contents

List of figures

List of tables

List of abbreviations

ACQ	Asthma control questionnaire
Δ/Delta X_{rs}	Difference in inspiratory and expiratory respiratory system reactance
DR1 volume	De-recruitment 1: lung volume at which airways begin to close
DR2 volume	De-recruitment 2: lung volume at which rapid airway closure occurs
ECG	Electrocardiogram
FEV_1	Forced expire volume in the 1st second
FiO_2	Fraction of inspired oxygen
FOT	Forced oscillation technique
FVC	Forced vital capacity
FVL	Flow volume loop
IC	Inspiratory capacity
LLN	Lower limit of normal
MBNW	Multi-breath nitrogen washout
MR	Magnetic resonance
MRI	Magnetic resonance imaging
PAM	Pause after measurement
PREFUL	Phase Resolved Functional Lung Imaging
RF	Radiofrequency
RV	Residual volume
ROI	Region of interest
R_{rs}	Resistance of the respiratory system
Sacin	Ventilation heterogeneity in the acinar region
Scond	Ventilation heterogeneity in the conductive region
SnIII	Normalised slope of alveolar plateau (phase 3) from MBNW trace

SVI	Specific ventilation imaging
T1	Longitudinal relaxation time
Ti	Inversion time
TLC	Total lung capacity
TR	Repetition time
ULN	Upper limit of normal
VC	Vital capacity
RVent	Regional ventilation
X_{rs}	Reactance of the respiratory system

Chapter 1: Introduction and background

1.1. Human respiratory system in health

The main role of the lungs is to maintain blood gas homeostasis by exchanging oxygen and carbon dioxide with the external environment. The airway-tree consists of approximately 23 generations of dichotomous branches starting at the trachea. As we breathe, gas moves through this branching network to access the gas exchange area of the lung (Weibel and Gomez, 1962), figure 1.1. The first 15 generations of branches constitute the conducting airways which do not take part in gas exchange and are therefore considered anatomical dead space (McNulty and Usmani, 2014). Distal to this are the respiratory bronchioles from which alveoli start to bud, which along with the subsequent alveolar ducts and sacs form the site of gas exchange (Venegas et al., 2005).

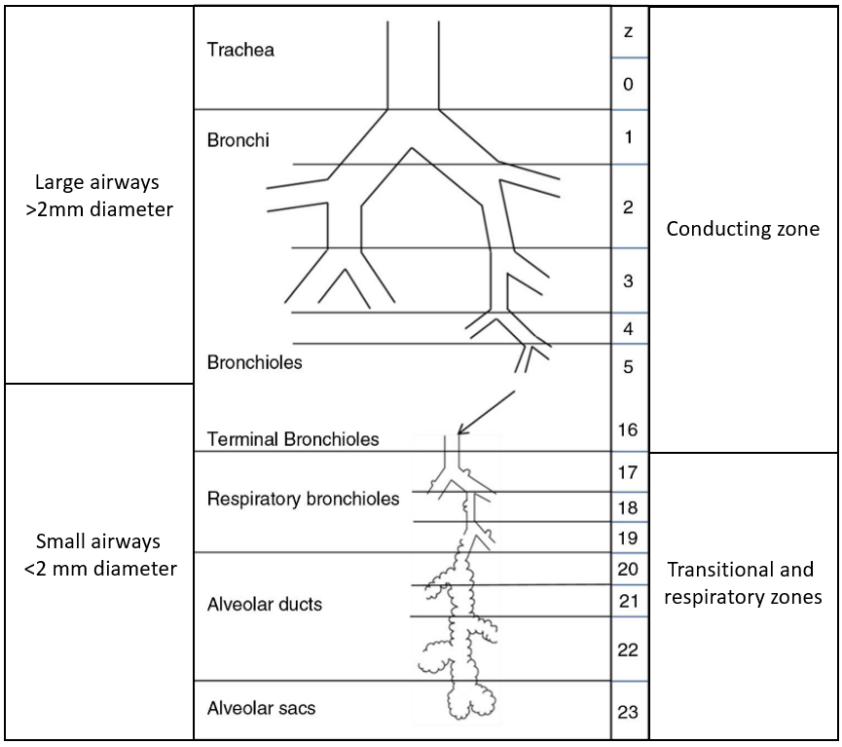

Figure 1.1. *Schematic diagram depicting the dichotomous branching of the airways starting at the trachea and continuing throughout the airway tree. Regional distinctions based on airway size (large vs small airways around generation 5) and function (conducting vs respiratory zones around generation 16) are depicted. Adapted from (Weibel, 1963).*

Traversing the respiratory tract towards the periphery the airways become shorter and lumen diameter reduces, conversely overall lumen cross sectional area increases exponentially by the factor of 2^n, where n is airway generation number. Due to the exponential increase in cross sectional area the peripheral airways contribute very little to overall airway resistance, in dogs the peripheral airways of diameter 1.5-2.5mm have been shown to contribute only 15% of total resistance at lower lung volumes, further peripheral resistance was undetectable at higher lung volumes (Macklem and Mead, 1967). Thus, in health resistance to gas movement is least in the lung periphery (Weibel and Gomez, 1962), figure 1.2.

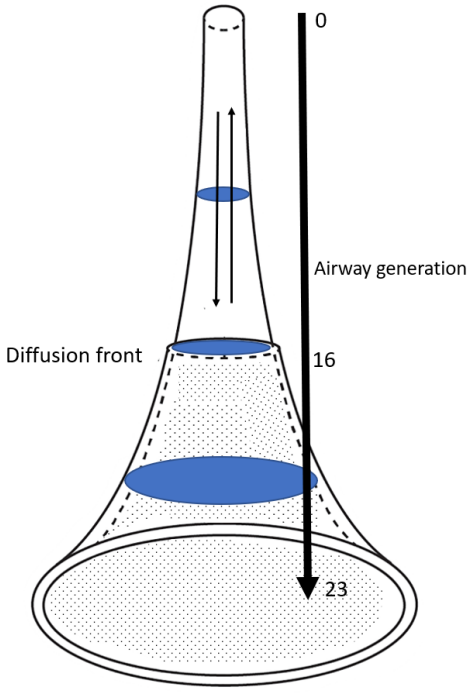

Figure 1.2. *Representation of the airway tree in a trumpet like model. Airway lumen size reduces as distance from the trachea increases, conversely the sum of airway lumen cross sectional area increases. Up to ~generation 15 there is bulk flow movement of gas, beyond this at the diffusion front, where cumulative large cross-sectional area is large and resistance is low, movement of gas is diffusive.*

The bulk flow movement of gas that occurs in the larger airways is described as convective, and happens in response to pressure changes (Verbanck and Paiva, 2011). Beyond this, as cross-sectional area increases, movement of gas molecules transitions from convective into

diffusive transport where gas molecules move along concentration gradients. The theoretical boundary where gas movement becomes diffusive is known as the 'diffusion front' and occurs at ~generation 16 in the adult human lung (Verbanck and Paiva, 2011).

1.2. Asthma overview

The Global Initiative for Asthma, GINA, describes the disease as heterogeneous and characterised by chronic airway inflammation (Reddel et al., 2019). In 2019 Asthma was reported to affect 300 million people worldwide (Annesi-Maesano and Forastiere, 2019) and carries a huge societal burden; responsible for significant morbidity (Denlinger et al., 2017), mortality (Garner et al., 2022), use of healthcare resources with outpatient management, presentation at emergency departments, and admissions to hospital (Nwaru et al., 2020, Loftus and Wise, 2015).

The common presenting respiratory symptoms include; wheeze, shortness of breath or dyspnoea, chest tightness, and cough. Symptoms occur secondary to bronchospasm, airway inflammation (Thien and Thompson, 2018, Garner et al., 2022), and mucus plugging (Garner et al., 2022) which limit airflow. Asthma is described as an obstructive lung disease due to the limitation of airflow through the airways, impeding ventilation in affected regions of the respiratory system. A distinguishable feature of asthma, compared with other chronic respiratory disease, is the variability of airflow limitation and associated symptoms. Variation may be diurnal, associated with exposure to work place or seasonal allergens, or associated with physical exertion. This inherent variability can make diagnosis with objective measures challenging, and is reliant on a comprehensive clinical history. The cause of asthma is unknown, however there are numerous genetic abnormalities associated with development of asthma when combined with environmental factors (Annesi-Maesano and Forastiere, 2019) such as pollution (Khreis et al., 2019).

'Asthma' is now accepted as an umbrella term or syndrome that encompasses many distinct endotypes with different biological mechanisms that cause the observable characteristics recognised as the phenotype asthma (Custovic et al., 2015, Moore et al., 2010, Lötvall et al.,

2011, Zedan et al., 2015, Fitzpatrick and Moore, 2017). Arguably the use of a single term to describe numerous endotypes has slowed progress in our understanding of asthma pathophysiology, as well as progress in management strategies, with poorly defined asthma cohorts, particularly in large clinical trials (Erzurum and Gaston, 2012).

Inhaled corticosteroid and bronchodilator medications form the mainstay of asthma treatment, and despite high doses of inhaled and additional oral medications many patients remain uncontrolled and experience exacerbations of asthma (Chung et al., 2014).
Poor patient compliance with inhaled medications routinely used to treat asthma is recognised as a contributing factor, a problem which does not apply to other administration routes such as injections (Sulaiman and Costello, 2021). The practicalities of taking inhaled medication; cost, forgetfulness and insufficient education on inhaler technique have been highlighted as barriers to adherence, which in turn lead to additional, but potentially unnecessary additional prescribed medication (Sulaiman and Costello, 2021) (Kerr et al., 2022).

We are now in the era of biologics, which have dramatically improved asthma management for many patients with severe asthma by reducing exacerbations, oral corticosteroid use, and improving asthma control and quality of life (Bleecker et al., 2016, Castro et al., 2015, Rabe et al., 2018). The overall positive outcomes of these large randomised controlled trials are not the full story, and for some these expensive agents are ineffective at reducing exacerbations, long term oral corticosteroid use, or in improving asthma control (Bleecker et al., 2016, Castro et al., 2015, Rabe et al., 2018). Trials of the biologic agents Mepolizumab (Pavord et al., 2012), Reslizumab (Castro et al., 2015) and Benralizumab (Bleecker et al., 2016) all reported success in treating uncontrolled asthma, however the mean reduction in clinically significant exacerbations reported was approximately 50% which equates to a large number of remaining non-responders. Thus, there is much more to be done to understand why some patients with asthma do not respond to traditional or novel therapies in order to achieve asthma remission.

Within the context of airways disease, a 'bottom up' approach that focuses on specific identifiable features that can be targeted, termed 'treatable traits', has taken steps towards achieving personalised medicine (Agusti et al., 2016, McDonald et al., 2019). And, this approach has achieved improved asthma control and health related quality of life for a cohort with severe asthma (McDonald et al., 2020).

1.3. Asthma pathophysiology

1.3.1. Underlying inflammation

The many cellular processes and mechanistic pathways that result in the asthma syndrome can broadly be divided into two categories; eosinophilic and non-eosinophilic airway inflammation (Busse, 2019). The inflammatory processes at play result in impeded function of asthmatic airways due to; inflamed and thickened airway walls, hypertrophy of airway smooth muscle (AWSM) that is hyperresponsive (Gillis and Lutchen, 1999), hyperplasia of mucus producing cells which further take up lumen area and produce excessive mucus, and infiltration of inflammatory cells (Nihlberg et al., 2010).

1.3.2. Airway hyperresponsiveness

Asthmatic airways may inappropriately constrict in response to certain stimuli. This tendency to constrict is termed airway hyperresponsiveness, the causes are multifactorial and include airway smooth muscle hypertrophy and hyperplasia (Lambert et al., 1993). During acute asthma, reduced airway lumen size and consequent increase in resistance to gas flow is worsened as airway smooth muscles contracts, figure 1.3. As ventilation is impeded, an increase in symptoms ensue. When ventilation is impaired to the point that perfused areas of the lung are no longer supplied with fresh oxygenated gas, there is a ventilation and perfusion mismatch. If, due to impaired gas exchange, the metabolic demands of aerobic respiration cannot be met, the outcome can be catastrophic. The 2014 National review of Asthma deaths revealed an annual death rate of 195 in the UK, and in 65% of cases the review panel identified aspects of patient management that could have

prevented death (Levy, 2015), highlighting the need to improve asthma care and reduce asthma related deaths.

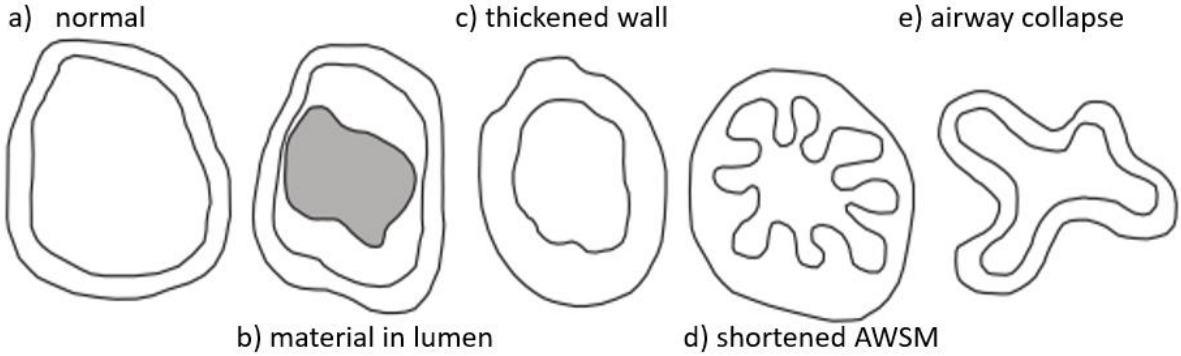

Figure 1.3. *Schematic airway cross-sections demonstraing the range of mechanism for a reduced lumen in asthma relative to in health (a), including mucus, cells or other material within lumen (b), thickened airway wall (c), constracted and shortend airway smooth mucsle (d) and airway closure of collapse (e). Adapted from (James and Wenzel, 2007).*

1.3.3. Airway remodelling

Chronic inflammation of the airways in poorly treated or refractory asthma can lead to long term structural changes of the airways, or airway remodelling. Airway remodelling can lead to irreversible effects on lung function, so that the variable obstructive component becomes fixed. Some have hypothesised that the development of fixed airflow limitation may be a protective adaptation that prevents further severe bronchoconstriction (Milanese et al., 2001). Whereas other research suggests the reverse mechanism of pathology in terms of cause and effect whereby airway remodelling in childhood is hypothesised to be the precursor to inflammatory lung disease later in life (Castro-Rodriguez et al., 2018, Bush and Saglani, 2018). Irrespective of the aetiology, preventing chronic structural changes is of paramount importance in maintaining lung function and reducing symptom burden for patients with asthma.

1.3.4. Respiratory mechanics in asthma

The underlying inflammation, acute and chronic structural and cellular makeup changes occurring within the airways and parenchyma in asthma, impact on the mechanics of the respiratory system.

Airways resistance

Poiseuille's law states that the resistance to flow through a tube is inversely related to the 4^{th} power of the radius, therefore small reductions in airway diameter result in relatively large increases in resistance to gas flow. In the classical example of asthma, airway smooth muscle, located in the large airway walls, contracts in response to stimuli, reducing airway diameter and making ventilation more difficult. The interplay of many other pathological processes including; cellular infiltration (Holgate, 1998), inflammation and airway remodelling (Ward et al., 2002) play a role in increasing resistance to gas flow along the airway tree.

The pathological processes in asthma extend to the airway exterior, reduced elastic fibre content relative to healthy controls results in weakened connections between the airways and the parenchyma which surround them (Mauad et al., 2004). Reduced traction and expansion during inspiration equates to reduced airway diameter, and an increase in airways resistance.

Modelling studies of the airway network have demonstrated how minor increases in resistance to gas flow in one area are capable of a large negative impact. Venegas *et al*. describe this phenomenon as the "propagation of constriction" whereby local increases in airway resistance affect airways in series and parallel causing major disturbances in gas flow promoting ventilation heterogeneity (Venegas et al., 2005), figure 1.4.

Airway closure

In health the airways are supported and held open by the forces that tether the airway walls to the parenchyma. In asthma both a reduction in lumen size, and a reduction in airway wall tethering increase the propensity of airways to close. Airway closure differs along the airway tree, the airways without supporting collagen, and with smaller baseline lumen size, i.e. the small airways, are more vulnerable to closure, or near closure. As discussed, the interconnected nature of the small airways leads to a "domino like effect", which results in hysteresis, whereby clusters of airways remain closed during inspiration and regions of lung are non-ventilated (Venegas et al., 2005), figure 1.4. Small airway closure and associated ventilation inhomogeneity is known to be problem particularly within severe asthma (King et al., 2018).

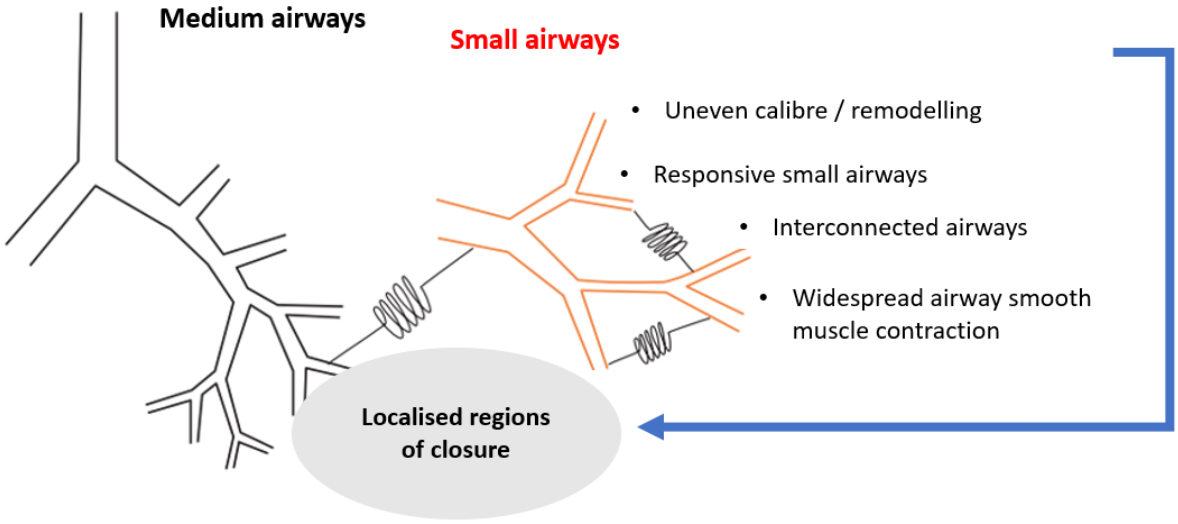

Figure 1.4. *Schematic diagram highlighting precursors to closure of airways within a region of the lung preventing gas exchange in the affected area. Adapted from (King et al., 2018).*

Compliance

In Asthma pathological mechanisms both increase and decrease respiratory system compliance. Scarring of asthmatic airways with laydown of collagen and fibrosis result in decreased compliance, or in other words, increased elastic recoil and harder to inflate lungs (Williamson et al., 2011) (Brown et al., 2007). Conversely, the reduction in elastic fibres and airway tethering discussed reduces elastic lung recoil (Nilsen et al., 2019). Evidence of reduced elastic fibre content and breakdown of lung parenchyma, both factors associated with airway closure, have been found in fatal asthma (Mauad et al., 2004) and in frequently exacerbating asthma (Gelb et al., 2015). Overall, the structural changes to the lung found in asthma serve to increase; compliance, airflow obstruction and airway closure.

1.5. Small vs large airway debate

Historically, the small airways are under studied compared with their larger upstream counterparts (Kraft et al., 2022). The small airways are not visible under the resolution of the radiation doses in conventional human imaging methods, and are inaccessible or unsafe for live tissue sampling for histological assessment, and have been termed the ‘silent zone’ in the context of traditional physiological assessment which are insensitive in the detection of abnormality in the lung periphery.

Within asthma, the importance of the small airways relative to large has been debated for some time (Donovan and Noble, 2021a). There is no true boundary or point of separation between large and small airways, making a binary approach over simplistic. Nevertheless, isolating regions of the airway tree to determine the area, if any, that presents more dysfunction is helpful in implementing a targeted management (McDonald et al., 2020).

Asthma diagnosis or management does not utilise histology, therefore lung tissue sampling is not routine in clinical care, further histological assessment of asthmatic airways in the research setting is limited and samples are often obtained from surgically resected or autopsied lungs (Ivancsó et al., 2013). Histology has confirmed 1) raised inflammatory cell

profiles and 2) abnormal structure in asthmatic airways. Pro-inflammatory cytokines were more prevalent in the large and small airways of asthmatics (Minshall et al., 1998) but the responsible transcription material (mRNA) was predominantly in the small airways (Minshall et al., 1998), and in severe asthma, overall inflammatory cell count was greater in the periphery (Balzar et al., 2005). Airway wall area was greater in asthma compared with controls (James et al., 1989) and within the periphery in fatal asthma, the small airways had reduced elastic fibres and abnormal alveolar attachments (Mauad et al., 2004).

1.5.1. Physiological measures of small and large airway function

In the clinical setting spirometry is commonly used in the assessment and management of asthma. Spirometry measures flow and volume of gas during a forced expiration and can identify reduced flow due to obstructed airways, however but this technique has limited sensitivity and may fail to detect abnormalities localised to the small airways (Wagner et al., 1998). In the research setting, the application of sensitive tests of physiology, including inert gas washout techniques and oscillometry, is building a body of evidence demonstrating that dysfunction of the small peripheral airways plays a significant role within the expression of asthma.

The multi-breath nitrogen washout test involves the subject inspiring 100% oxygen to clear nitrogen from the lungs, the gas concentration of each expired breath is used to calculate regional measures of ventilation heterogeneity from convection dependent and diffusion-convection dependent regions. Ventilation heterogeneity in the convective region of conducting airways is denoted by S_{cond} and ventilation heterogeneity in the diffusive or acinar region is denoted by S_{acin}. The methodology and theoretical basis pertaining to multi-breath nitrogen washout is described in detail in Chapter 2.

Oscillometry superimposes soundwaves on tidal breathing, the resultant changes in flow and pressure are used to calculate the impedance of the respiratory system, which is differentiated into resistance, and reactance (stiffness). The penetration of input signal into

the respiratory system is dependent on the oscillation frequency. The methodology and theoretical basis pertaining to oscillometry is described in detail in Chapter 2.

When the physical effects of bronchoconstriction in asthma are induced artificially, parameters of ventilation heterogeneity in both the proximal convective, S_{cond}, and peripheral diffusive, S_{acin}, regions increase, as does resistance to gas flow and reactance or stiffness of the respiratory system, measured via oscillometry (Downie et al., 2013). S_{cond}, and S_{acin} were shown to be worse for those with greater symptom burden, as scored by the asthma control questionnaire (Farah et al., 2012a, Farah et al., 2012b). Further, S_{cond} and S_{acin} were both predictive of symptom improvement following medication up-titration (Farah et al., 2012a, Farah et al., 2012b), however, only the marker of peripheral diffusive ventilation heterogeneity, S_{acin}, demonstrated the additional power to predict which subjects, who were initially well controlled, would not tolerate de-escalation in treatment. This suggests that in contrast to low symptoms scores residual dysfunction in the periphery is a warning signal for vulnerable or at-risk patients (Farah et al., 2012b).

Ventilation heterogeneity in the conductive or convective dependent region, S_{cond}, is an independent predictor of airways hyperresponsiveness, and of airway hyperresponsiveness that persists after treatment (Downie et al., 2007). Further, S_{cond} was worse during acute asthma (Thompson et al., 2013), whereas it was S_{acin} or ventilation heterogeneity in the acinar region, that improved post exacerbation following the intensive treatment administered (Thompson et al., 2013).

Raised ventilation heterogeneity in the peripheral acinar region was also associated with an increase in reactance, suggesting that airway closure occurring in the periphery is responsible for acute changes in lung mechanics (Downie et al., 2013). In addition, dysfunction of the peripheral small airways has been shown to be associated with worse symptoms, and with greater small airway closure in uncontrolled asthma (Kelly et al., 2013).

Whilst the issue may not solely lie in the small or large airways (Donovan and Noble, 2021b), it is recognised that measures reflecting peripheral ventilation heterogeneity and airway

closure are associated with poor control, susceptibility for further decline, and are responsive to treatment. Thus, incorporating more sensitive and regional assessments of airway physiology in asthma may be helpful in guiding a more targeted approach therapeutically, as well as, through generation of treatable traits for individualised and precision medicine in asthma.

1.6. Application and efficacy of inhaled therapies

1.6.1. Inhaled therapies

Inhaled therapies in asthma are topical treatments and require direct application to the target site of inflammation and bronchoconstriction, the airways, for which drug formulations are produced as aerosols for inhalation. The benefits of inhaled medications include; quick onset of action, and efficacy at lower doses compared with other drug administration routes (Darquenne, 2012). Due to the inaccessibility of the airways, drug delivery can be challenging, and understanding drug deposition patterns which include non-target sites is important for expected clinical response and side effects caused by systemic absorption or deposition in unwanted areas (Newman, 2000). The fraction of initial dose administered that successfully deposits in the airways, as well as the pattern of deposition throughout the airway tree vary dependent on delivery method (Zainudin et al., 1990). The deposition fraction, and pattern are affected by flow (Laube et al., 2011), breath hold time (Darquenne et al., 2000), particle size (Usmani et al., 2005, Hultquist et al., 1992, Dolovich, 2000), and airway diameter (Dolovich, 2000).

1.6.2. Particle size and airway deposition

Particle size, which is often described by the median mass aerodynamic diameter (MMAD) in micrometres (μm), is the most important aspect of aerosol characteristics affecting deposition (Dolovich, 2000). It has been shown that particles between MMAD 2–6μm preferentially deposit in the lung, particles of MMAD <2 μm reach the alveoli, (Usmani et al.,

2005, Usmani, 2012) and have greater peripheral deposition compared with larger particles (Usmani et al., 2003).

1.6.3. Overview of particle size and drug efficacy

The site of deposition of inhaled drugs is dependent on aerosol particle size, hence the response the drug is able to elicit is also affected by particle size. Many studies have investigated the effect of particle size on efficacy for common inhaled bronchodilator and anti-inflammatory medications in asthma.

Short acting beta agonists (SABA)

SABAs bind with β2 receptors and mimic the effects of the sympathetic nervous system to produce bronchodilation, the mode of action is fast so response can be measured within a few minutes of administration. The results described below used common preparations of SABA including: albuterol or salbutamol, isoproterenol and terbutaline.

Two studies that measured response to different particle size preparations using spirometry, found that fine particle SABA elicited the greatest bronchodilation compared with medium and large particle preparations: SABA MMAD 1.8µm was superior to 4.6µm or 10.3µm (Clay et al., 1986) and 1.5µm produced greater effects than 3.2µm (Ruffin et al., 1981). In contrast, three other studies in mild and chronic asthma that also assessed bronchodilation with spirometry found mid-range particle size preparations to be most effective; 2.5µm and 2.8µm were superior compared with 1.5µm and 5µm (Zanen et al., 1994, Patel et al., 1990) and 3.3µm achieved greater bronchodilation over 7.7µm (Johnson et al., 1989). The latter finding is not surprising due to increased deposition in the oropharynx with larger particles, however in mild and moderate asthma two studies demonstrated large particle SABA at 6µm MMAD to be a more effective bronchodilator than 1.5µm and 3µm (Usmani et al., 2005, Usmani et al., 2003). Further, some studies simply found no difference in the bronchodilation achieved with 1.5µm and 4.8µm (Hultquist et al., 1992) or 1.4µm vs 5.5µm (Mitchell et al., 1987).

Inhaled corticosteroids (ICS)

ICS are a glucocorticoid medication which work at a cellular level to stop inflammatory pathways, thereby reducing inflammation, thus maximum benefit can take some weeks. The literature investigating particle size preparation of ICS uses a dichotomous approach, comparing traditional larger particle size and extra-fine preparations. Due to the duration of treatment required prior to assessing response more detailed assessments can be used.

The research into the effect of fine particle ICS provides conflicting results. Studies that have switched subjects from traditional to fine particle ICS preparations and looked at the change in induced sputum eosinophils, a signal of asthma-causing inflammation, found a reduction compared to baseline and compared with the placebo group for patients who treated with fine particle ICS Ciclesonide (Hodgson et al., 2015). A reduction in sputum eosinophils was found from baseline with a switch to fine particle beclomethasone propionate at 4weeks, and the reduction was maintained at 1 year (Ohbayashi, 2007). However, data detailing functional response following the swap to fine particle formulations is contradictory. Some studies demonstrate improvement in spirometric parameters (Hauber et al., 2003, Bateman et al., 2006), and reduced airway hyper-responsiveness measured by methacholine challenge test (Goldin et al., 1999). Whereas, of the studies that showed reduced inflammation there was no functional improvement (Hodgson et al., 2015, Ohbayashi, 2007). Analysis of response to ICS for a large cohort of subjects with moderate to severe asthma showed no difference in spirometric response between those treated with fine particle preparation versus those treated with coarse particles (Molimard et al., 2005). A recent Cochrane review that compared fine particle Ciclesonide to coarse particle ICS in treating children found no improvement in symptoms, exacerbations, or side effects (Kramer et al., 2013). And, patients with mild asthma who were switched to fine particle ICS showed no improvement in spirometric parameters, but they did demonstrate an improvement in function as a reduction in small airways resistance, measured via impulse oscillometry (Hoshino, 2010). This suggests that the use of traditional tests, such as

spirometry, alone, is insufficient to monitor response to treatment or categorise patients with asthma, particularly if there is airway dysfunction residing in the lung periphery.

Combination long-acting beta agonists (LABA) with ICS

ICS/LABA preparations aim to reduce airway inflammation and produce bronchodilation. The active ingredients in LABA have slower dissociation from receptors compared with SABA, therefore have longer lasting benefit. Again, the results reported in the literature do not clearly point toward a superior particle size preparation in terms of efficacy.

Treatment with extra-fine ICS/LABA resulted in a greater reduction in airway hyperresponsiveness when compared with non-fine preparation (Scichilone et al., 2010), whereas in another cohort of sub-optimally controlled asthmatics a switch to extra-fine ICS/LABA from current coarse combination therapy despite improvement self-reported asthma control, there was no improvement in objective markers of lung function or airway inflammation overall (Popov et al., 2013).

The consensus

Despite extensive research there is no consensus on what inhaled particle size medication is best (El Baou et al., 2017), or which particular aerosol particle size, fine or coarse, is best for whom.

The conclusions that are able to be drawn from the research are limited by two key deficits:

1 Inappropriate or insensitive measures

The tests used in much of the published research that investigates response to fine particle application lack the capability to identify changes occurring in the periphery. Conventional measures such as spirometry produce robust and reproducible parameters, however, lack sensitivity to assess response in specific lung regions, in particular the periphery. The absence of measurable change in spirometry with corresponding objective improvement in

peripheral airway resistance detected by oscillometry, supports the idea of using more sensitive techniques in the assessment of asthma, that are also sensitive to changes in the lung periphery, both in the research and clinical setting.

2 Poor differentiation or characterisation of patients

Insufficient characterisation of recruited participants is another possible reason for the findings of no difference between groups. It is usual practice to discount differences between groups as a confounding factor when investigating response to different treatments. However, in this context if the treatments being investigated are differentiated by particle size distribution, and particle size is the major determinant of drug deposition, then baseline regional assessments of airway physiology are necessary to truly understand baseline characteristics of subjects with asthma. Further, stratifying treatment groups according to region of airway dysfunction may be more appropriate than lumping everyone in together.

Secondary analyses of some of the research previously discussed has highlighted the need to implement more complex and sensitive testing in the assessment of asthma. The initial finding of a reduction in peripheral ventilation heterogeneity following a switch to fine particle ICS, although significant, was dampened by non-responders. The subgroup analysis revealed that for some participants there was no benefit following a switch to fine particle ICS, whereas those with abnormal baseline acinar ventilation heterogeneity had greater normalisation (reduction) in S_{acin} (Verbanck et al., 2006).

The need for a nuanced approach in asthma patient grouping when assessing efficacy of inhaled drug particle size and airway function, is made clear in the Popov et al. study (2013). The group who was switched to treatment with fine particle ICS demonstrated a small statistically significant improvement in spirometry, with uncertain clinical significance. However, further subdivision of the cohort according to change from baseline revealed that the response was hugely varied, therefore they were retrospectively separated into ‘responder’ and ‘non-responder’ groups (Popov et al., 2013). The ’non-responders’, not only had no functional benefit but also experienced a decline in forced vital capacity (FVC), which

is used as a surrogate for airway closure, indicating worse control. Although not emphasized in the discussion, these findings suggest that inhaled therapy should be targeted according to the specific needs or phenotypes of individual asthma patients. Unfortunately, none of the measures included were able to distinguish the 'responders' from the 'non-responders' at baseline. Overall, understanding the individual presentations of asthma is important for prescribing appropriate medication that targets site of dysfunction.

1.7. Summary

The pathogenesis of asthma is multifaceted and complex. While the involvement of the larger airways in asthma has been extensively studied, evidence suggests that the small airways also play a critical role in its pathophysiology. Despite this, clinical assessment of the small airways remains limited, leaving a significant gap in our understanding.

Research investigating the efficacy of inhaled medication often fails to include appropriate tests that adequately assess the small airways. This omission is problematic, as the optimal particle size for inhaled medication delivery may vary depending on the location within the respiratory tract that requires treatment. Without accurate assessment tools, it is impossible to determine the most effective treatment approaches for individual patients.

To address these gaps in knowledge, a more nuanced approach is needed in the categorisation of patients with asthma. In terms of lung function, this can be achieved by using more sensitive tests that can assess regional airway function, particularly in the small airways. As well as imaging techniques, such as ventilation MRI scans that provide additional spatial information about ventilation.

It is imperative that researchers and clinicians adopt these more rigorous assessment methods to aid patient stratification, subgroup analyses, and even individual-level analysis, when evaluating the efficacy of inhaled medications of different particle sizes.

Through implementing more specialised tests, it is possible to create a clearer picture of how regional airway function relates to the clinical picture of asthma, to identify potential treatment target sites, and to ensure that the benefits and the risks of altering inhaled drug particle size are accurately assessed. By adopting a more personalized approach to asthma management, clinicians may be better equipped to identify at risk patients, and the specific areas of the respiratory system that require treatment, which could lead to improved clinical outcomes.

1.8. Thesis aim and outline of chapters

The work described in this thesis has aimed to use sensitive tests of respiratory system function that detail; airflow limitation, regional ventilation heterogeneity and respiratory system mechanics, to comprehensively evaluate respiratory pathophysiology in individuals with asthma. The research focuses on assessing the involvement of specific airway regions in acute clinical events in asthma and investigates the potential of controlling the particle size of bronchodilator medication to target regional airway dysfunction. Additionally, novel MR imaging methods were sought and developed to enhance the interpretation of targeted bronchodilator treatment and expand on the understanding and applicability of these innovative scans in an asthma cohort.

Chapter 2 reports the findings of retrospective data analysis completed during a period of suspended non-essential research due to COVID-19 lockdowns. The results of traditional and complex physiological tests were analysed to ascertain links between airway function characteristics and clinically important exacerbations of asthma.

Chapter 3 describes the work completed to develop the ventilation scan 'specific ventilation imaging' for application with MR scanners double the strength of those previously used. The finalised protocol was tested and compared using datasets gathered according to the original published scan protocol for 2 healthy subjects, prior to implementation in the subsequent chapter.

In the final investigational chapter, chapter 4, the work undertaken to test the efficacy of bronchodilator medication of two distinct particle sizes is described. Subjects with asthma completed comprehensive assessments of respiratory function using physiological and MRI techniques on two occasions; a small particle and large particle visit, where the peripheral and proximal airways, respectively, were targeted.

Chapter 2. Investigating the link between small airways dysfunction and exacerbations of asthma

Prior to completion of this chapter, the following project milestones had been accomplished: the literature review to identify gaps in knowledge had been completed, the aims of the thesis were established, the research study protocol was developed, the methods were finalised, necessary resources and equipment were procured, and an application to the human research ethics committee was submitted. Unfortunately, ethical approval was granted shortly before the first local lockdown due the global COVID-19 pandemic. This prohibited 'non-essential' research and prevented subject recruitment and prospective data collection.

It transpired that a body of data requiring analysis existed at The Alfred Hospital, Melbourne, and so formed the contingency plan to maintain momentum in the PhD in a work package that was both relevant to the thesis (asthma) and still possible to do under mandatory lockdown/remote learning circumstances. The physiological lung function data was collected from a cohort of subjects with asthma, using sensitive measures, thus serendipitously served as a resource to address some of the questions highlighted in chapter 1. The multi-breath nitrogen washout (MBNW) methodology and data analysis also resonated with the subsequent imaging section of the thesis that applies gas wash-in to MR imaging. The data collected was funded by National Health and Medical Research Council, Department of Health, Australian Government (Grant number: APP1008548).

The work described in this chapter has been published in the American Physiological Society's Journal of Applied Physiology as an original research article entitled: "Small airways dysfunction is associated with increased exacerbations in patients with asthma" Authors: Claire F. O'Sullivan, Kris Nilsen, Brigitte Borg, Matthew Ellis, Pam Matsas, Frank Thien, Jo A. Douglass, Chris Stuart-Andrews, Gregory G. King, G. Kim Prisk, and Bruce R. Thompson. Journal of Applied Physiology, 2022, 133:3, 629-636, as such the content of this thesis chapter necessarily closely reflects the content of the published article (O'Sullivan et al., 2022).

2.1. Background

Phenotyping of asthma patients and identifying specific characteristics of those who exacerbate is deemed a priority to improve patient outcomes (King et al., 2018, Postma et al., 2019). Exacerbations pose a significant acute risk to patients, leading to unplanned healthcare and systemic corticosteroid use (Reddel et al., 2009), as well as avoiding chronic pathophysiological consequences such as loss of FEV_1. Therefore, understanding the physiological mechanisms behind exacerbations and identifying clinical markers of exacerbation risk is crucial for personalized medicine.

Peripheral airway dysfunction, which can be measured by increased ventilation heterogeneity, has been associated with uncontrolled or unstable asthma characterized by symptoms and airway hyper-responsiveness (Farrow et al., 2012, Farah et al., 2012b, Tang et al., 2020). Precision medicine in chronic airway disease requires identifying treatable characteristics rather than just managing symptoms (Agusti and Pavord, 2018). Such as; airflow limitation, airway smooth muscle contraction, airway inflammation, and mucosal oedema are some of the treatable traits that are all identified via conventional lung function tests and imaging (Agusti et al., 2016). However, peripheral airway dysfunction has been relatively overlooked due to a lack of mechanistic data using sensitive measures.

Spirometry is commonly used clinically in the management of asthma despite being insensitive to the narrowing, closure, or destruction of peripheral airways with a lumen size of less than 2mm (Wagner et al., 1998). On the other hand, more complex respiratory function tests such as multi-breath washout and oscillometry are sensitive to changes in the lung periphery. Multi-breath nitrogen washout (MBNW) measures ventilation heterogeneity in the conducting and acinar regions (Robinson et al., 2009), both of which have been found to be abnormal in people with asthma and responsive to treatment (Tang et al., 2020, Verbanck et al., 2006). Oscillometry measures impedance of the respiratory system, from which resistance and reactance are derived (Bates and Lutchen, 2005, King et al., 2020). Resistance is a measure of airway calibre, while reactance is a measure of dynamic compliance. Both measures can detect small airway dysfunction, particularly reactance,

which is sensitive to airway closure and heterogeneous airway narrowing. (Kelly et al., 2013, Tang et al., 2020). However, to use these measures as a biomarker for exacerbation and a treatable trait, it is necessary to identify markers of small airway function associated with exacerbations.

Further, in much of the literature physiological assessment of airway function in asthma is limited to those who are deemed 'stable'. That is research study inclusion criteria stipulate a period of ≥6 weeks that the subjects must be clear from antibiotics, oral corticosteroids and/or an increase in asthma symptoms that may indicate exacerbation of asthma. Therefore, there is a paucity of data on the airway function of patients with asthma during or close to an exacerbation.

2.1.1 Study aim

The aim of this cross-sectional study was to assess the difference in small airway function in terms of ventilation heterogeneity and respiratory system mechanics in subjects with asthma who exacerbate versus those who do not.

2.1.2. Hypothesis

The hypothesis was that subjects with asthma who exacerbate will demonstrate more abnormal peripheral airway function compared with subjects who are stable in terms of exacerbations. Further, those that have had a recent exacerbation will demonstrate the greatest degree of peripheral airway dysfunction.

2.2. Methods

Ethical approval was granted by The Alfred Hospital (Melbourne, AUS) Ethics Committee (No: 160-11). All participants provided written informed consent to participate. Participants were

recruited from the severe asthma clinic following routine appointment or via referral from emergency department following presentation due to an exacerbation of asthma.

2.2.1. Subjects

Subjects with severe asthma were categorised into three phenotypic groups based on exacerbation history.

1) The "Stable" group was defined as subjects who had no reported exacerbations or increase in asthma symptoms that required up titration of asthma medication for greater than 12 months.

2) The "Treated-exacerbation" group were recruited and tested no more than 30 days following their most recent exacerbation. In some cases (n=3) this was as soon as the day of presentation due to exacerbation. An exacerbation was defined as worsening asthma symptoms requiring a course of oral corticosteroids +/- antibiotics.

3) "Exacerbation-prone" group. Since an asthma exacerbation within the last 12 months is associated with risk of recurrence of exacerbation (Bloom et al., 2019), we recruited subjects who had had at least one exacerbation at least 30 days ago, but within the last 12 months, requiring oral corticosteroids +/- antibiotics.

Exclusion criteria were current smoking, smoking within the last year, or smoking history of more than 10 pack years, and any comorbid lung disease.

2.2.2. Study visits

Subjects attended the laboratory on one occasion and completed the asthma control questionnaire (ACQ6) (Juniper et al., 2006) relating to their asthma symptoms and control. At this time post bronchodilator lung function testing was performed.

Spirometry

Spirometry is a common test of lung function that measures both volume and flow of gas expired during a maximal (forceful) expiration from the position of total lung capacity. The graphical traces produced during a spirometry test are given in figure 2.1.

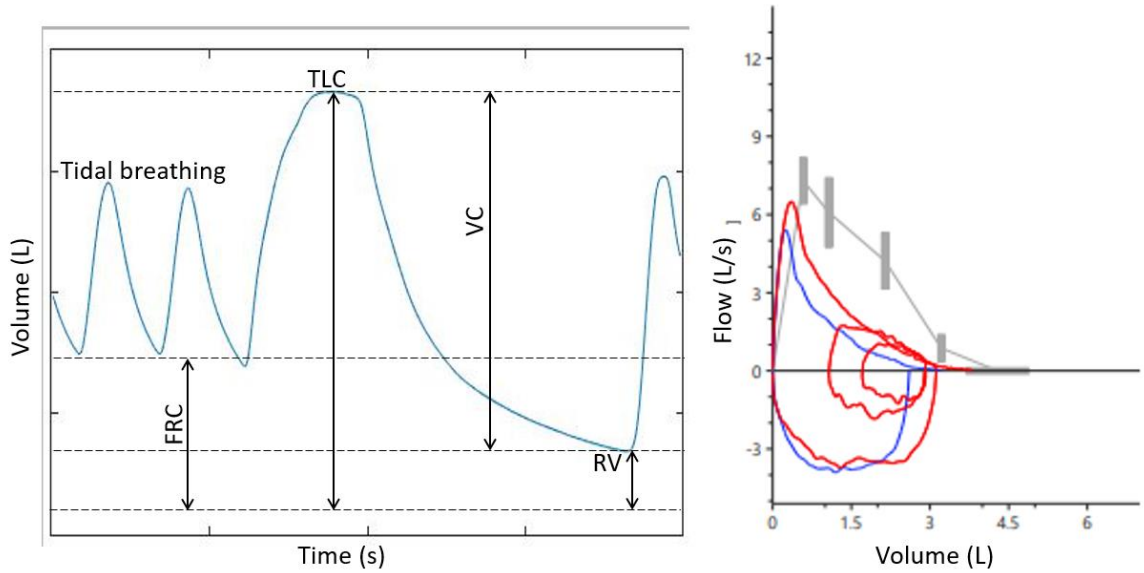

Figure 2.1. *Graphical representation of a spirometry manoeuvre. Left, time (x axis) volume (y axis) trace, the subject begins breathing normally (tidally) inspires to total lung capacity (TLC) and expires forcefully with an open glottis to residual volume (RV). The volume expired is the vital capacity, denoted as FVC during a forced manoeuvre (forced vital capacity). Right, flow volume graph for a subject with asthma. The predicted result for this subject indicated by grey trace, the baseline result in blue shows scooping of the expiratory limb, the post-bronchodilator result is in red, shows an improvement in flow and total volume expired, but incomplete reversal of airflow obstruction.*

Spirometry was performed using the 'preVent' pneumotachograph (Medgraphics, Platinum Elite series, St. Paul, MN). To which the subject was connected via a mouthpiece containing a bacterial filter, whilst they wear a nose peg to allow for mouth breathing with no leaks. The preVent contains tiny tubes through which expiratory and inspiratory gas can flow. The pressure changes across the series of tiny tubes are measured by a differential pressure transducer, this signal is translated to flow and volume measurements. Equipment specifics and maintenance as well as subject testing were completed in accordance with the ATS/ERS published standards for spirometry (Miller et al., 2005). A minimum of 3 technically acceptable efforts were obtained for each subject, achieving 2 values for FEV_1 and FVC within 150mL of the highest acceptable recording value, the greatest value was reported.

The 'Global Lung Initiative' reference equations of Quanjer *et al.* were used to determine mean predicted spirometric values based on subjects age, sex, height and ethnicity (Quanjer et al., 2012). The FEV_1, FVC and their ratio (FEV_1/FVC) were expressed as absolute values, percentage of predicted mean, and Z-scores. Z-scores describe the degree of abnormality within the context of expected variation for a parameter in healthy individuals, and were calculated using standardised residuals from the Global Lung Initiative healthy cohort (Quanjer et al., 2012).

Body plethysmography

The lung volumes measured during spirometry are known as dynamic lung volumes, whereas static lung volumes such as total lung capacity (TLC) are measured via body plethysmography, among other methods such as gas dilution techniques. To perform this measurement subjects are placed in a body plethysmograph (a large box, sealed for the short duration of the test) and breath tidally on the aforementioned flow measuring device. At the point of functional residual capacity (FRC) (shown in figure 2.1) a shutter is closed to prevent movement of gas in and out of the lung whilst the subject makes small inspiratory and expiratory efforts, with their hands placed flat on their cheeks to prevent them from ballooning out. During this panting stage pressure changes are measured at the mouth and are assumed to reflect intrathoracic pressure. Pressure and volume changes within the box are also measured, the remaining unknown volume is the thoracic gas volume (TGV) which can be calculated based on the principle that at constant temperature the pressure and volume of a gas are inversely related. Once TGV is known TLC can be calculated. The measurements were performed on Platinum Elite series, (Medgraphics, St. Paul, MN), according to the ATS/ERS published standards for body plethysmography (Wanger et al., 2005) whereby 3 acceptable manoeuvres produced 3 TGV volume recordings within 5% of the median value.

The reference equations of Goldman *et al.* for static lung volumes (Goldman and Becklake, 1959) were used to calculate expected normal values. Absolute volumes and percentage of predicted mean were reported for; RV (residual volume), total lung capacity (TLC), as well as

their ratio RV/TLC. Gas trapping was defined as RV/TLC > upper limit of normal (ULN), hyperinflation was defined as TLC >ULN.

Multi-breath nitrogen washout

The multi-breath nitrogen washout (MBNW) technique can be used to measure both the static lung volume, functional residual capacity (FRC), as well as measures of ventilation heterogeneity. In theory the FRC is the same volume as the Thoracic Gas Volume (TGV), however the distinction is made as the differences in methodological approach to measure TGV (plethysmography) vs FRC (gas dilution) lead to different results, particularly in the presence of obstructive lung disease. For example, if an obstructive defect resulted in some areas of the lung that are 'non-communicating' and are not reached by the dilution gas, FRC will be underestimated by a method based on gas dilution.

To complete the MBNW the subject is connected to the system via a mouthpiece and wears a nose peg. Once a stable baseline of tidal breathing has been achieved the subject is 'switched in' to breathing 100% oxygen. With each successive exhalation the concentration of nitrogen gas reduces as the inspired oxygen replaces, or washes out, the nitrogen (N_2) from the lungs. The FRC, specifically from the breath immediately preceding switch in, is calculated using the end expired concentration of N_2 (<2%) and the volume of gas inspired to achieve washout.

When using the MBNW technique to also provide measurements of ventilation heterogeneity it is required that the inspired volume of 100% oxygen is 1L. That is to both maintain a close to usual breathing pattern, as well as provide sufficient data to complete analysis of the exhaled gas concentration (Robinson et al., 2009), (see figure 2.2).

The Lung Clearance Index (LCI) is a global measure of ventilation heterogeneity and is calculated by dividing the cumulative expired volume by FRC (Robinson et al., 2009).

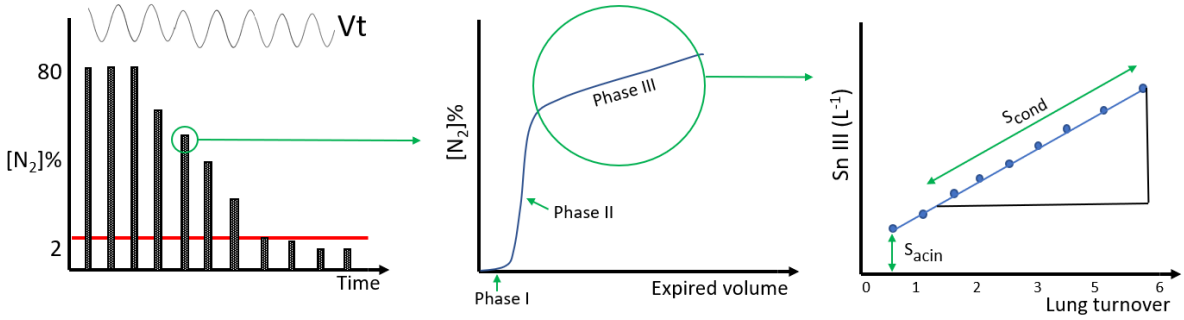

Figure 2.2. *Graphical schema of left) MBNW trace, tidal breathing displayed above, concentration of exhalate displayed breath by breath, the first 3 breaths represent breathing air therefore exhaled nitrogen concentration is ~80%, after the switch to 100% oxygen, nitrogen concentration reduces and the test is terminated after the concentration is <2%. Middle) a close-up of a single exhalate, the plateau is the phase III slope and represents alveolar gas. Right) the normalised slope of each phase III slope is plotted against lung turnover (cumulative expired volume/FRC). The gradient of the slope for the first breath represents diffusion-convection dependent inhomogeneity denoted as S_{acin}, the increasing degree of normalised phase III slopes between lung turnover 1.5 to 6 represents convection dependent inhomogeneity denoted as S_{cond}.*

Regional measures of ventilation heterogeneity are calculated using the traces of nitrogen concentration of each 1L expiration following the switch to 100% oxygen throughout the test. The change in nitrogen concentration over the 1L exhalate is determined by lung anatomy and function and can be altered in disease.

Phase I of the exhalate trace represents anatomical dead space where no gas exchange occurs, thus nitrogen concentration is at or close to zero (figure 2.2.). Phase II, depicted by a steep inflection of rising nitrogen concentration, represents a mixture of dead space and alveolar gas. The plateau in nitrogen concentration is Phase III which represents alveolar gas, it is the slope of Phase III that is used to calculate regional measures of ventilation heterogeneity (Stuart-Andrews et al., 2012).

Segmented linear regression analysis is used to detect the point of transition between phases (Stuart-Andrews et al., 2012). The phase III slope from each exhaled breath trace is normalised by dividing by the mean expired nitrogen concentration and denoted as SnIII. The SnIII values are plotted against lung turnover:

lung turnover = cumulative expired volume / FRC

The increase in SnIII between lung turnovers 1.5 and 6 from least squares regression, details convection dependent inhomogeneity, known as S_{cond}. The SnIII of the first breath minus the S_{cond} contribution details diffusion-convection dependent inhomogeneity known as S_{acin}. The boundary between the convection dependent and diffusion-convection dependent region of gas movement is known as the diffusion front and is located around the acinar entrance (Verbanck and Paiva, 2011).

Pathology that result in increased ventilation heterogeneity where movement of gas is via convection will result in a greater increase in SnIII slopes and raised S_{cond}. Whereas pathology that causes increased ventilation heterogeneity in the convection-diffusion dependent region will be seen as an increase in the first SnIII slope and raised S_{acin}.

The MBNW test was conducted using an in-house built system in accordance with published recommendations (Robinson et al., 2013). Automated software to determine the phase III slopes was used in the calculation of ventilation heterogeneity parameters S_{acin} and S_{cond} (Stuart-Andrews et al., 2012). The reference equations of Verbanck *et al.* were used to calculate predicted values (Verbanck et al., 2012) and results were expressed as absolute values and Z-scores.

Forced oscillation technique

The forced oscillation technique, or FOT, measures the impedance of the respiratory system, consisting of resistance and reactance, by superimposing soundwaves over tidal breathing, figure 2.3. Oscillations over a range of frequencies are applied at the mouth by a loudspeaker and the resultant changes in flow and pressure are measured and used to calculate the impedance properties (King et al., 2020).

Resistance of the respiratory system, R_{rs}, is thought to reflect the resistance to gas flow that occurs within the airways. Reactance of the respiratory system, X_{rs}, can be thought of as the elastic properties of the lungs, airways, parenchyma, and chest wall, and is reported in negative integers. Small negative values indicate a more compliant respiratory system,

whereas increasing magnitude of negative X_{rs} values indicates an increasingly stiff respiratory system.

The frequency of the input oscillation signal affects the level of penetration through the respiratory system, whereby the low frequencies travel deeper and reach the periphery. The R_{rs} and X_{rs} measurements are reported at 6Hz, and the R_{rs} measurement at 6Hz minus R_{rs} at 20Hz is used to described peripheral resistance. Inspiratory and expiratory reactance were measured at 6Hz and from these Delta X_{rs} was derived.

FOT was performed using an inhouse built forced oscillation system (Salome et al., 2003), according to the published standards at the time of data collection (Oostveen et al., 2003). Parameters were reported as absolute values and the reference equations of Oostveen *et al.* were used to report R_{rs} and X_{rs} as Z-scores (Oostveen et al., 2013).

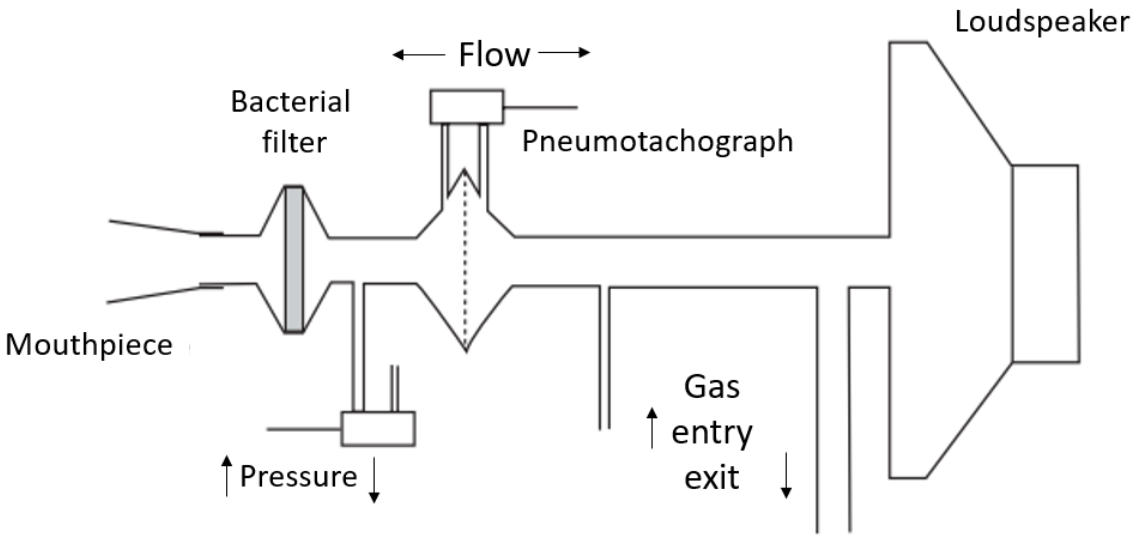

Figure 2.3. *Schematic of oscillometry set up, adapted from (Oostveen et al., 2003). The system delivers the oscillatory signal from a loudspeaker, to which the subject is connected via a single use mouthpiece containing a bacterial filter. The pressure transducer measures pressures change at the airway opening or mouth, and the pneumotachograph measures airflow to measure respiratory system impedance.*

2.2.3. Statistical analysis

Statistical analysis was performed using GraphPad Prism 8 (V8.3.1). Differences between 3 groups were assessed using one-way ANOVA for parametric and Kruskal-Wallis for non-parametric data. Differences between 2 groups were assessed using independent Student's t-tests for parametric and Mann-Whitney test for non-parametric data. Correlations were assessed using Pearson's correlation coefficient for parametric data and Spearman's rank correlation coefficient for non-parametric or categorical data. Receiver operating characteristic (ROC) analysis was used to determine to the ability of parameters to discriminate between stable and exacerbation-prone subjects. Significance for comparisons was defined as $p<0.05$. Z-scores less than -1.645 or greater +1.645, which correspond to the 5^{th} and 95^{th} percentiles respectively, were used to identify abnormal lung function parameters as recommended by international guidelines (Stanojevic et al., 2021).

2.3. Results

Thirty-nine subjects with asthma were studied. All subjects were classified as severe based on Global Initiative for Asthma, GINA, treatment step (https://ginasthma.org/wp-content/uploads/2019/01/2011-GINA.pdf). Subjects were GINA step>3 and prescribed combined moderate to high dose inhaled corticosteroids and long-acting beta agonists, some were also prescribed, leukotriene receptor antagonists (n=4), continuous low to high dose oral corticosteroids (n=19), and biologics (n=5). Mean age was 49.8±14.0 years and 34 (87%) had fixed airflow obstruction defined as a post bronchodilator FEV_1/(F)VC ratio below the lower limit of normal (Z-score<-1.64). 18 subjects had been stable with no asthma exacerbations for >12 months (Stable group), 21 patients had had at least one exacerbation within 12 months (range 1-6 exacerbations), 12 of those were tested within 30 days of their most recent exacerbation (Treated-exacerbation-group). Thus 9 subjects formed the Exacerbation-prone group. Demographics are listed in Table 2.1. Ventilation heterogeneity in the acinar region was raised (S_{acin} Z-score>1.645) for 13/18 (72%) of the Stable group, 9/9 (100%) of the Exacerbation-prone group, and 11/12 (92%) of the Treated-exacerbation group. Ventilation heterogeneity in the conductive region was raised (S_{cond} Z-score>1.645)

Table 2.1. Subject demographics

	Stable	Exacerbation-prone	Treated-exacerbation
Subjects (n)	18	9	12
Females/Males (n)	10 / 8	2 / 7	6 / 6
Age (years)*	53.7 ± 14.6	54.0 ± 11.7	40.6 ± 11.2
Height (cm)	168 ± 10	169 ± 8	169 ± 7
Weight (kg)	75.3 ± 15.9	81.2 ± 10.7	81.4 ± 24.4
BMI (kg/m^2)	26.6 ± 4.8	28.5 ± 4.1	28.3 ± 7.0
GINA step score (2012) †	4.0 (1.25)	4.7 (0.50)	4.7 (0.70)

Data are represented as mean ± SD, median (IQR).
BMI, body mass index; GINA, Global Initiative for Asthma treatment step score 2012.
*ANOVA p=0.02, treated-exacerbation vs exacerbation-prone p=0.01.
†Kruskal-Wallis p=0.04, stable vs treated-exacerbation p=0.03

for 5/18 (28%) of the Stable group, 4/9 (44%) of the Exacerbation-prone group and 4/12 (33%) of the Treated-exacerbation group.

ACQ6 score was higher in the Treated-exacerbation group indicating worse self-reported asthma symptoms and control. In the Stable group, 9 (50%) had an ACQ>1.5 which is consistent with uncontrolled asthma (Jia et al., 2013). There was no difference in symptoms between the stable and exacerbation-prone groups. For all asthma subjects combined ACQ6 correlated with FEV_1 %predicted (R^2=0.33, p=0.002), FVC %predicted (R^2=0.20, p=0.02), S_{cond} (R^2=0.20, p=0.02), and X_{rs} Z-score (R^2=0.17, p=0.04). Lung function and ACQ6 scores are listed in table 2.2.

Table 2.2. Lung function and asthma symptom scores for three asthma groups

	Stable (n=18)		Exacerbation prone (n=9)		Treated exacerbation (n=12)		ANOVA/ Kruskal Wallis p value	Stable vs Exacerbation prone p value
Spirometry								
FEV_1 (L)	2.03	(1.03)	1.86	(0.77)	2.20	(0.68)	0.3	
FEV_1 Z-score	-2.32	(1.06)	-3.58	(1.13)	-3.23	(0.59)	0.046	**0.03**
FVC (L)	3.68	(1.55)	3.4	(1.04)	3.29	(1.11)	0.7	
FVC Z-score	-0.92	(1.24)	-1.52	(0.99)	-2.06	(0.97)	0.03	**0.09**
FEV_1/(F)VC (%)	59.4	(15.2)	49.0	(13.4)	62.5	(10.8)	0.0005	**0.003**
FEV_1/(F)VC Z-score	-2.91	(1.18)	-4.03	(1.17)	-2.71	(0.88)	0.02	**0.01**
Static lung volumes								
TLC (L)	6.20	(1.50)	6.30	(0.66)	5.39	(1.06)	0.054	
TLC (%predicted)	110.0	(15.3)	106.0	(18.0)	100.0	(13.3)	0.01	0.6
RV (L)	2.84	(0.71)	3.16	(0.60)	2.19	(0.56)	0.004	0.3
RV (% predicted)	139.5	(21.3)	129.0	(35.0)	121.0	(28.0)	0.2	
RV/TLC	42.9	(14.2)	45.4	(9.7)	42.2	(14.1)	0.2	
TGV (L)	3.58	(0.74)	3.79	(0.41)	2.97	(0.66)	0.005	0.3
TGV (% predicted)	117.0	(18.0)	115.0	(22.0)	103.0	(27.5)	0.08	
TGV - FRC difference	0.96	(0.40)	1.16	(0.62)	1.19	(0.38)	0.1	
MBW								
Sacin (L^{-1})	0.206	(0.098)	0.308	(0.232)	0.178	(0.143)	0.007*	**0.001†**
Sacin Z-score	3.63	(3.88)	7.43	(8.59)	3.46	(4.87)	0.02*	**0.006†**
Scond (L^{-1})	0.040	(0.028)	0.049	(0.030)	0.048	(0.031)	0.3*	
Scond Z-score	0.03	(2.20)	0.95	(2.15)	0.92	(2.89)	0.3	
LCI	8.40	(1.36)	9.63	(1.94)	8.78	(2.31)	0.01*	**0.002†**
LCI Z-score	6.24	(5.57)	8.51	(7.21)	7.23	(5.34)	0.03*	**0.01†**
FOT								
R_{rs} 6Hz ($cmH_2O.s.L^{-1}$)	4.01	(1.51)	4.45	(1.09)	3.81	(0.30)	0.4	
R_{rs} 6Hz Z-score	0.69	(1.10)	0.94	(1.10)	0.24	(0.80)	0.4	
X_{rs} 6Hz ($cmH_2O.s.L^{-1}$)	-1.32	(1.94)	-2.74	(3.82)	-1.55	(2.03)	0.04*	**0.01†**
X_{rs} 6Hz Z-score	-0.11	(0.60)	-0.45	(1.19)	-0.19	(0.43)	0.2	
Inspiratory X_{rs} ($cmH_2O.s.L^{-1}$)	-1.31	(1.17)	-2.16	(1.26)	-1.43	(1.02)	0.08*	
Expiratory X_{rs} ($cmH_2O.s.L^{-1}$)	-1.36	(2.25)	-3.24	(4.91)	-1.56	(2.49)	0.04*	**0.01†**
Delta X_{rs} 6Hz ($cmH_2O.s.L^{-1}$)	0.22	(1.01)	1.08	(3.63)	0.12	(1.17)	0.04*	**0.02†**
R_{rs} 6-19Hz ($cmH_2O.s.\ L^{-1}$)	0.57	(0.86)	1.56	(0.34)	0.63	(1.09)	0.1	
ACQ6	1.71	(0.71)	1.86	(1.70)	3.60	(1.49)	<0.0001	0.4

Data are presented as median (IQR)

Difference between groups assessed with One-way ANOVA for parametric and Kruskal Wallis* for non-parametric, difference between Stable and Exacerbation prone groups assessed with t-test for parametric data, and Mann-Whitney† for non-parametric. FEV_1, forced expired volume in 1s; FVC, forced vital capacity; TLC, total lung capacity; RV, residual volume; TGV, thoracic gas volume measured via plethysmography; FRC, functional residual capacity measured via multi-breath nitrogen washout; Sacin, index of ventilation heterogeneity in the diffusion-convection dependent region; Scond, index of ventilation heterogeneity in the convection dependent airways; Rrs 6Hz, respiratory system resistance at 6Hz; Xrs 6Hz, respiratory system reactance at 6Hz; ACQ6, 6-item Asthma Control Questionnaire.

2.3.1. Exacerbation-prone vs Stable groups

The Exacerbation-prone group had greater fixed airflow limitation (lower FEV_1 and FEV_1/VC Z-scores) compared with the Stable group, and worse (greater) ventilation heterogeneity in the acinar region, (S_{acin}) (figure 2.4), however there was no significant difference in ventilation heterogeneity in the conducting region (S_{cond}) (table 2.2).

Table 2.2 shows that the Exacerbation-prone group had more impaired (more negative) respiratory system reactance, X_{rs}, suggestive of stiffer lungs or airway closure in the context of obstructive defects (Nilsen et al., 2019). The Exacerbation-prone group also had greater Delta X_{rs} (difference in inspiratory and expiratory reactance). There was a trend for more abnormal Inspiratory reactance in the Exacerbation-prone group, but this did not reach significance, whereas Expiratory reactance was worse. Expiratory reactance is therefore driving the difference in Delta Xrs (difference in inspiratory and expiratory reactance) which is worse in the Exacerbation-prone group and suggestive of dynamic airway narrowing/collapse, consistent with obstructive pathologies such as asthma.

ROC analysis was completed for parameters that were significantly different between the Exacerbation-prone and Stable groups, figure 2.5. The area under the curve (AUC) for S_{acin} Z-score (0.82, $p<0.01$), X_{rs} AUC (0.80, $p=0.01$) and Delta X_{rs} (0.79, $p<0.02$) were similar. The discriminative power in identifying the Exacerbation-prone group for FEV_1 was less (AUC 0.76, $p=0.03$). Within this cohort the threshold of S_{acin} Z-score above 6.84 has 88.9% specificity and 55.6% sensitivity in identifying the exacerbation-prone subjects, X_{rs} threshold of below -1.59 has 61.1% specificity and 88.9% sensitivity, and Delta X_{rs} threshold of above 1.05 has 77.8% specificity and 55.6% sensitivity.

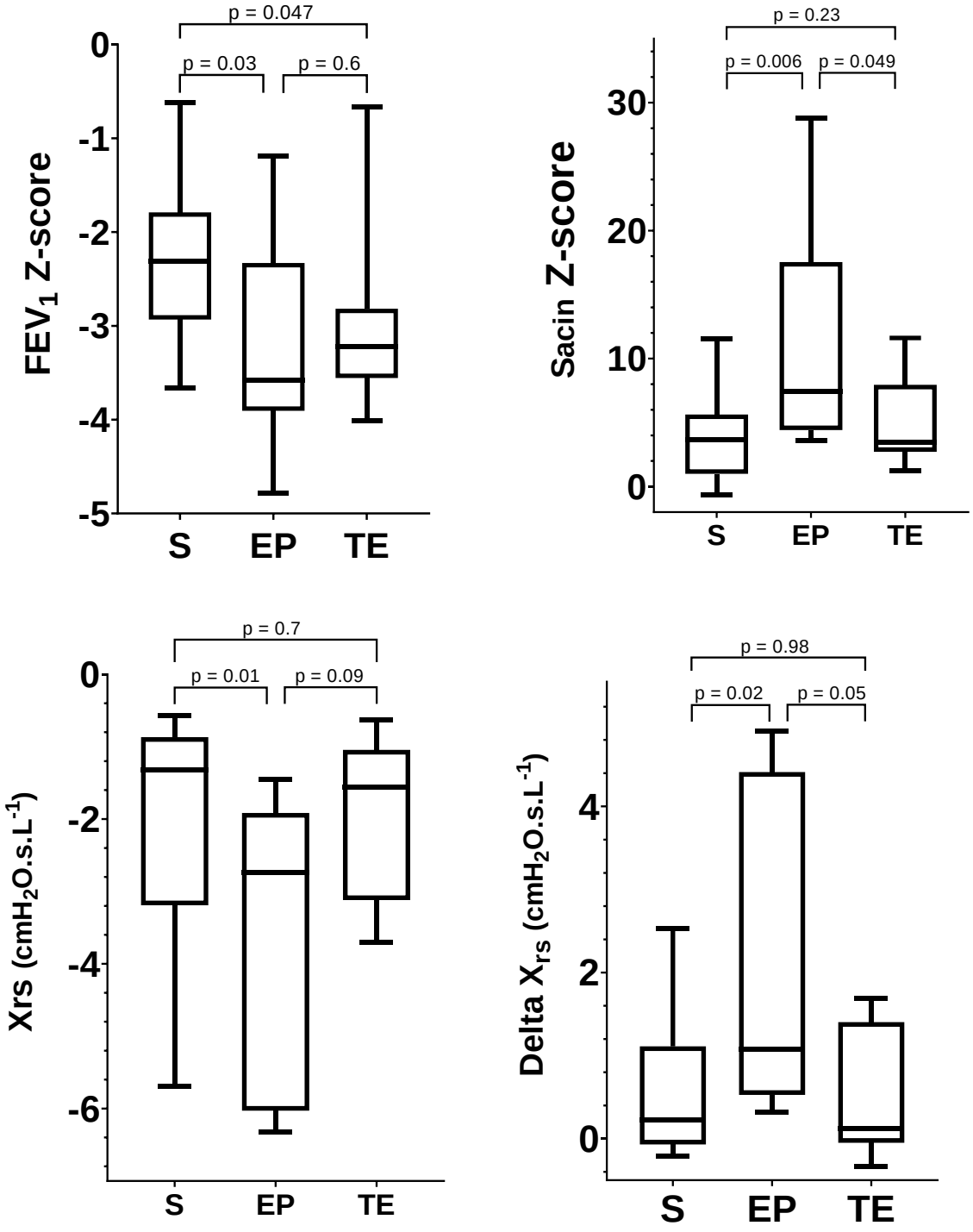

Figure 2.4. *Parameters with significant difference Stable (S) vs Exacerbation-prone (EP) group, with Treated-exacerbation group (TE) displayed for comparison.*

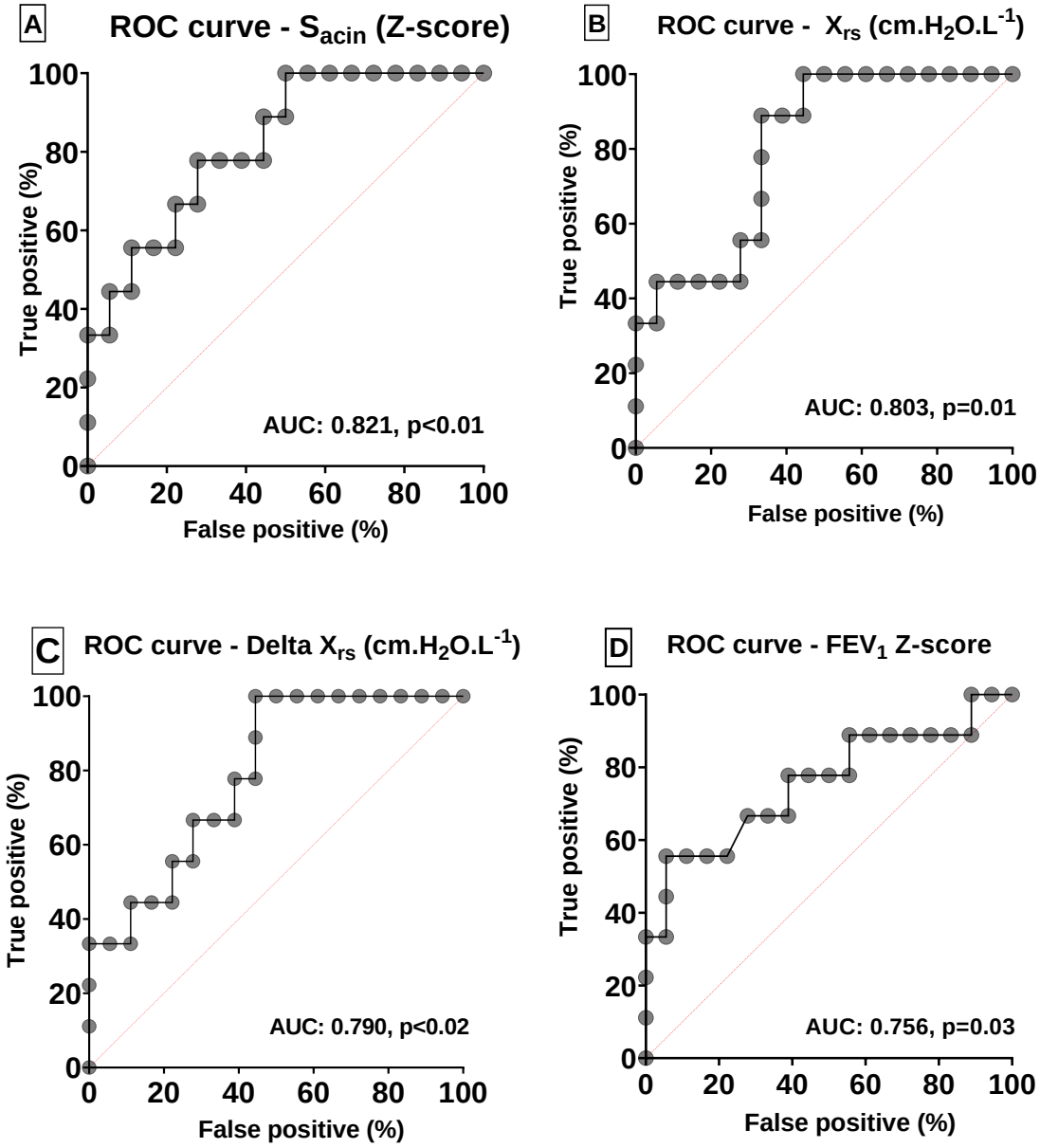

Figure 2.5. *ROC curves for* ***A)*** *S_{acin} Z-score* ***B)*** *X_{rs}* ***C)*** *Delta X_{rs} and* ***D)*** *FEV_1 Z-score*

2.3.2. Treated-exacerbation group vs Stable group

Compared with the Stable group the Treated-exacerbation group had worse obstruction (FEV_1 Z-score -3.23(0.59) vs -2.32(1.06), p=0.047), with reduced FVC (FVC Z-score -2.06(0.97) vs -0.92(1.24), p=0.01). There was no evidence of gas trapping, in the Treated-exacerbation group who had lower residual volume (RV %predicted 121.0(28.0) vs 139.5(21.3), p=0.01), or

of hyperinflation, with lower total lung capacity (TLC %predicted 100.0(13.3) vs 110.0(15.3), p<0.01). The Treated-exacerbation group were on higher level of prescribed treatment (GINA 4.7(0.7) vs 4.0(1.3), p=0.04), and were more symptomatic (ACQ6 3.60(1.49) vs 1.71(0.71), p<0.001) compared with the Stable group.

Despite being tested within 30 days of an acute exacerbation of asthma the Treated-exacerbation group displayed similar peripheral airway function to Stable subjects. There was no difference between the Stable and Treated-exacerbation groups for parameters of ventilation heterogeneity; (S_{acin} L^{-1} 0.178(0.143) vs 0.206(0.098), p=0.3; S_{cond} L^{-1} 0.048(0.031) vs 0.040(0.028), p=0.7) or respiratory system mechanics (R_{rs} $cmH_2O.s.L^{-1}$ 3.81(0.30) vs 4.01(1.51), p=0.9; X_{rs} $cmH_2O.s.L^{-1}$ -1.55(2.03) vs -1.32(1.94), p=0.7).

2.4. Discussion

The results indicate that asthmatic patients who experience exacerbations exhibit higher ventilation heterogeneity in the acinar region of the lung and more abnormal respiratory system reactance compared to those who do not experience exacerbations. However, patients who were tested shortly after receiving treatment for exacerbation showed similar peripheral airway function to non-exacerbators likely a result of treatment for their exacerbation. The findings suggest that S_{acin} elevations and X_{rs} decreases could serve as treatable traits before exacerbation (Verbanck et al., 2006), and therefore may be important in the management of a specific (acinar) endotype within asthma. Identifying such traits may aid in preventing future exacerbations in these patients.

2.4.1. Peripheral airway function in patients with asthma

In this study, S_{acin} was above the upper limit of normal for those with stable asthma (Verbanck et al., 2006) and it was further elevated in those who have had an asthma exacerbation in the previous year (figure 2.4), whereas S_{cond} did not differ between the groups. Previous research links increased ventilation heterogeneity in both the acinar (S_{acin}) and conducting zone (S_{cond}) of the lung in patients with acute asthma or uncontrolled

asthma according to symptoms (Downie et al., 2007, Bourdin et al., 2006, Thompson et al., 2013, Farah et al., 2012a), and S_{acin} is predictive of airway hyperresponsiveness, AHR, measured by both responses to challenge agent with spirometry (Verbanck et al., 1997) and ventilation imaging (Farrow et al., 2017). Ventilation heterogeneity in the conducting region has been shown to correlate with AHR at baseline and with the reduction in AHR following treatment (Downie et al., 2007). However, the link with exacerbations has not been examined. This study clearly demonstrates elevated S_{acin} in those with asthma who experience exacerbations compared to those who do not, whereas there was no difference in S_{cond}. These data demonstrates that elevated S_{acin} is a marker of those at risk of bronchoconstriction and having worse asthma control. Previously, it has been shown that those with asthma and elevated S_{acin} had a greater response to small particle inhaled corticosteroids (Verbanck et al., 2006) which target the small airways. Therefore, S_{acin} appears to be a useful biomarker in detecting asthma patients at risk of exacerbations that can be targeted with therapy and, as such, is a treatable trait. Prevention of exacerbations is a major target within asthma management, therefore validation of S_{acin} as a biomarker for use in the prediction of exacerbation risk has the potential to form an important contribution to asthma evaluation.

2.4.2. Respiratory system mechanics in asthma

Patients with asthma display reduced airway distensibility (Kelly et al., 2012) and increased airway closure compared with controls (Nilsen et al., 2019). The oscillometry data from this study supports and furthers these observations in patients who have exacerbations demonstrating they have more negative respiratory system reactance, X_{rs}, than the Stable group. A possible reason for the appearance of stiffer lungs in the Exacerbation-prone group may be airway closure or near closure; whereby the oscillometry signal does not reach regions of lung distal to closed airways, these regions are therefore described as 'non-communicating lung volumes' (Nilsen et al., 2019). The Exacerbation-prone group also had a greater difference in their inspiratory and expiratory reactance measurements compared with the Stable group, which was driven by a difference in expiratory reactance. The more negative expiratory reactance relative to inspiratory suggests that the Exacerbation-prone group are exhibiting dynamic airway collapse (Dellacà et al., 2007) in agreement with the

airway closure theory. Previously it has been shown that more negative X_{rs} was associated with worse asthma control in terms of symptoms (Kelly et al., 2013) and now validation of X_{rs} as a biomarker for use in identifying patients at risk of clinically important acute exacerbations of asthma is warranted.

It is not clear whether a raised S_{acin} and more negative X_{rs} are causative of, or result from, asthma exacerbations. However, the lack of difference in S_{acin} and X_{rs} between the stable group and the Treated-exacerbation groups suggests that the responsible mechanism is reversible and corrected in the short term by the rescue medications given at the time of exacerbation. Airway remodelling is a chronic pathophysiological consequence of asthma and includes the thickening of adventitial, submucosal and muscle layers and has been shown to affect the peripheral airways (Kuwano et al., 1993). The resulting narrowing of peripheral airways and poorer gas mixing would raise acinar ventilation inhomogeneity as described by S_{acin}. Decreased luminal area would also result in abnormal X_{rs} as airways would demonstrate an increased propensity for airway closure or near closure, and less lung volume is reflected in the measurements obtained from the oscillometry signal.

It is possible that the mechanism behind the differences unique to the Exacerbation-prone group is inflammation occurring at the level of the most distal airways proximal to acinus detected by S_{acin}, which is resistant to maintenance therapy, but responsive to high dose systemic corticosteroids that target inflammation. Inflammation causes airway mucosal infiltration of inflammatory cells and is associated with edema. The accumulation of fluid, inflammatory cells and mucus in these peripheral airways would account for raised S_{acin} and more negative X_{rs}, by increasing asymmetry in peripheral airways and render them prone to closure as well as blockage.

Routine measures of gas mixing and or oscillometry in a clinical setting could aid an individualised approach to predicting asthma exacerbations. Variability in inspiratory resistance was predictive of acute exacerbations in COPD (Zimmermann et al., 2020), and within asthma, variability in inspiratory resistance was predictive of spikes in inspiratory

resistance (Gulotta et al., 2012); therefore, serial monitoring may have the potential to forewarn of asthma exacerbations.

2.4.3. Difference in peripheral airway function between groups

The Treated-exacerbation group included those subjects who are within 30 days of their most recent exacerbation, this group are under investigated in the literature as exacerbation within 4-6wks is usually listed in exclusion criteria. Unexpectedly, the Treated-exacerbation group have similar small airway physiology to the Stable group, (figure 2.4). One explanation for the difference in peripheral airway function between the Exacerbation-prone and Treated-exacerbation groups may be that the effect of the intervention on the lung periphery at time of exacerbation is not maintained.
The treatment of exacerbations, which includes high dose oral corticosteroids (Thompson et al., 2013) appears to correct peripheral airway dysfunction in the short term, but due to the significant adverse side effects incurred, oral corticosteroids should be avoided for long term management plans (Bateman et al., 2006).

2.4.4. Airway physiology and symptoms

The evidence surrounding the link with asthma control and symptoms measured using ACQ and sensitive measures of airway function such as MBW and oscillometry is conflicting. Improvement in ACQ following up-titration of inhaled medications was predicted by baseline S_{cond} (Farah et al., 2012b), whereas in other cohorts ACQ was unrelated to all MBW parameters (Tang et al., 2020, Farrow et al., 2012) even when there was a relationship with both resistance and reactance from oscillometry (Tang et al., 2020). In this cohort although there were associations of ACQ with spirometric parameters, S_{cond} from MBW and reactance from oscillometry, there was no difference in symptoms between the stable and exacerbation-prone groups.

2.4.5. Study limitations

Due to the inherently small normative values of S_{acin} and S_{cond} the associated Z-scores are very sensitive which may limit utility; however, our conclusions are supported by both Z-scores and absolute values. This study is limited by the cross-sectional experimental design and small numbers in each study group. Nevertheless, the results provide evidence to support the use of more sensitive tests of lung function in the assessment of airway physiology in asthma. According to these data, parameters pertaining to the peripheral airways have the ability to differentiate between subjects who have experienced exacerbations and those who have not. As previous exacerbation is a risk factor for future events (Miller et al., 2007), these findings highlight the need for monitoring of the lung periphery in patients with poor peripheral airway function, which may allow for intervention to prevent future exacerbations. Larger prospective studies are required to address this. Longitudinal assessments of patients at stages pre, during and post exacerbation are warranted to help understand the mechanisms behind exacerbation so that they may be avoided.

2.5. Conclusion

Patients with asthma who exacerbate have worse small airway function as evidenced by increases in S_{acin} measured by MBW and delta X_{rs}, both markers of small airway dysfunction, compared with those that do not. These findings suggest that dysfunction in the small airways, perhaps a result of worsening peripheral airway inflammation, is linked to the mechanism behind exacerbations of asthma. With further longitudinal research it may be possible to identify these patients before such exacerbations occur.

Chapter 3. MRI protocol development

The site available for prospective subject testing, including MRI ventilation scans and physiological tests, was the research institute Monash Biomedical Imaging. The MRI scanner located there is a 3-Tesla Siemens Skyra. As the published protocol for the specific ventilation scan to be performed uses a 1.5-T scanner, development of a protocol for use on the 3-T scanner was required. In this chapter the investigations completed in the development of a 3-T protocol, the final protocol parameters and a comparison of datasets collected at 3-T with data collected in accordance to the original 1.5-T protocol are described.

3.1 Principles of Magnetic Resonance Imaging

3.1.1. Hydrogen nuclei are MR active

Magnetic resonance imaging, or MRI, uses the magnetic properties of hydrogen nuclei, ^{1}H, or protons, as they are abundant in the human body existing mainly in water (H_2O) and fat (HCO). Hydrogen nuclei are MR active as a magnetic moment is created by the spin of each single proton, contained within the hydrogen nucleus. In MRI, protons align and spin either parallel, or anti-parallel to the strong magnetic field imposed by the scanner (Westbrook and Talbot, 2018), figure 3.1.

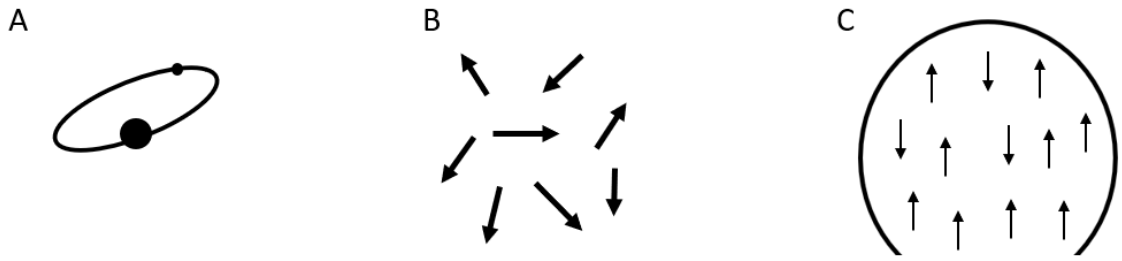

Figure 3.1. *A) represents a single hydrogen atom, the negatively charged electron orbits the nucleus, the nucleus contains a single positively charged proton which spins on its axis. B) The spin of each nucleus creates a magnetic field or magnetic moment, the direction of the magnetic moment of hydrogen nuclei throughout the body is random, represented by the arrows. C) In the presence of a strong external magnetic field the magnetic moment of hydrogen nuclei aligns either parallel, or anti parallel (parallel>antiparallel) and this phenomenon is utilised in nuclear magnetic resonance, NMR, imaging.*

The alignment of nuclei magnetic moments is not static, however at any given time more proton spins are aligned in parallel with the external magnetic field and are low energy spin-up nuclei, whereas the smaller proportion are in antiparallel alignment and termed high energy spin-down nuclei (Westbrook and Talbot, 2018) figure 3.1. The overall magnetisation of a subject in a scanner in parallel with the external magnetic field is the sum of the magnetisation of spin-up nuclei minus the magnetisation of spin-down nuclei, which is known as the net magnetic vector. As the external magnetic field strength increases, the number of nuclear magnetic moments in the antiparallel direction reduces, consequently net magnetic vector increases (Westbrook and Talbot, 2018).

3.1.2. Larmor frequency and phase

Although the net magnetic vector is parallel to the external magnetic field along the z-axis, the magnetic moments of the hydrogen nuclei are actually spinning around the z-axis, which is called precession (Westbrook and Talbot, 2018), figure 3.2. The rate at which nuclei spin on their axis is termed precession frequency, or Larmor frequency, which is proportional to the strength of the external magnetic field (Westbrook and Talbot, 2018). Within the external magnetic field, the precession of the magnetic moments, in both the parallel and anti-parallel directions are at different points along the 360^{o} rotation, and are considered out of phase. The application of a radiofrequency (RF) pulse knocks the magnetic moments to the same point of rotation so that they are in phase, the net magnetic vector is no longer along the z-axis, figure 3.2.

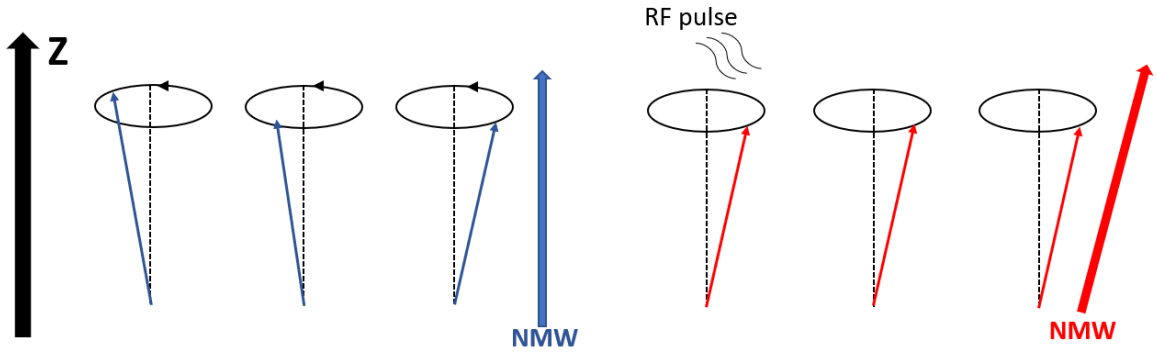

Figure 3.2. *Left) Direction of the z axis, or longitudinal plane which is in line with the external magnetic field. Middle) Arrows represent the precession of magnetic moments all at different phases around the z-axis, the resultant net magnetic vector (NMV) is parallel to z. Right) Application of a radiofrequency pulse knocks the precession of magnetic moments in to phase, which is reflected in the NMV.*

Energy from the radiofrequency pulse, at the resonant frequency of hydrogen nuclei, is absorbed, in this process the hydrogen nuclei are altered from a low energy, to a high energy state. The strength of the radiofrequency pulse determines the extent to which the net magnetic vector deviates from the z-axis. When the radiofrequency pulse is switched off, the hydrogen nuclei revert back to the low energy state. This involves two processes; dephasing of hydrogen nuclei in the transverse plane, and re-growth of magnetisation in the longitudinal plane. The latter is a much slower process. These processes release energy emitted as radio waves, and this signal is detected by an RF coil and used to generate MR images.

3.1.3. Inversion recovery imaging

Inversion recovery imaging, or T_1 weighted imaging, uses signal created by the longitudinal recovery of magnetisation as it re-grows along the z-axis after the radiofrequency pulse is switched off (Westbrook and Talbot, 2018). Speed of inversion recovery differs between tissues and is therefore an inherent source of contrast, inversion recovery is also changed in different external magnet field strengths. Therefore, the time at which signal from longitudinal magnetisation is measured at inversion time, known as Ti, affects the amplitude of the signal and contrast between tissues, figure 3.3.

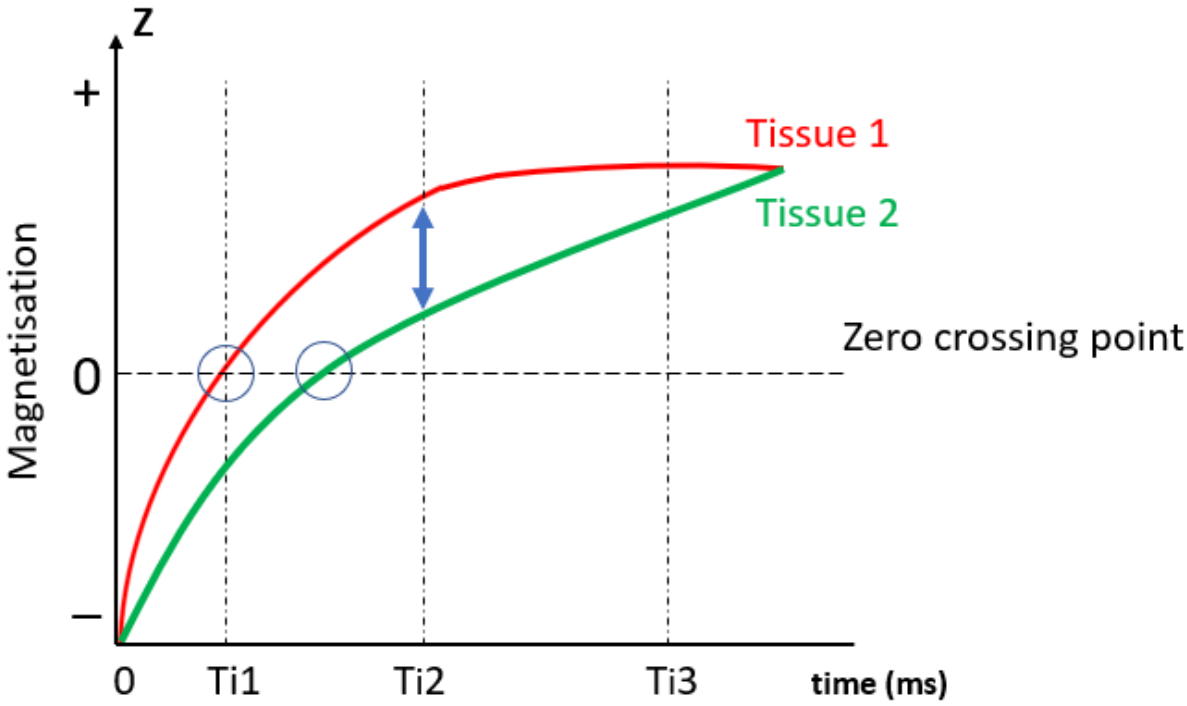

Figure 3.3. *Inversion recovery of magnetisation along the z-axis following RF excitation pulse at time point 0. The red and green lines represent different rates of inversion recovery for two different tissues. Inversion time, Ti, is the time following RF pulse at which signal is measured. The difference in magnetisation is greatest at Ti2 which therefore provides the greatest contrast between tissue 1 and 2. At Ti3 recovery is complete or almost complete for both tissues therefore difference in signal and ability to differentiate tissues is limited. At Ti1 recovery of magnetisation for tissue 1 crosses the zero point, this is known as the null point where minimal signal is generated. Selection of Ti in inversion recovery imaging is therefore important as it determines signal and contrast between tissues.*

As the magnetisation recovers along the longitudinal axis there is a point at which net magnetisation is zero (Westbrook and Talbot, 2018). If Ti occurs when inversion recovery is at or close to zero, little to no signal is detected, this is known as the null point (Westbrook and Talbot, 2018), figure 3.3.

3.1. MRI of the lung

The lungs are a unique spongey structure within the body, and thus have low proton density compared with other tissues, this presents one of the challenges to MR imaging of the lungs. The use of contrast agents such as hyperpolarised noble gases e.g. Helium-3 (Samee et al., 2003, Nilsen et al., 2021, Fain et al., 2008, Svenningsen et al., 2013), Xenon-129 (Svenningsen et al., 2013), and fluorinated gases e.g. Sulphur-hexafluoride and Perfluorocarbon (Kuethe et al., 2000) enable visualisation of gas distribution throughout the lung, and identification of poorly or non-ventilated regions, albeit often with limited quantification (Prisk and Sá, 2014). Monash Biomedical Imaging research facility does not have the capabilities to perform scans with such gases, therefore this thesis focuses on ventilation scans using non-special gases or no contrast agents at all, these techniques may be more applicable in the clinical space.

3.2. Oxygen enhanced MRI

Oxygen is weakly paramagnetic and shortens the inversion recovery time when dissolved in lung tissue and pulmonary venous blood (Ohno and Hatabu, 2007, Edelman et al., 1996). The longitudinal relaxation time, or T_1, has a linear inverse relationship to inspired oxygen flow rate prior to reaching a plateau (Mai et al., 2002), which represents the point of saturation. By increasing the fraction of inspired oxygen (FiO_2), alveolar partial pressure of oxygen, and thereby the concentration of dissolved oxygen in lung parenchyma, it is possible to generate contrast within the lung relative to baseline status whilst breathing air at FiO_2 0.21.

If this scenario is applied to the example in figure 3.3. inversion recovery of lung tissue is represented by the green line (tissue 2), whereas the shortened inversion recovery of lung tissue saturated with dissolved oxygen is represented by the red line (tissue 1), and measurement of signal at Ti2 would allow visualisation of this contrast. The regional signal intensity changes reflect changes in alveolar partial pressure of oxygen, which is dependent

on ventilation, and so this phenomenon is utilised in functional ventilation imaging with oxygen.

3.3. Specific ventilation

Specific ventilation, SV, refers to the volume of fresh gas delivered on inspiration relative to the end expiratory volume of gas (Lewis et al., 1978, Sa et al., 2010).

$$SV = \Delta V / V_0$$

where ΔV is inspired volume and V_0 is end expiratory volume (Sa et al., 2010).

In the lungs on a global scale this could be described as the ratio of tidal volume (Vt) to functional residual capacity (FRC) (resting lung volume at the end of a normal expiration). In the case of obstructive lung disease, SV is more heterogeneous. Lung regions with impaired ventilation receive less fresh gas on inspiration, therefore for each breathing cycle, changes in alveolar partial pressure of oxygen are lessened and the wash-in takes longer. Many different methods can be used to estimate SV, either on a global scale for the lungs using inert gas washout (Lewis et al., 1978), or for a region of interest using imaging with gases such as He-3 (Arai et al., 2018) and oxygen (Sa et al., 2010).

3.3.1. Specific ventilation imaging

Specific ventilation imaging, SVI, uses the rate of signal change within the region of interest, as an indirect measure of ventilation. SVI using oxygen as the contrast agent was first described by Sá et al. in 2010 (Sa et al., 2010) and involves inhalation of 100% oxygen to washout nitrogen from the lungs, just like in a multi-breath nitrogen washout.

As described in Chapter 2 during a multi-breath nitrogen washout, the subject is connected to a pneumotach to measure flow, and to an oxygen gas analyser, via a mouthpiece. Throughout the test breathing is relaxed, so that expiration is to FRC (resting lung volume)

and inspirations are guided to achieve 1-litre inspired volume. The test starts with the subject breathing air, when tidal breathing is stabilised the subject is switched to breathing 100% oxygen at the point of FRC. The test continues until the nitrogen concentration of the exhalate is 1/40th of the starting concentration. In healthy lungs with relatively homogenous ventilation the washout of nitrogen is quick, whereas in the presence of lung disease, ventilation is impaired and gas mixing throughout the lung is more heterogenous, therefore the washout of nitrogen is slower, shown in figure 3.4.

In specific ventilation imaging, rather than oxygen concentration of exhaled breath, it is the signal intensity of a lung slice or slices that is measured. Again, the subject breathes in a relaxed fashion, exhaling to FRC, it is at this lung volume that images are acquired and one breathing cycle occurs between each successive image. The first block of images is taken whilst the subject breathes air, the next block of images is acquired after the subject is switched to breathing 100% oxygen, and this continues until a series of air-oxygen switches have taken place. The rate of oxygen wash in is measured as MR signal change (due to shortening of T_1 relaxation), the rate of change is used to calculate the SV of each single volume element (voxel) of the slice(s) of lung being imaged. In healthy lungs the rate of nitrogen washout and replacement with oxygen is faster, which is reflected in the rate of change of MR signal change, and corresponds to a greater SV. In obstructed lungs with areas of low SV, oxygen wash in is slower, and so is the change in MR signal, this is represented in figure 3.4.

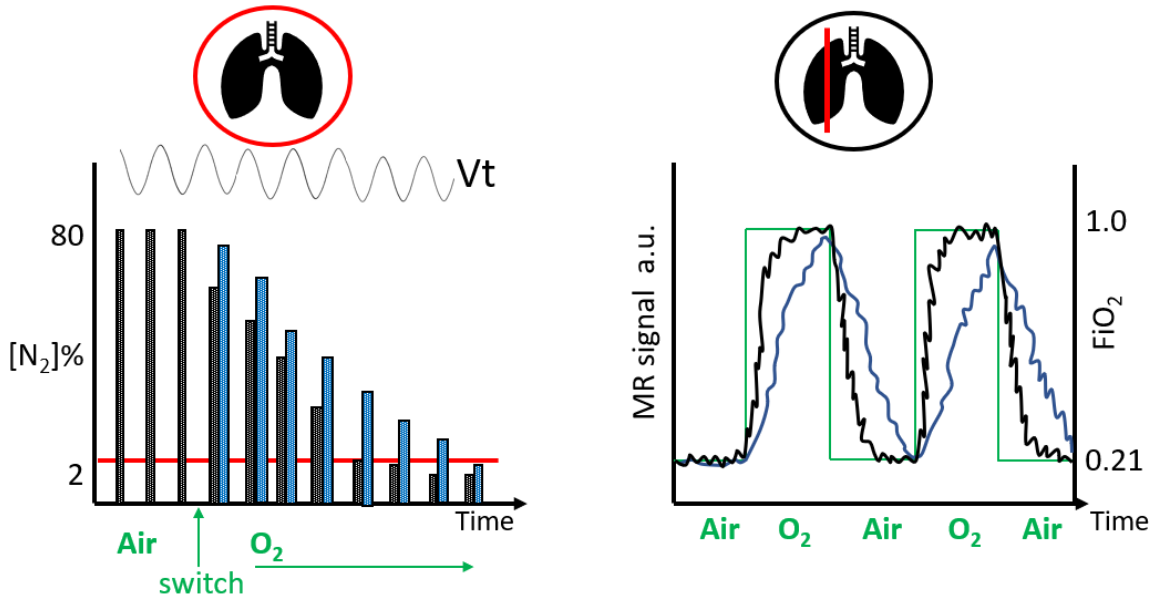

Figure 3.4. *Two methods of assessing ventilation homogeneity via breathing 100% oxygen that washes nitrogen out of the lungs. Left: Multi-breath nitrogen washout, a global measure of ventilation. The trace at the top of the graph represents tidal breathing, Vt. The columns beneath are nitrogen concentration measured during exhalation at the mouth, after the 'switch' to breathing 100% oxygen the nitrogen concentration reduces with each successive breath to below 2%, black columns show a normal washout, blue columns show a slower washout expected in the presence of obstructive lung disease. Right: Specific ventilation imaging, schematic represents a spatial element of the lung which may be a slice of lung or a single voxel. The green trace depicts the driving function i.e. FiO_2 0.21 and 1.0. The black trace represents the change in signal measured for region of interest with normal SV, the blue trace represents the change in signal of an area with low SV.*

3.3.2. Performing SVI

Subject preparation

First, safety screening was completed by a qualified radiographer and the scan protocol was explained to the subject. This included how to 'respiratory gate' whereby the subject was coached to time their breathing to be at FRC during image acquisition, this was practiced using a pre-recorded example of scanner noises which act as cues. The subject was prepared for scanning by removing any artefact causing items, or items with safety contraindications in a high magnetic field environment, such as metal containing clothing /

underwear, and they were positioned supine on the scanner table with cushioning to aid comfort throughout scan which lasted for 20-30minutes. Earplugs were supplied for ear protection, as well as headphones to allow communication from the console room.

The torso coil was placed over the subject directly beneath their chin to overlay the lung apices and secured with clips and/or Velcro straps. An airtight mask was fitted to the subject to enable oxygen delivery during the scan, to this a T-piece was attached. The T-piece acts as a flow bypass device, this allows inspirations of 100% medical grade oxygen during delivery of high flow oxygen, as well as inspirations of room air when the oxygen source is turned off, this system negated the need for valves that present a potential safety risk (Cook et al., 2015, Geier et al., 2019). The oxygen tubing ran from the T-piece connection to the console room where it was connected to the oxygen source via a turn-valve which allowed instantaneous switching from air-oxygen and vice-versa. All connectors and tubing inside the scanner room were MR compatible and the diameter of tubing transitioned to ½ inch for the final 2m section to reduce noise from gas flow. Finally, the subject was moved to within the scanner bore, bean bags were used to secure oxygen tubing and prevent drag on the mask (Geier et al., 2019).

Scanning

Initially a localiser scan was completed to view the subjects' position inside the scanner. Then a 15mm thick sagittal slice of right lung, selected to maximise the volume of lung imaged whilst avoiding major hilar vessels, was chosen. The subject was coached at the start of the 220-image acquisition protocol to time their breathing cycle so that image acquisition was after a relaxed expiration (respiratory gating), intermittent reminders were given throughout. The aim was to acquire each of the 220 images at the same lung volume (FRC), with one relaxed breathing cycle completed in between each consecutive image. Initially the subject breathed air, they were then switched to inspire 100% oxygen at intervals of 20 breaths or images, a 40 breath or image block of inspired oxygen was included to increase sensitivity for slow space (poorly ventilated regions) that may take more than 20 breaths to reach equilibrium. The time between images or repetition time, TR, was around 5seconds

which allowed for a natural breathing frequency of ~12 breaths or images /min, therefore scan completion time was around 18minutes. Specific acquisition parameters as published in (Geier et al., 2019) are given in table 3.3 below.

3.3.3. MR data processing and SV calculation

Region of interest volume quality assurance and selection

A complete SVI data set consists of 220 images. The data was imported (e.g. as DICOM files) into analysis software (MATLAB). First, the 128x128 matrix was reconstructed to 256x256. Then, images underwent volume registration (Arai et al., 2012) to correct for small deviations from the ideal lung volume, FRC, and to remove signal intensity changes due to changes in lung tissue density. Images were registered to the sagittal slice with the most frequently occurring lung volume from the 220-image stack, assumed to represent FRC. FRC is the point at which elastic recoil of the lungs is equal and opposite to the recoil of the chest wall, as no energy is being exerted it is a resting lung volume, and FRC is reproducible if position is constant, in this case supine. Volume registration is reliable for volume corrections of up to 10% (Arai et al., 2012) therefore images <0.9 or >1.1 of the most frequently observed lung area are considered 'bad breaths', these were excluded from the analysis. The remaining image stack was inspected manually, images that were poorly registered or affected by motion were discarded.

The region of interest, ROI, i.e. the sagittal lung slice, was manually selected from the field of view containing the subjects' supine thorax, figure 3.5. All voxels included in the selected ROI, for each remaining image underwent the SVI temporal analysis.

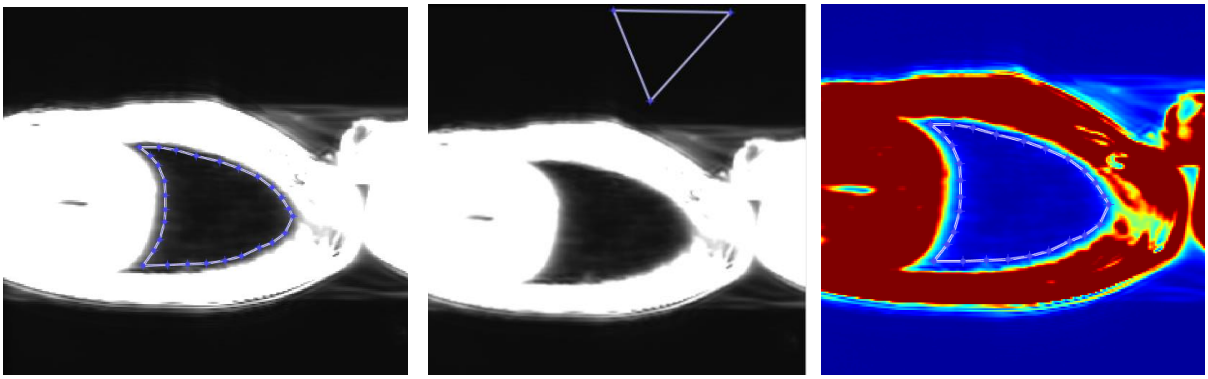

Figure 3.5. *Left, manual selection of the ROI represented by blue line outlining periphery of lung area, Middle, selection of background for noise determination, Right, verification of ROI illustrating exclusion of extreme lung periphery/chest wall that are susceptible to motion artefact.*

Specific ventilation map creation

Specific ventilation maps were created by assigning each voxel within the ROI a value of SV. The voxel-wise temporal analysis used the rise time, or rate of T_1 signal change to equilibrium value after switch in FiO_2, to determine SV (Sa et al., 2010), explained below.

Signal interpretation

MR signal change over a full SVI run of 220 images is displayed in figure 3.6. There are 5 switches from air to oxygen, each set of images was acquired at FiO_2 0.21 or 1.0, alternating in blocks of 20 images, with the exception of the first block of FiO_2 1.0 which was 40 images, and increases the sensitivity for determining low SV in regions with poor ventilation (Geier et al., 2019). Graphically, the driving function of the measured response is represented by a square wave, i.e. FiO_2 0.21 immediate increase to 1 when the switch is made from inspired air to 100% oxygen.

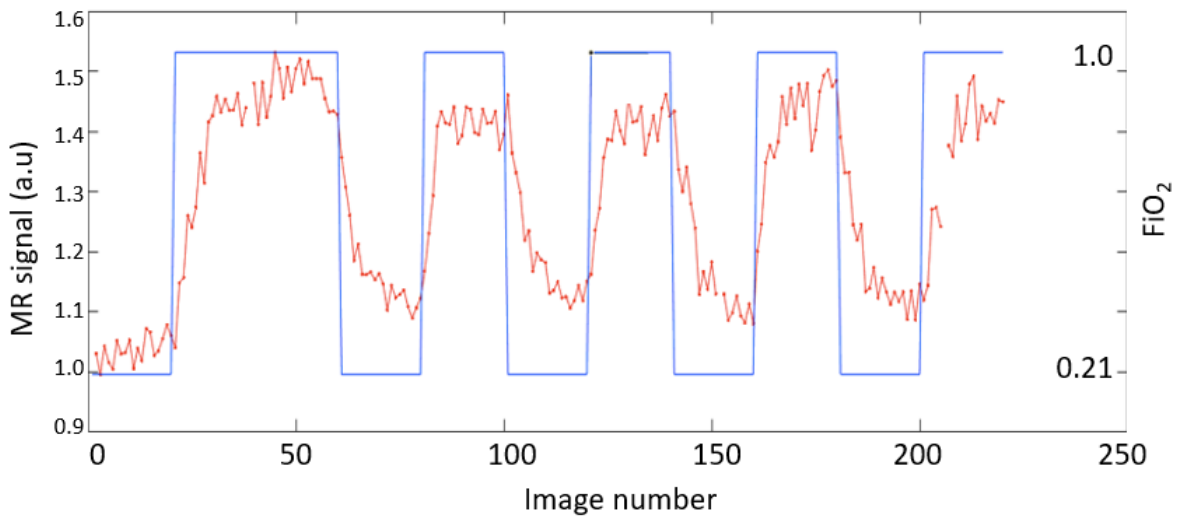

Figure 3.6. *Plot of MR signal for region of interest throughout the SVI scan protocol. Blue line is the driving function alternating between FiO_2 0.21 and 1 as the subject is switched between air and oxygen, the red trace represents whole ROI signal intensity.*

The shape of the trace illustrating signal change for each voxel is determined by; the SV of that voxel, and the amount of additional noise measured. Experiments to work out how SVI voxel signals correspond to values of SV were completed by Sa et al. (Sa et al., 2010). The wash in of oxygen for a single lung unit model, representing a single voxel, was simulated to calculate the rate of MR signal change to equilibrium after a switch to FiO_2 1.0, example in figure 3.7. This was completed for a range of SVs from well ventilated (SV = 1.0) to poorly ventilated (SV = 0.05) creating a library of SV functions (Sa et al., 2010). The signal trace from each voxel was mapped to the library of SV functions, the function with the greatest correlation to measured signal was assigned to that voxel, or, if no SV functions correlate significantly ($p \geq 0.05$) that voxel was discarded, (Sa et al., 2010).

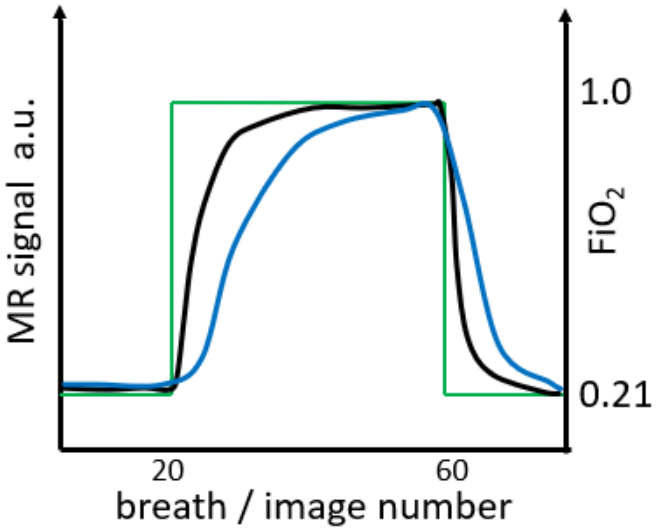

Figure 3.7. *Schematic representing driving function (FiO_2) in green, and example modelled noise-less traces of MR signal from a voxel. Following change in FiO_2 the gradient of the black trace is steeper demonstrating faster MR signal change and greater SV compared to the blue trace.*

SVI outputs

SVI map

The SVI map is the spatial output displaying SV for each voxel within the lung slice ROI, figure 3.8.

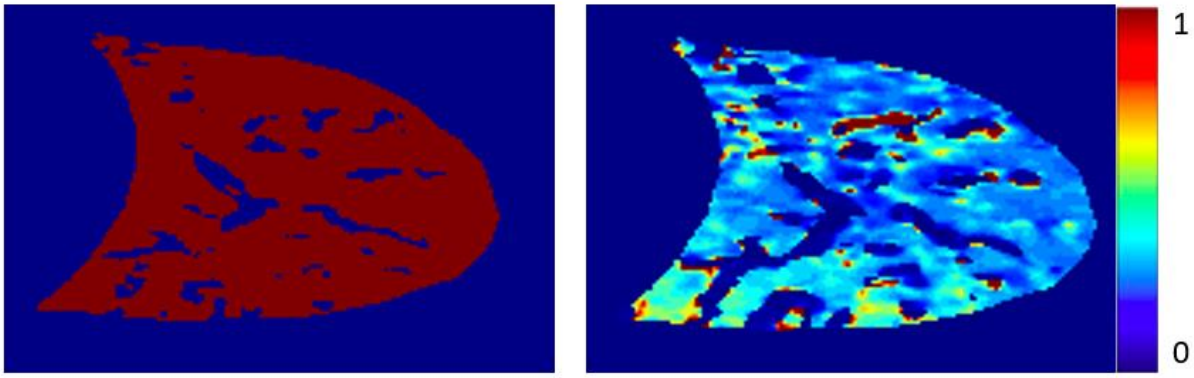

Figure 3.8. *Left, whole ROI 'p map' displays voxels that correlate with a library function of SV in red and discarded voxels that do not correlate in blue. Right, SVI map displays regional SV described by colour, cooler colours = low SV, warmer colours = higher SV.*

Histogram

The distribution of voxel SVs were viewed as a normal distribution on a log scale, the best fit normal distribution symmetrical bell curve was applied, as shown in figure 3.9. The width of the best fit normal distribution is a measure of variance of SV within the ROI and therefore describes heterogeneity of SV, or ventilation heterogeneity.

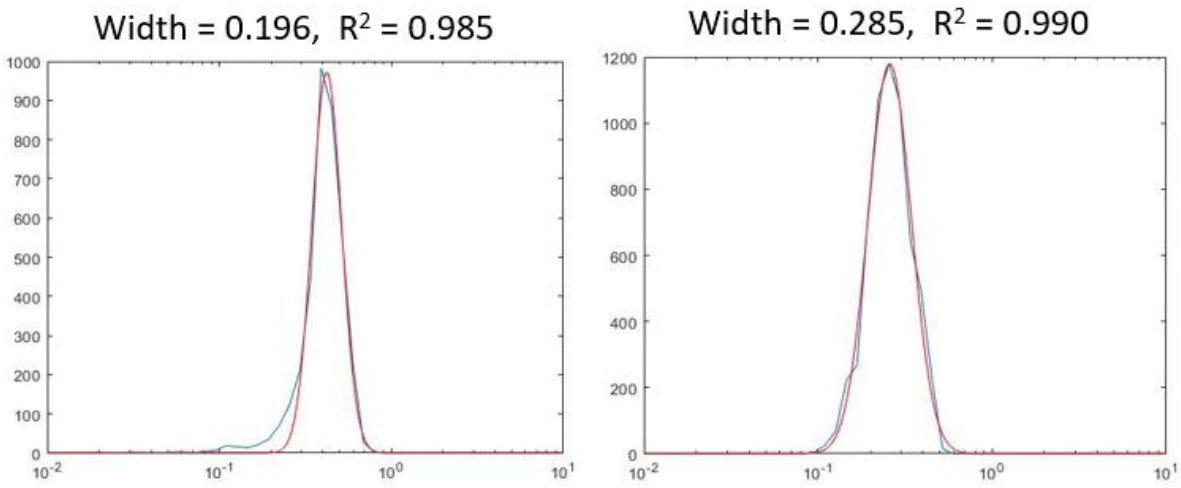

Figure 3.9. *y-axis = number of voxels, x-axis = log SV. Blue trace represents the log distribution of SV, red trace represents the best fit normal distribution curve. Left histogram is narrower representing a more homogenous distribution of SV, right histogram is wider representing more heterogenous SV.*

Height plot

The average SV of ascending lung portions in the isogravitational plane are displayed in a height plot, figure 3.10. Dependent lung is beneath non-dependent lung in the direction of gravity, thus, the posterior aspect of lung slice forms the dependent region for a supine SVI dataset. Due to gravity, the alveoli in the non-dependent lung are stretched, and have a higher baseline volume relative to those in the dependent lung (Hopkins et al., 2007). Therefore, in the healthy lung, the ratio of fresh gas to resident gas in the non-dependent lung region is less, hence SV is lower (Geier et al., 2019, Sa et al., 2010).

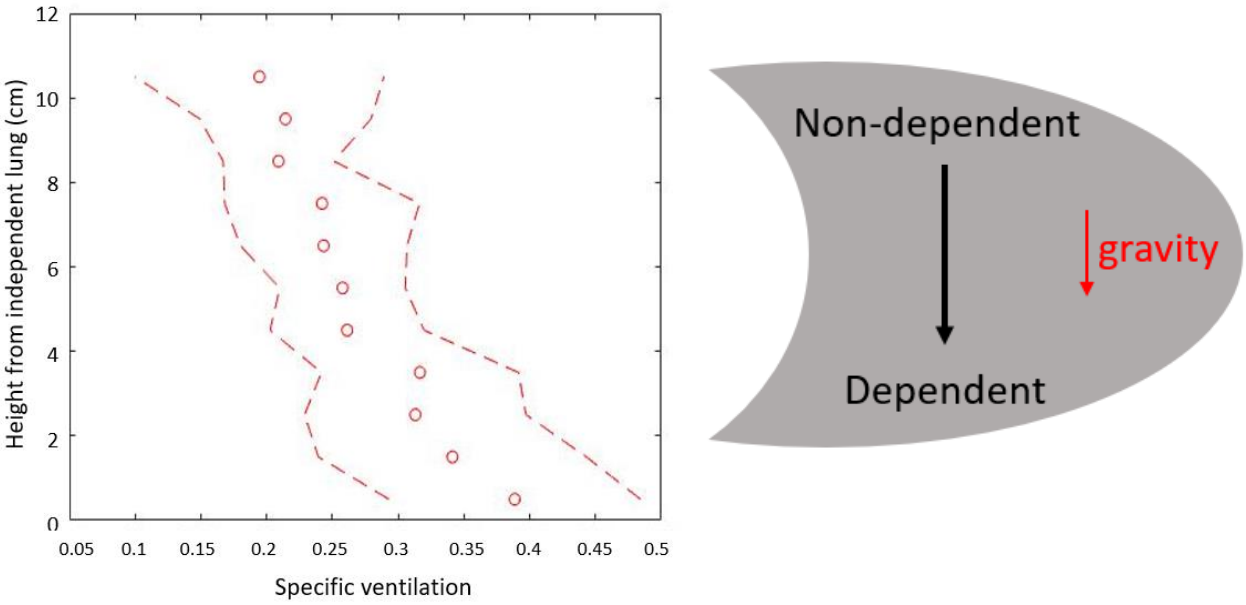

Figure 3.10. *Left) Average SV for isogravitational lung slices plotted against cm from dependent lung that resides inferiorly in the gravitational plane. Depicted in Right) schema of sagittal lung slice. There is a negative association between height from dependent lung and SV, SV is greater in the dependent lung which receives more fresh gas on inspiration relative to non-dependent lung.*

3.4. Specific Ventilation Imaging at a higher magnetic field

The SVI technique described has previously been performed on scanners of magnet strength 1.5-Tesla (T), whereas the MRI scanner available for subject testing in this research was 3-T. As scan protocols are not transferable to different field strengths, development of a 3-T SVI protocol was required. Further, although 1.5-T MRI scanners are used clinically, MR imaging at 3-T has become more common (Stanisz et al., 2005, Thieme et al., 2011), therefore, development of a 3-T protocol may serve to expand the utility of this technique.

The move to MR scanners with stronger magnets is in part driven by the improvement in signal to noise ratio, SNR which enable generation of higher quality images. For some tissues increase in SNR is proportional to the increase in field strength (Dietrich et al., 2008), however, this does not translate to MR of the lung. The lung is prone to susceptibility artefacts caused by numerous gas to tissue interfaces, the differences in magnetisation of solid lung parenchyma versus air spaces cause local field inhomogeneities which promotes dephasing of magnetic moments (Thieme et al., 2011). MR signal measured from the lung is

inherently low, further the greater propensity for dephasing at gas to tissue interfaces results in faster signal decay. Precession of magnetic moments, as well as dephasing due to magnetic susceptibility is greater at 3-T than at 1.5T (Westbrook and Talbot, 2018), therefore, the SNR gains seen in other tissues at higher fields do not necessarily apply to the lung.

3.4.1. 3T Protocol development process

Two healthy volunteers were recruited to complete a series of experiments to optimise the SVI scan protocol, in terms of both scan parameters and procedure, for testing at 3-T.

Constants throughout the 3-T testing process

Scanner and location

Testing sessions were completed at Monash Biomedical Imaging research facility, Melbourne, Australia, using Siemens Skyra 3-Tesla magnetic resonance imaging scanner (bore width: 70cm, 18-channel body coil). A qualified radiographer completed subject preparation including all safety checks prior to subject scanning and operated the scanner implementing investigational protocols.

Slice selection

For each scan a 15mm sagittal slice of the right lung was selected to achieve the largest area within the region of interest, ROI, whilst avoiding the major hilar vessels by lateral positioning. Slice position relative to spinal column was recorded for each subject to reproduce location of imaged ROI between scans.

Sequence

Single shot turbo spin echo sequencing was used, or specifically Half-Fourier Acquisition single-shot turbo spin-echo (HASTE) as trademarked by Siemens. This sequence obtains all

the data required to create an image after a single radio-frequency excitation, which undergoes Fourier-transformation to generate the MR image (Westbrook and Talbot, 2018).

Oxygen delivery

The oxygen source was located in the console room and delivered via a high flow meter set at maximum flow with a 180^{o} turn valve to facilitate rapid switches from air to oxygen and vice versa. Oxygen tubing was fed into the scanner room and attached to MR safe connector and custom-made 3D printed T-piece which fitted the face mask (Hans Rudolph Inc., Kansas City, MO, USA, 8930 Series, size Medium) (Geier et al., 2019). To achieve inhalation of 100% oxygen the flow of delivered oxygen must be greater than the peak inspiratory flow of the subject being imaged (Geier et al., 2019), to account for this the flow meter was set at maximum delivery of 70L/min.

Subjects

Subject	**Sex**	**Age (yrs)**	**Height (cm)**	**Weight (kgs)**
1	Male	38	185	70
2	Female	31	167	61

Titration of inversion time

Signal from longitudinal magnetisation is generated at inversion time (Ti) and as T_1 is different at 3T a series of Ti titrations were completed. The objective was to optimise the signal to noise ratio, SNR, for both air and oxygen, as well as to achieve the greatest signal enhancement, or contrast, with oxygen.

Calculations

SNR = average signal within ROI ÷ average background signal

Contrast ratio = average signal O_2 ÷ average signal AIR

Average SNR = (Air SNR + O_2 SNR) ÷ 2

Contrast to noise (%) = Contrast ratio ÷ Average SNR · 100

Subject 1 completed a session in the scanner testing Ti values from 800ms to 1200ms at increments of 50ms. The subject practiced respiratory gating so that each image was acquired after one respiratory cycle after the tidal expiration at the volume of functional residual capacity. An electrocardiogram (ECG) was applied to cardiac gate using the 'R' portion of the QRS complex (ECG trace depicting ventricular depolarisation) as the trigger and a pause time calculated based on subject heart rate so that image acquisition coincided with diastole to minimise blood flow. The subject completed one switch only, completing 20 breaths of air followed by 40 breaths of oxygen, or vice versa. The average signal measured from the ROI, its variation as standard deviation for both air and oxygen, and resulting SNR are reported in table 3.1.

Table 3.1. Signal and variation for differing Ti values at 3T for Subject 1

	Air			**Oxygen**			**Contrast ratio**
Ti (ms)	Average signal	SD	SNR	Average signal	SD	SNR	
800	393	26	15.1	285	9	31.7	0.7
850	201	25	8.0	174	3	58.0	0.9
900	189	10	18.9	185	7	26.4	1.0
950	191	9	21.2	204	4	51.0	1.1
1000	181	5	36.2	227	6	37.8	1.3
1050	185	5	37.0	285	17	16.8	1.5
1100	256	19	13.5	403	41	9.8	1.6
1200	396	28	14.1	578	49	11.8	1.5
1300*	76.5	31.1	2.5	82.6	32.1	2.6	1.5

Results for Ti range 800-1200ms from tests conducted at Monash Biomedical Imaging research facility, Ti 1300ms* reported from literature (Thieme et al., 2011)

SNR was calculated at 3-T for air and oxygen using the whole ROI, excluding only the extreme periphery to avoid motion artefact of the chest wall and diaphragm, which includes

expected variation across a supine sagittal slice due to gravitational effects on SV (Sa et al., 2010). Calculated SNR was greater than that reported in the literature at all Ti values for both air and oxygen, table 3.1. (Thieme et al., 2011)

The greatest SNR for air and oxygen was achieved at Ti 1000ms, however the signal enhancement with oxygen versus air was low. Insufficient contrast ratio in the context of an inherently noisy signal results in a higher proportion of discarded voxels, as SV cannot be deciphered. For each voxel, if the measured signal change that occurs after the switch from FiO_2 0.21 to 1.0 does not correlate with any of the SV library functions ($p \geq 0.05$) the voxel is excluded and classed as missing data, figure 3.11.

The contrast ratio was greatest for Ti values 1050, 1100 and 1200ms, Table 3.1, and as 1050ms had the greatest average SNR over air and oxygen and the majority of voxels correlated with the driving function, figure 3.11, 1050ms was selected as the optimal Ti value.

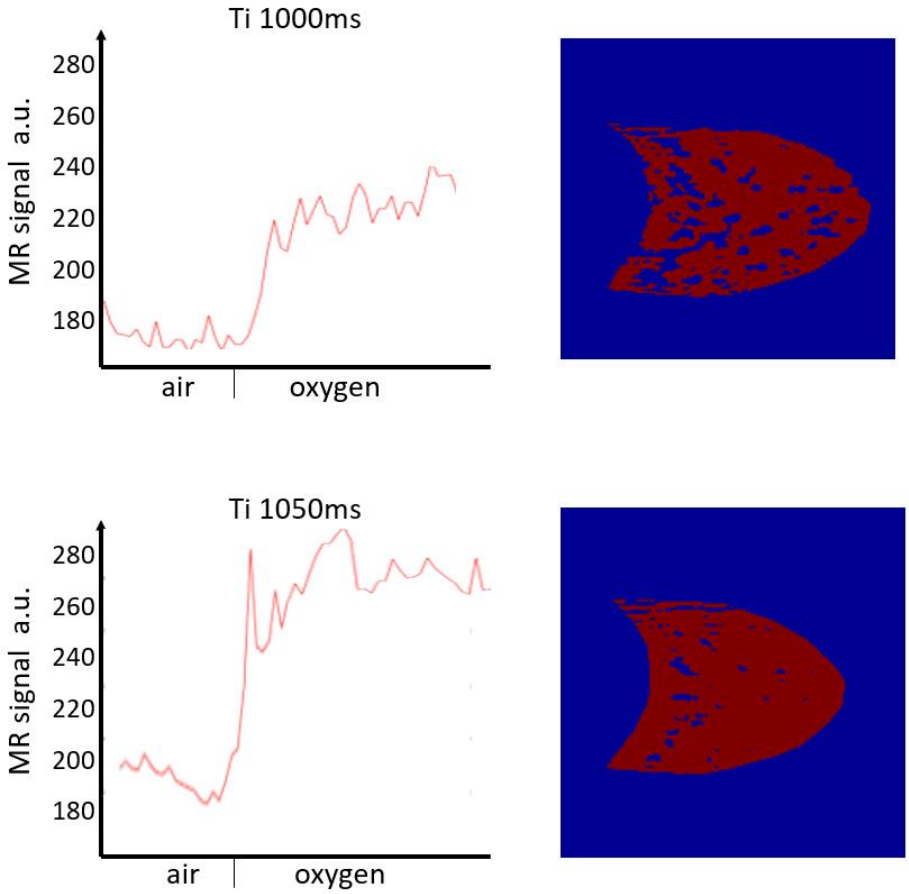

Figure 3.11. *Left: graphs displaying signal intensity change over one switch from air to oxygen for Ti 100ms (top) and Ti 1050ms (bottom). Right: Corresponding 'p maps' that display the voxels discarded due to no correlation with SV functions as blue areas within the red sagittal slice ROI, for Ti 1000ms (top) and Ti 1050ms (bottom). Ti 1050ms provides greater increase in signal following the change in FiO_2 which translates to a greater contrast ratio and results in fewer discarded voxels and less missing data.*

Ti assessment confirmation with a second subject

A series of Ti titration assessments were completed with subject 2 to test and confirm the results obtained from subject 1, results in Table 3.2.

Table 3.2. Signal and variation for differing Ti values at 3T for Subject 2

	Air			Oxygen			
Ti (ms)	**Average signal**	**SD**	**SNR**	**Average signal**	**SD**	**SNR**	**Contrast ratio**
975	283	7.9	35.8	359	20.8	17.3	1.3
1000	283	8.3	34.1	366	16.6	22.0	1.3
1030	284	6.9	41.2	388	18.3	21.2	1.4
1050	286	13.6	21.0	390	11.5	33.9	1.4
1070	291	10.9	26.7	436	40.1	10.9	1.5
1100	313	14.3	21.9	506	38.7	13.1	1.6

The greatest SNR achieved for air was at Ti 1030ms and the greatest SNR for oxygen was at Ti 1050ms, confirming that Ti around 1030-1050ms is optimal for SVI imaging at 3T, producing a contrast ratio ~1.4. For subsequent scanning Ti 1040ms was chosen.

Trial of non-cardiac gated scan with optimal Ti

The aim of cardiac gating is to time image acquisition during diastole thereby avoiding unwanted vascular MR signal when blood is pulsatile. The 'R' wave, from the QRS complex responsible for instigating systole, is the trigger, and heart rate is used to determine the delay so that image acquisition occurs immediately prior or during the next QRS complex during diastole.

Producing a clean ECG recording in an MR scanner can be challenging. The trace quality is affected by the magnet field, as the currents created by ions in blood flow that are perpendicular to the magnetic field interfere with the recording of currents within cardiac muscle, this is exacerbated at higher magnet field strengths (Dietrich et al., 2008). An artefactual ECG trace may prevent correct selection of the QRS complex resulting in mistimed image acquisition.

SVI at 1.5-T uses a Ti of 1100ms which, conveniently, is the null point for blood, this allows assessment of ventilation without interference from vascular signal. As T_1 is altered by external magnet strength and oxygen partial pressure the impact of vascular signal at the selected Ti 1040ms for 3-T was assessed by conducting both cardiac gated and non-gated scans for subject 2.

The signal intensity trace representing the whole ROI, from a cardiac gated and non-cardiac gated full SVI scan, was compared for subject 2, figure 3.12. Both the gated and non-gated signals demonstrated a clear relationship with the driving function, however the non-gated dataset produced a noisier signal with a greater number of and larger excursions from the trend due to inclusion of vascular signal from pulsatile blood. Therefore, cardiac gating is a worthwhile step in the pursuit of a cleaner and easier to interpret signal in SVI at 3-T.

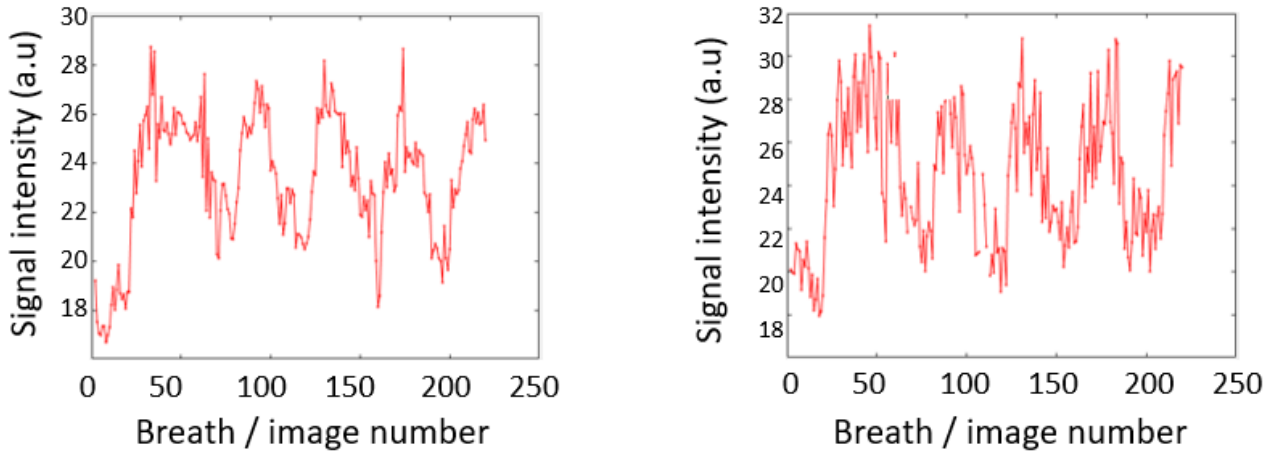

Figure 3.12. *Signal intensity taken from whole ROI (15mm sagittal slice of medial right lung) as a function of breath number for cardiac gated, left, and a non-cardiac gated run, right. The increase and decrease in signal following change in FiO_2 is visible for both runs, however due to avoidance of unwanted vascular signal the cardiac gated run generated a cleaner signal. A less noisy signal is easier to map to library of SV functions.*

Exploring the possibility of a shorter scan

Consideration must be given to the duration of the SVI protocol, this lengthy scan runs for 220 breaths which works out to about 18 minutes with a dynamic scan duration of 5 seconds. Reduction in scan time would be a practical step in promoting use of this technique, as well as being more attractive to potential study participants, that is if comparable results can be produced.

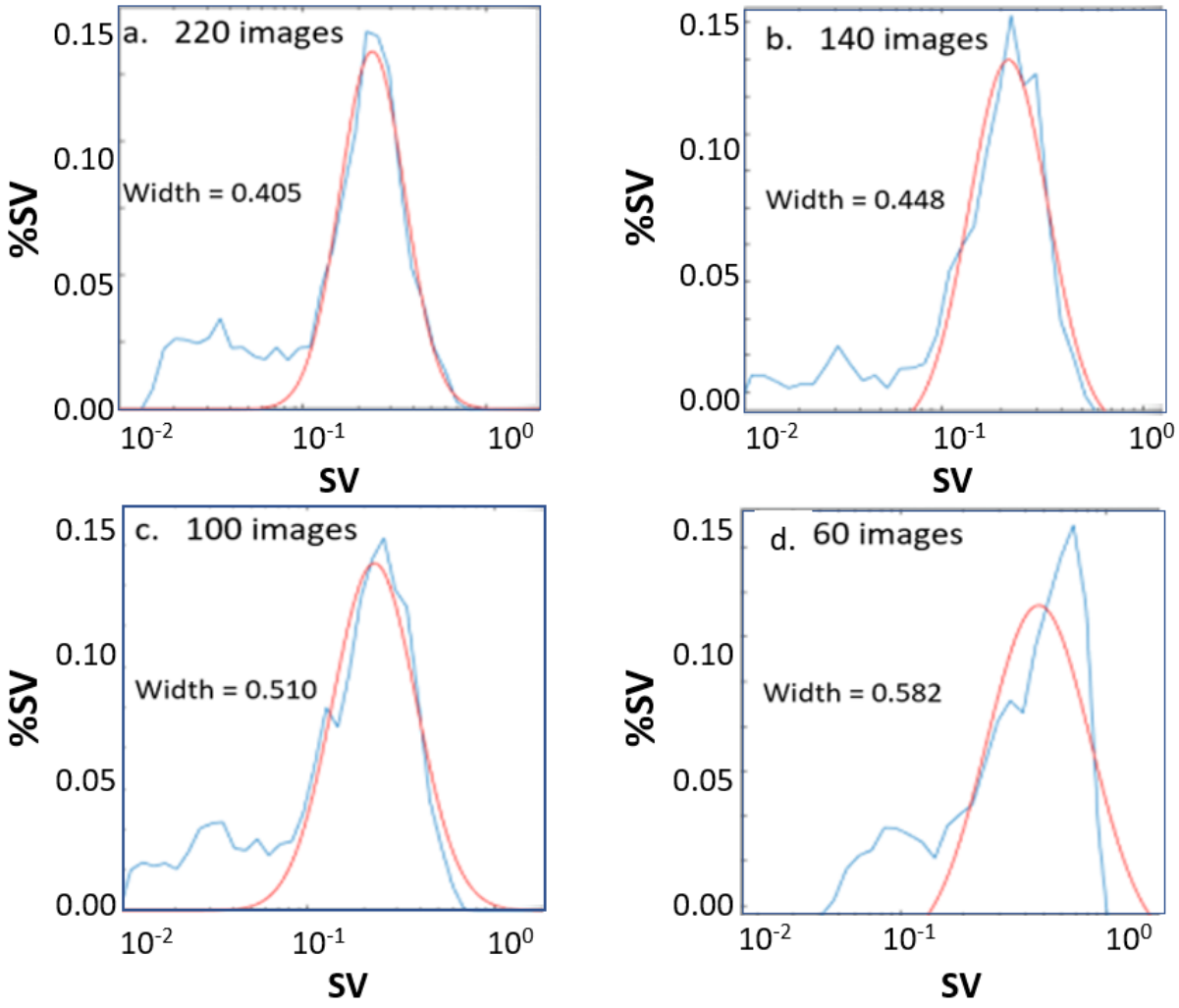

Figure 3.13. *SV distribution histograms in blue on log scale, with fitted Gaussian distribution in red for the same dataset for subject 2. Each tile represents the analysis with reducing number of images and therefore fewer switches in FiO_2. a) 220 images, b) 140, c) 100, d) 60. The top row demonstrates that results produced by analysis using 140 images are largely unchanged compared with 220 images, SV distribution width to 1 significant figure is 0.4. As the datasets reduce further SV distribution width increases; 0.5 for 100images, and 0.6 for 60 images.*

Figure 3.13. demonstrates the effect of reducing scan length and analysing datasets with fewer air to oxygen switches for subject 2. The SV distribution of the 140-image dataset is mostly unchanged compared to the full 220-image dataset, the key metric SV distribution width is unchanged, assessed at 1 significant figure. For subsequent reductions in the number of images, width of fitted Gaussian distribution increases, and there is a dramatic shift rightward for dataset 60-images. These results suggest that an SVI protocol of 140 images is sufficient, for this subject, on this occasion. These results also demonstrate that reducing the amount of data acquired and analysed can significantly change the output. Further, the effect on datasets of poorer quality would be exacerbated, and the effect on a dataset representing pathology is unknown. Therefore, erring on the side of caution, the 220-image acquisition protocol from 1.5-T was retained.

The final scan parameters for SVI at 3-T agreed within the research group are detailed in table 3.3. with 1.5-T parameters shown for comparison. SVI results for both subjects obtained with the developed protocol are shown in figures 3.14.

Table 3.3. Final SVI scan protocol parameters for SVI at 3T on Siemens Skyra with 1.5T for comparison

Parameter	**1.5T**	**3T**
Echo time Single slice	21.6 ms	39 ms
Repetition time (TR)	5s (Any values >4s, adjusted for patient comfort / breathing frequency)	1 respiratory cycle ~5s Achieved by TR 1250ms + PAM (pause after measurement) 3s + QRS trigger time
Repetitions	220	220
Inversion time (Ti)	1100ms (single slice)	1040ms
Matrix	256 x 128 (single slice)	128 x 128 Reconstructed to 256x256
Field of view	40cm (32 – 40 cm)	40cm
Bandwidth	125 kHz	831 Hz/Px
Slice thickness	15mm	15mm
Cardiac gating	No	Yes

3-T SVI results

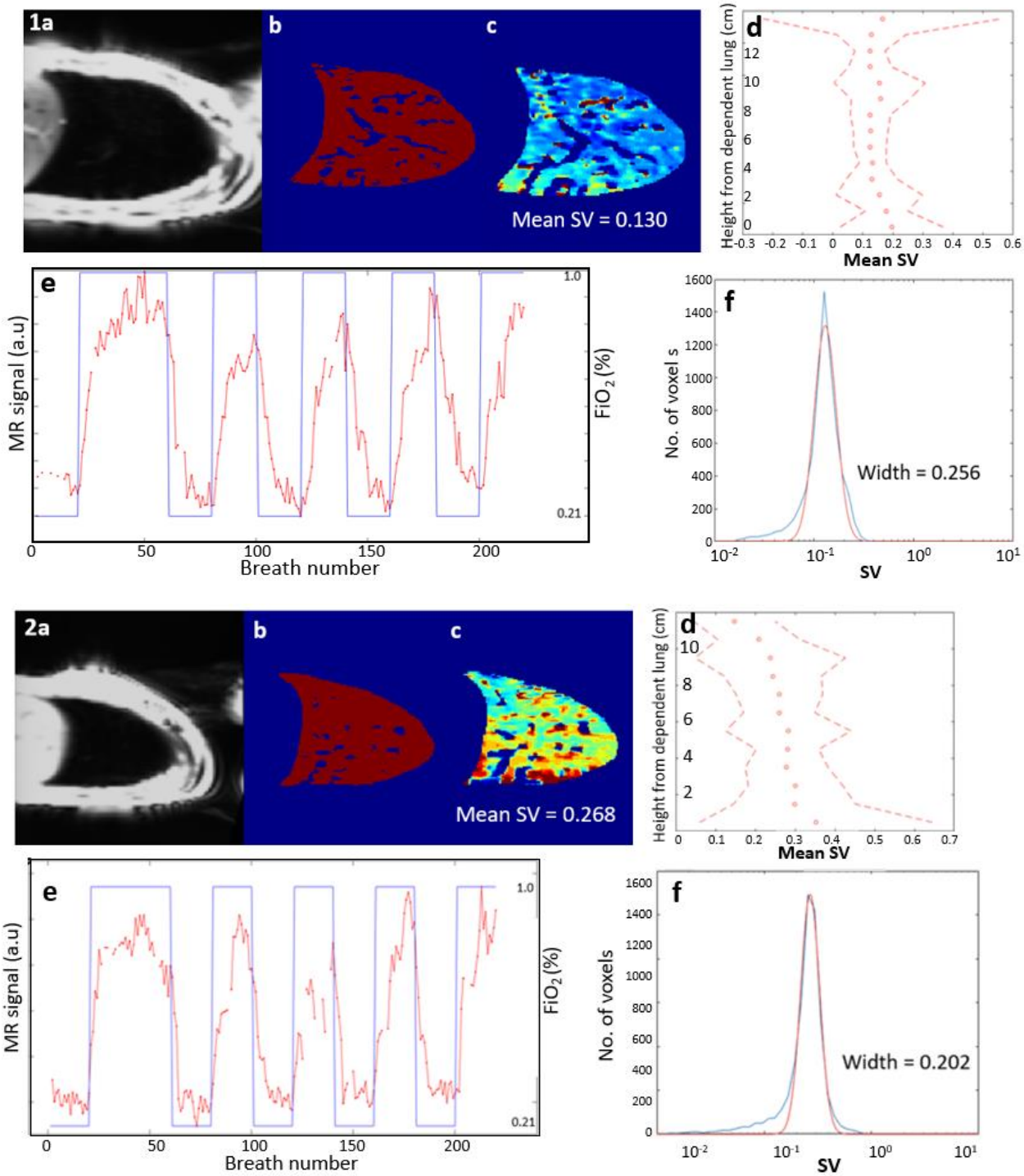

Figure 3.14. *3-T SVI results for subjects 1 (top) and 2 (bottom) from a single full run. a) Sagittal slice ROI. b) p-map displays voxels discarded due to lack of correlation with SV library functions as blue within red ROI. c) SVI map. d) height plot. e) plot of MR signal versus driving function f) distribution of SV on a log scale in blue, with best fit normal distribution curve in red. Subject 1 has a greater proportion of discarded voxels (b), mean ROI SV is less for subject 1 (c), there is a trend for greater SV in dependent lung subject 2 but not for subject 1 (d), ventilation heterogeneity is greater for subject 1 who has a wider fitted Gaussian distribution.*

Addition of median filter to SVI post processing

The addition of cardiac gating produced a cleaner signal compared with the signal obtained in non-cardiac gated scans. Despite this the traces of MR signal for whole ROI still contain noise in the form of abrupt excursions, figure 3.12, which are caused by suboptimal cardiac gating. A poor ECG trace or variable heart rate may result in some images acquired during systole and the inclusion of vascular signal. To rectify this a median filter was added into the SVI data analysis process. Median filters are effective at removing sharp spikes (increased signal due to poor cardiac gating and inclusion of vascular signal) whilst preserving edges or transitions (change in signal sue to switch in FiO_2) (Pratt, 2007), demonstrated in figure 3.15.

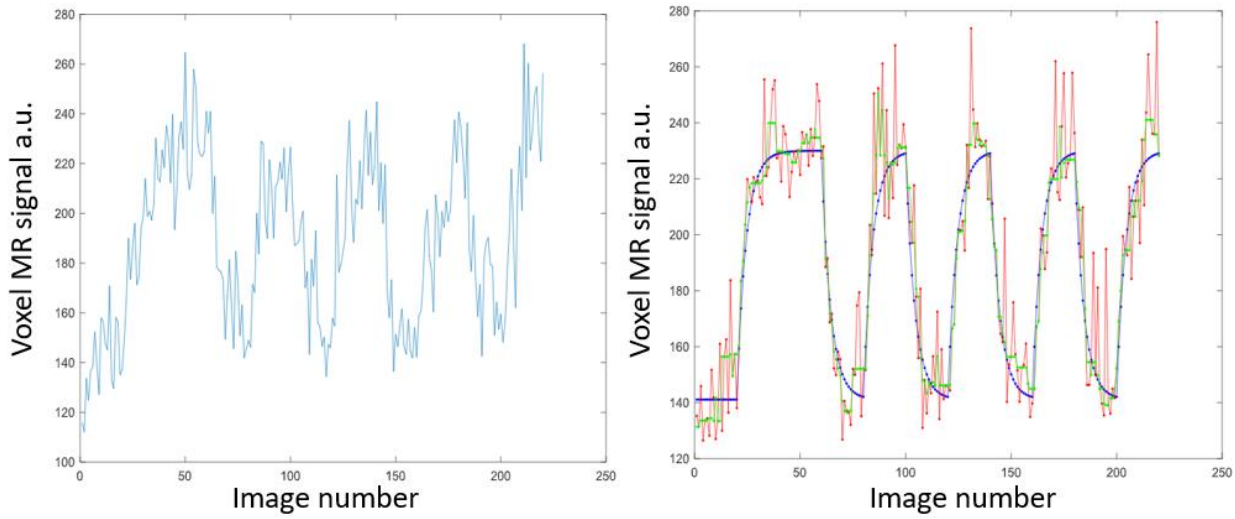

Figure 3.15. *Left, signal trace from a single voxel for a full SVI run measured at 3T. Right, blue = library function of SV, red = library function with the addition of expected noise, the trace is similar to the 'real' voxel MR signal trace displayed on the left graph, green = median filtered signal*

A median filter of 5th order was applied to 3-T datasets. The order refers to the number of consecutive datapoints from which the median is selected; i.e. 5th order median filter will assess 2 values either side of the value to be reported and assign the median of those 5 consecutive datapoints (Pratt, 2007), the result is shown in figure 3.16.

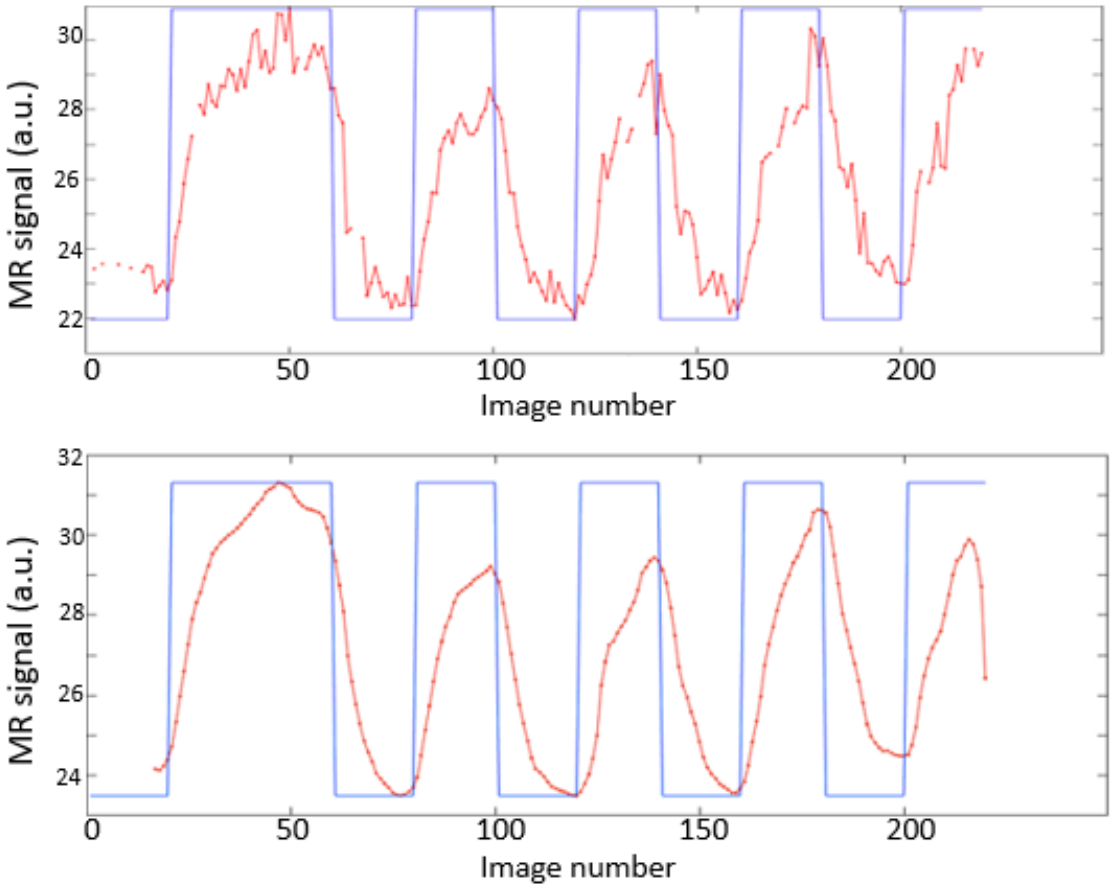

Figure 3.16. *Subject 1 3-T SVI scan signal trace in red, with driving function in blue. Top = original analysis, bottom = 5th order median filter applied. The filtered version is smoother as high spikes in MR signal captured due to inclusion of vascular signal have been removed, the transitions following switch in FiO_2 are preserved.*

3.5. Comparison of 3-T SVI with 1.5-T SVI

To evaluate the SVI results produced with the developed 3-T protocol against the 1.5-T published protocol further SVI testing, both at 3-T for repeat measures and at 1.5-T for comparison datasets, was required. Access to a 1.5-T scanner was possible through research team connections, located at the Centre for Advanced MRI, University of Auckland, New Zealand. The research trip was made possible through funding from the International Partnerships Seed Funding scheme, Newcastle University. Study personnel, including the two healthy volunteers attended the research facility in Auckland and completed SVI scans in the 1.5-T Siemens Avanto Fit MRI machine.

The 1.5-T and 3-T scanning, in Auckland and Melbourne respectively, took place during the time of intermittent and extensive lockdowns due to the COVID-19 pandemic. Therefore, the datasets collected were limited to: Subject 1 = 1x 1.5-T scan and 2x 3T scans, Subject 2 = 2x 1.5T scans, and 2x 3T scans. 1.5-T results are displayed in figure 3.17. SV is dependent on resting lung volume and volume of gas inhaled and exhaled in tidal breathing during scanning, both of which vary between subjects, and this is reflected in differences in mean SV. The critical parameter is SV distribution width which details the heterogeneity of SV or ventilation throughout the ROI.

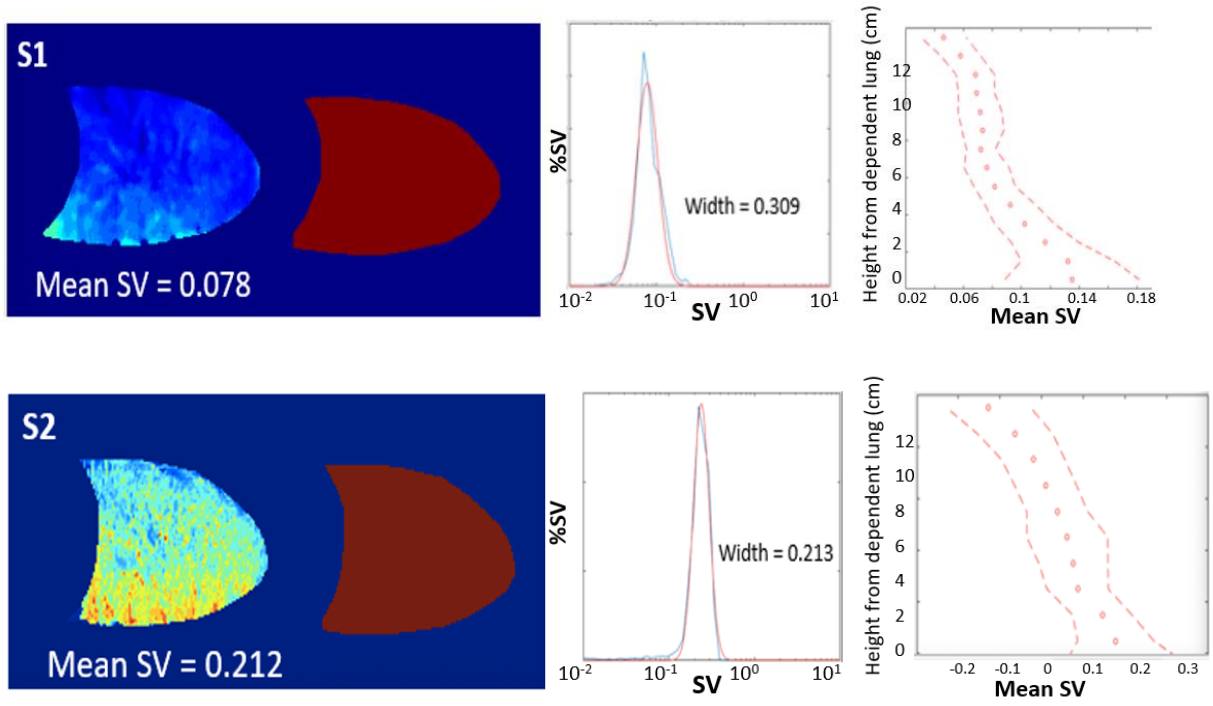

***Figure 3.17**. Results from a single 1.5-T SVI scan for subject 1 top and subject 2 bottom. All voxels within the ROI correlate with the driving function for both subjects. Subject 2 has greater mean SV, subject 1 has a wider distribution of SV representing greater ventilation heterogeneity, the gravitational relationship of SV, with greater SV in dependent lung is visible for both subjects.*

3.5.1. SV distribution comparison

Distribution of SV, which provides a measure of ventilation heterogeneity, is denoted as the width of the fitted normal distribution bell curve. The absolute difference in SV distribution width was similar for both subjects (0.050 and 0.048), however there was no pattern relative to magnet strength. Subject 1 had a greater SV distribution width at 1.5T (0.309 vs 0.259) whereas subject 2 had a narrower distribution at 1.5T (0.200 vs 0.248), table 3.4.

The centre of distribution, corresponding to mean SV was lower for subject 1. There was no pattern in difference 1.5 vs 3T. Subject 1 centre of SV distribution was lower at 1.5T (0.078 vs 0.124) and for subject 2 centre of SV distribution was greater at 1.5T (0.211 vs 0.194), table 3.4.

Table 3.4. ROI SV distribution width comparison

	1.5T		3T	
Subject	**Centre of SV distribution**	**SV width**	**Centre of SV distribution**	**SV width**
1	0.078*	0.309*	0.124	0.259
2	0.211	0.200	0.194	0.248

SV values are average of 2 datasets apart from S1, 1.5T *values from the single dataset obtained reported.

3.5.2. Spatial comparison - voxel-wise

To complete a voxel-wise spatial comparison of SV the 256x256 matrix was down sampled by applying a 12x12 grid over the ROI sagittal slice, figure 3.18. The peripheral voxels of the ROI from within the 12x12 grid were discarded as incomplete data.

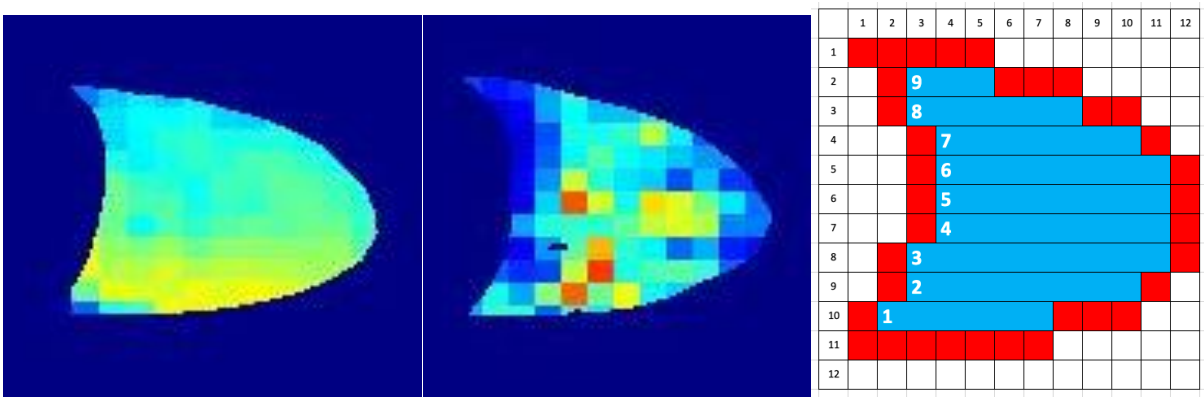

Figure 3.18. *Example down-sampled SVI maps to 144 large voxels for subject 2 at 1.5-T, left and 3-T, middle. Right, schematic of down sampled ROI processing from 12x12 grid. Lung ROI is supine, diaphragm concave aspect viewed on the left, and apex on the right of each example. Filled area represents ROI, outer red portion is removed from analysis due to partial filling, the remaining blue area is included in the voxel-wise comparison. The blue rows numbered 1 through 9 form isogravitational slices in order from posterior (dependent) to anterior (non-dependent) lung.*

Remaining large voxels from the 12x12 grid were plotted 1.5 versus 3T, figure 3.19, and correlation was assessed with Pearson's correlation and Deming regression reported in table 3.5. Deming regression applies a line of best fit that reduces the distance of datapoints in the direction perpendicular to the line, rather than in parallel with the axes. It is the appropriate regression method when assessing agreement in two variables that contain error, i.e. in the absence of a gold standard (Martin, 2000).

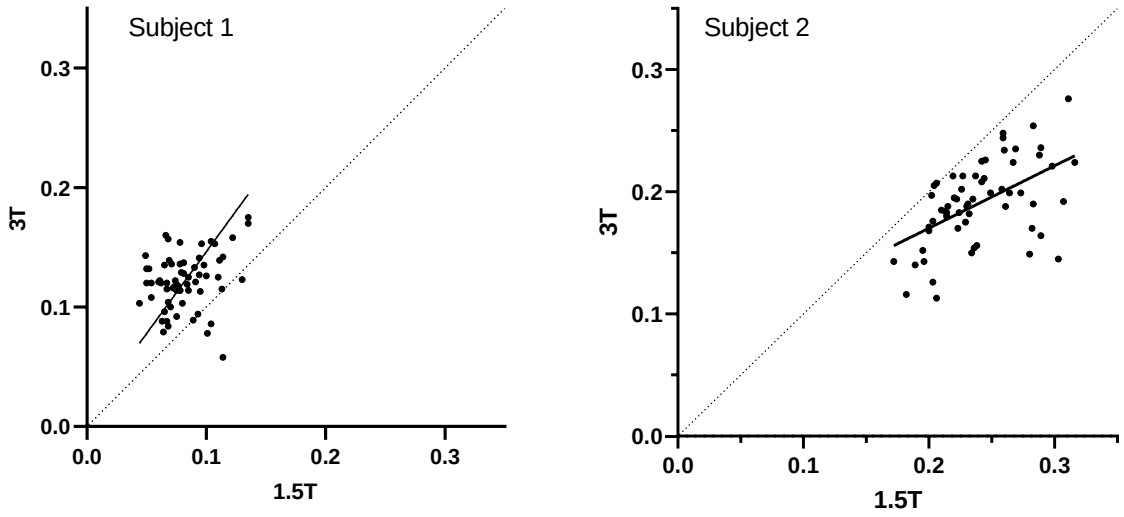

Figure 3.19. *Down sampled 12x12 corresponding large voxels for 1.5 (x axis) vs 3T (y axis). Deming regression slope and Pearson's r displayed in table 3.5. Deming regression slope for subject 1 is steeper than the line of unity demonstrating that overall large voxel SV at 3T>1.5T, Deming regression slope for subject 2 is <1 demonstrating that large voxel SV at 3T<1.5T.*

Table 3.5. Voxel-wise comparison Pearson's correlation r value and Deming regression for data displayed in figure 3.7

Subject	r	Deming regression slope
1	0.25	1.37
2	0.53	0.94

Large voxel value of SV measured at 1.5T showed poor correlation with the 3T measurement for subject 1, and moderate correlation for subject 2 (r= 0.25 and 0.53 respectively). The slope gradient was not consistent between subjects, overall subject 1 SV values were greater at 3T with slope >1. Overall subject 2 SV values were greater at 1.5T, with slope <1.

3.5.3. Gravitational effect on SV

To assess the gravitational effect on SV for both 1.5 and 3T datasets the supine 15mm sagittal ROI was divided into 9 isogravitational slices, as shown in figure 3.19. The slice average SV values were plotted against slice number, 1 representing the most posterior slice to 9 the most anterior slice, moving from dependent to non-dependent lung, figure 3.21.

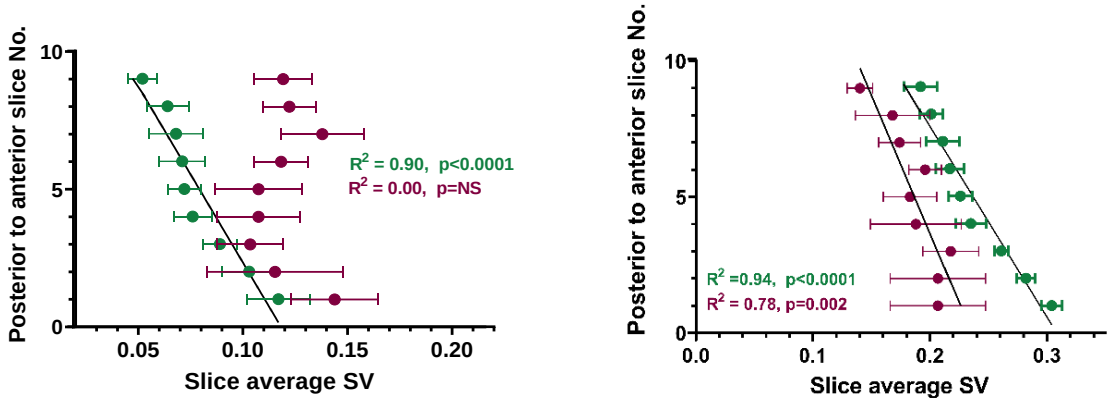

Figure 3.21. *Gravitational effect on SV for subject 1, left and subject 2, right. Isogravitational slice SV averages and SD (error bars) are plotted in ascending order for 3T (magenta) and 1.5T (green). Slice average SV values were greater at 3T for subject 1, but greater at 1.5T for subject 2. The significant negative correlation between posterior to anterior slice number and slice average SV seen at 1.5T for subject 1 and at 1.5 and 3T for subject 2 confirms greater SV in dependent lung, this relationship is not present for subject 1 at 3T. There was greater variability (wider error bars) in slice SV for both subject at 3T.*

The expected increase in SV in the posterior (dependent) portion is evident in all 1.5T datasets, as well as in the 3T dataset for subject 2, but not for subject 1 at 3-T, figure 3.21, the reasons for this are unclear. figure 3.21. reiterates the absence of a pattern of SV measurement bias according to magnet strength. For subject 1 the 3-T measurement is shifted right (higher SV) and for subject 2 the 3-T measurement is shifted left (lower SV) for all isogravitational slices. There is less certainty in slice average SV measured at 3T as evidenced by the wide error bars at 3T, whereas error bars at 1.5T are narrow, for both subjects.

3.6. Discussion

This chapter described the successful development of a 3-T SVI protocol. The purpose was to enable spatial assessments of ventilation in the subsequent study where available facilities included a 3-T MRI scanner, with the potential to expand the reach of SVI beyond 1.5-T scanners.

Optimum inversion time was determined through assessments of two subjects to optimise signal obtained in T_1-weighted imaging and to maximise contrast between lung tissue while breathing air vs while breathing 100% oxygen. Steps to increase applicability and usability of this technique were unsuccessful. Whilst shortening of the scan protocol may be an option in the future, with negligible changes in outcomes demonstrated with a reduction from 220 to 140 acquired images, further investigation is necessary to determine the impact on shorter runs for datasets of poorer quality or representing significant respiratory pathophysiology. An additional practical step of an in-session ECG measurement, to carry out cardiac gating, is required to avoid vascular signal that presents at 3-T but not 1.5-T.

The estimates of ventilation heterogeneity via width of SV distribution, the key outcome parameter of SVI, for the 2 subjects tested was lower than normal values reported in literature measured via oxygen enhanced MRI (Sa et al., 2014, Sa et al., 2010) and within the range of that measured via multiple breath nitrogen washout (Lewis et al., 1978). The mean specific ventilation for subject 1 at both 1.5 and 3-T was lower than normative values reported in literature. This finding is somewhat expected due to their height. Subject 1 is 185cm tall and correspondingly has big lungs with a large resting lung volume or FRC. This results in a relatively small tidal volume to FRC ratio, and an inherently low SV during relaxed breathing. Expected ranges in SV and ventilation heterogeneity measured via this technique according to factors that affect this parameter e.g., age and height (affecting thorax A-P dimension) are not published.

This study is limited by the small number of participants recruited and further 3-T SVI studies are warranted to assess and confirm the 3-T specific protocol parameters produced.

The healthy subjects who were scanned have relatively homogenous ventilation and therefore a small distribution of SV values, the difference in 3-T SVI measurement compared with 1.5-T over a greater variation in SV remains unknown. Therefore, caution should be exercised when interpreting the 3-T SVI results obtained in the presence of respiratory pathophysiology.

3.7. Conclusion

SVI results obtained using a 3T magnet are noisier compared with those obtained at 1.5T despite refining techniques such as cardiac gating and post processing signal filtering. This research suggests that while 1.5T and 3T values for specific ventilation are obtainable, there is variability between individuals with no clear pattern relative to magnet strength. Conclusions are limited by the small sample size and further data collection is needed to determine how 1.5T and 3T measurements of SV compare across a wider range of values. This work has demonstrated that SVI at 3T is feasible, and has produced a protocol for SV imaging for use in the subsequent chapter with the caution that magnet strength and protocol should not be interchanged for SVI assessments pre and post intervention or when completing serial measurements.

Chapter 4. Assessment of physiological response to short-acting bronchodilator in subjects with asthma: a comparison of small and large particle aerosols

4.1. Introduction

Previous studies have used sensitive tests of respiratory physiology such as inert-gas washout and oscillometry to assess the relationship between the peripheral airway function, airway hyperreactivity and symptom burden in asthma (Farah et al., 2012a, Downie et al., 2007, O'Sullivan et al., 2022) . However, as highlighted in chapter 1, such tests were not commonly used in studies investigating the efficacy of inhaled medication targeting airway regions. Rarer still are deposition studies that incorporate medical imaging. This final investigational chapter incorporates sensitive physiological tests capable of assessing proximal and peripheral airway regions, as well as MR ventilation scans, to measure the response to inhaled bronchodilators administered as large and small particle aerosols to target the conductive and peripheral airways respectively.

The MR scans, including the 3-T SVI protocol developed in Chapter 3, are designed to complement the physiological tests by providing spatial assessments of ventilation heterogeneity.

4.2. Background

Inhaled therapies are topical treatments, therefore, to be effective in reducing inflammation and/or producing bronchodilation, it is imperative that they are applied directly to the site they are intended to treat. The pathophysiology of asthmatic airways does not exist in a uniform manner along the airway tree, variable levels of abnormality and dysfunction have been evidenced histologically (Ward et al., 2002, James et al., 2023) and with functional assessments (Farah et al., 2012a, Geier et al., 2018). As detailed in Chapter 2, some subjects with Asthma demonstrate an increased level of dysfunction in the peripheral airways compared with their upstream counterparts, with raised acinar ventilation inhomogeneity (S_{acin}) and evidence of dynamic airway closure (based on X_{rs} and Delta X_{rs}). Chapter 2

provided evidence showing the association of peripheral airway dysfunction with increased symptom burden and utilisation of healthcare due to acute exacerbations of asthma, highlighting that the difficult to reach small airways are an important treatment target in some cases.

It is possible to target specific airways with inhaled therapies, and of the variables pertaining to administration of inhaled medication, particle size has the greatest influence over where a drug deposits (Darquenne, 2012). Whilst smaller particles reach the periphery of the lungs (Usmani et al., 2005), and larger particles deposit more proximally, the relationship is not linear (Lippmann et al., 1980, Heyder et al., 1986). Particles that are too small may fail to deposit due to a low sedimentation rate and are therefore exhaled on expiration (Zanen et al., 1994), and particles that are too large may not reach the intrathoracic airways, depositing in the upper airway walls and back of the throat due to impaction (Ferron et al., 1985, Heyder et al., 1986), figure 4.1.

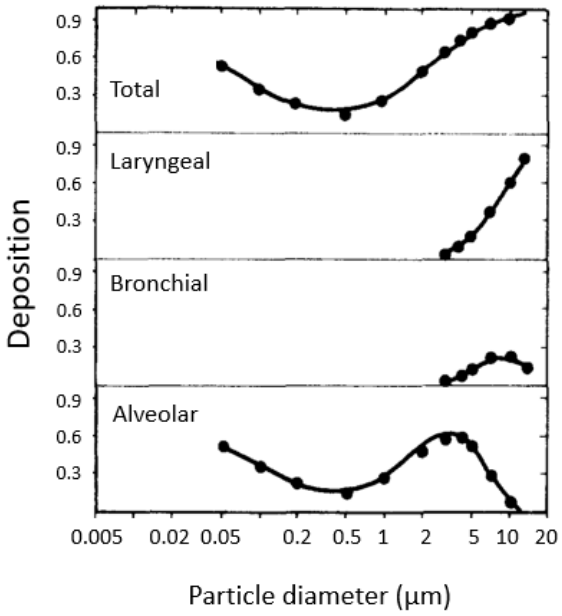

Figure 4.1. *Regional fractional deposition patterns of particles according to size in diameter (µm) during relaxed breathing. Laryngeal = extra-thoracic deposition. Adapted from (Heyder et al., 1986).*

Aerosol plumes generated by metered dose inhalers for inhalation contain a range of particle sizes (Usmani et al., 2003). The characteristics of an aerosol particle size distribution are described by the mass median aerodynamic diameter (MMAD) or the Dv50 (volume median), ± the geometric standard deviation (σ) in micrometres (μm). Drugs designed for inhalation are usually 'polydisperse' and contain a wide range of particle sizes within the aerosol, whereas 'monodisperse' aerosols display a much narrower distribution and contain particles similar in size.

When using appropriately sized "monodisperse" particle size preparations, large responses to inhaled drugs can be achieved with doses that are fractional compared to those usually prescribed clinically (see section 4.3.5 'selection of bronchodilator dose'). This implies that targeting specific airways with smaller doses or using larger targeted doses to achieve a greater treatment effect may be possible. This is particularly relevant for inhaled corticosteroids (ICS), where smaller doses could be used to avoid side effects while still achieving the desired therapeutic effect. Therefore, targeting specific airways with inhaled medication may lead to improved therapeutic outcomes or minimise side effects, and possibly both.

Previous existing literature investigating the efficacy of inhaled therapies of various particle sizes in the treatment of asthma relies on airway assessment using conventional measures such as the forced expired volume in the 1st second (FEV_1). The FEV_1 is a robust, reproducible parameter widely used in clinical practice to define airflow obstruction, and to assess response to bronchodilator. Nonetheless, it is insensitive to changes occurring in the small airways. A reliance on inadequate techniques and parameters such as the FEV_1, as well as poor differentiation of asthma subjects according to airway function, has led to conflicting results across the literature, a lack of consensus and no guidance for clinicians in the use of the various inhaled medication particle size options marketed by pharma.

The work described in this chapter addresses this problem by using techniques that are sensitive to small airway changes and specific lung regions, including MR ventilation techniques and using inhaled bronchodilator medication targeted to specific airways regions

by altering particle size. The methodology was designed to answer the question: do subjects with asthma who have peripheral airway dysfunction demonstrate a larger positive response to short acting beta-2 agonist delivered as small particles, compared to the large particle equivalent?

4.3. Methods

4.3.1. Recruitment

Between October 2020 and July 2021, a total of 10 subjects were recruited from the asthma clinic, Alfred Hospital, Melbourne. The study protocol was approved by Alfred Hospital ethics Committee (Project No: 55017) and subjects provided written informed consent. Inclusion and exclusion criteria are listed below:

Inclusion criteria

- Able to provide informed consent to participate in the study
- Physician diagnosis of asthma
- Evidence of suboptimal Asthma control defined as either: recent positive response to salbutamol on spirometry bronchodilator testing (within 6 weeks) or an Asthma Control Questionnaire (ACQ) score >1.5.
- 18–60 years of age
- Current Non-smokers with <10-year pack history and no smoking for 12 months

Exclusion criteria

- COPD, bronchiectasis, and any other lung disease apart from asthma based on clinical grounds and available HRCT scans
- Asthma exacerbation (increase in asthma symptoms >2days resulting in increased SABA +/- ICS or oral steroids) within the previous 6 weeks
- Attending emergency department or GP for worsening asthma symptoms in the last 12 weeks
- Current smoking (>1 cigarette/day>3months) within the last 12 months, or >10 pack

year history of smoking.

- Any cardiac disease
- Any reason prohibiting the patient from having an MRI scan, including possible metallic foreign bodies and claustrophobia
- Unable to provide written informed consent
- Allergy to salbutamol

The published guidelines current at the time of recruitment defined a positive response to bronchodilator as an increase in FEV_1 and/or FVC of ≥12% and 200mL compared to the baseline value (Pellegrino et al., 2005). If interested, subjects were provided with the patient information (appendix) and referred for the opportunity to discuss the research study, ask questions and arrange study visits if willing and able. Regional lung function was not determined prior to recruitment, but assessed during study visits. Recruitment was impacted by the COVID-19 pandemic (see Chapter 6).

4.3.2. Physiological testing

Subjects attended Monash Biomedical Imaging research facility for physiological testing on 2 occasions, one 'small particle' and one 'large particle' visit, thereby, all participants were assessed for their response to small and large particle preparations of 30µg salbutamol. Small and large aerosol particle sizes were median 2.6µm and 6.2µm respectively, particle size distributions are described in more detail in section 4.3.4 'targeting airway regions with bronchodilator'. Study visits were completed in a random order, and to minimise differences in baseline airway physiology due to intrinsic and external factors e.g. diurnal variation and allergens, study visits were completed at the same time of day and within 1 week (days between visits range 1-6). Subjects withheld bronchodilator therapy prior to study visits, as they would prior to routine lung function testing (Graham et al., 2019), detailed in table 4.1. All subjects were prescribed long acting bronchodilator therapy in combination with ICS; ICS/LABA, ICS/LAMA or ICS/LABA/LAMA, therefore ICS were also withheld prior to study visits.

Table 4.1. Inhaled medication withholding requirements for participants

Medication	**With-hold time**	**Examples**
Short-acting beta agonist (SABA)	4-6 hours	Salbutamol, albuterol
Short-acting muscarinic antagonists (SAMA)	12 hours	Ipratropium bromide
Long-acting beta$_2$-agonists (LABA)	24 hours	Formoterol, salmeterol
Ultra LABA	36 hours	Indacterol, Vilanterol, Olodaterol
Long-acting muscarinic antagonist (LAMA)	36-48 hours	Tiotropium, Umeclidinium, Aclidinium, Glycopyrronium
ICS (Inhaled corticosteroids)	12 hours	Beclomethasone, budesonide, Ciclesonide, fluticasone

The manoeuvres completed in the performance of certain tests of lung function incur physiological effects. For example, deep inspirations to TLC during spirometry cause bronchodilation with reduced diffusion-convection dependent ventilation heterogeneity and airway closure (Chapman et al., 2011). Conversely, in asthma deep inspirations may result in bronchoconstriction (Burns and Gibson, 2002). The order of tests was therefore configured to minimise the effect of each technique on subsequent test outcomes. Test order was; 1) oscillometry, 2) multi-breath nitrogen washout, and 3) spirometry. Figure 4.2. details the sequence of physiology and imaging tests throughout each study visit including baseline, administration of salbutamol and post-bronchodilator testing. All physiological tests were completed in the upright sitting position and imaging assessments were complete supine.

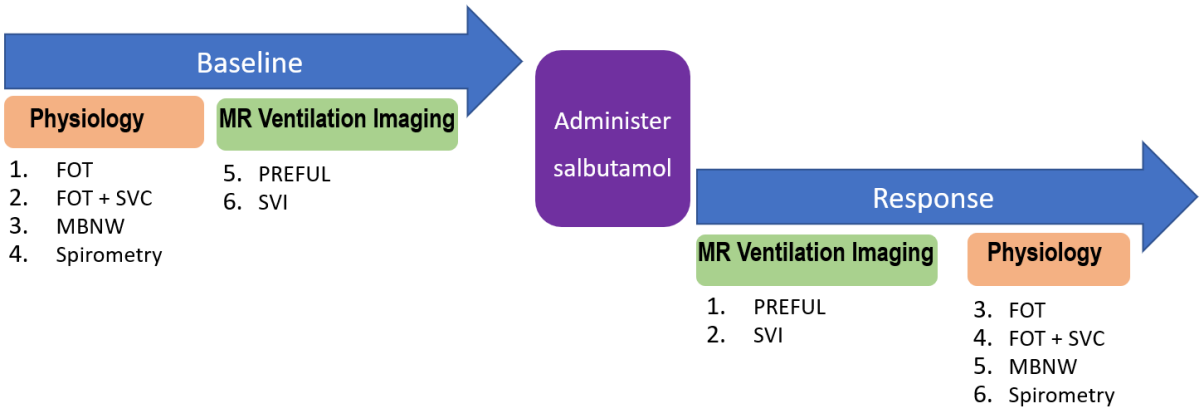

Figure 4.2. *Flow chart of study visit testing sequence, for both visit 1 and 2. This configuration serves to minimise effects of test manoeuvres on airway physiology that may alter parameters measured in subsequent tests. FOT, forced oscillation technique; SVC, slow vital capacity; MBNW, multi-breath nitrogen washout; PREFUL, phase resolved functional lung imaging; SVI, specific ventilation imaging.*

Forced oscillometry technique

The theoretical basis and practical steps involved in the assessment of the mechanical properties of the respiratory system using the forced oscillation technique, FOT, are described in chapter 2. The device used for data collection in this study was TremoFlo C-100 (Thorasys Medical Systems, Canada), which adheres to current European Respiratory Society technical standards for the performance of respiratory oscillometry (King et al. 2020). The TremoFlo was verified prior to each testing session with a 15cmH_2O.s.L^{-1} calibration load, and results were selected from acceptable 30-second FOT recordings (during relaxed tidal breathing, with no: coughs, swallows or other obstructions from the upper airway) to achieve 3 readings within a coefficient of variation ≤10% (King et al., 2020). The published reference values of Oostveen et al. (2013) were used to calculate predicted mean values, lower and upper limits of normal, and Z-scores based on subjects' sex, age, height and weight (Oostveen et al., 2013).

Oscillometry de-recruitment manoeuvre

The importance of achieving relaxed tidal breathing during FOT measurements is paramount, since respiratory system mechanics are greatly affected by lung volume or the extent of expansion or compression from relaxed volume FRC. However, in recent years

measurement of reactance, over lung volumes outside of the tidal breathing range has been shown to be a useful method to non-invasively assess lung de-recruitment (Nilsen et al., 2019, Kelly et al., 2012, Kelly et al., 2013). During expiration from total lung capacity intrapleural pressure increases, and when intrapleural pressure exceeds airway distending pressure, airway closure occurs. The lung regions that are distal to the closed airways are then inaccessible to the input signal from oscillometry, the result of this reduced effective lung volume is an increase in magnitude of the negative reactance value which indicates increased stiffness (Nilsen et al., 2019).

Subjects completed a minimum of 3 de-recruitment manoeuvres according to the published technique (Nilsen et al., 2019). Following tidal breathing, subjects completed a maximal relaxed expiration from total lung capacity to residual volume, during which reactance was measured at the usual sample rate of 0.1s. Total lung volume in litres was calculated using the inspiratory capacity (IC) from the de-recruitment manoeuvre from oscillometry and functional residual capacity (FRC) from multi-breath nitrogen washout:

$$TLC = IC + FRC$$

MATLAB was used to plot lung volume as percentage of total lung capacity (TLC) against reactance. Figure 4.3 displays an example of the resultant line graph; the gradient is relatively flat whilst reactance is stable at higher lung volumes. As lung volume reduces during expiration the point at which reactance begins to become more negative (exemplifying increased elastance due to lung decruitment) is identified as the $DR1_{volume}$, the point at which reactance reduces more rapidly is identified as the $DR2_{volume}$ (Nilsen et al., 2019). The term lung decruitment is the process through which regions of the lung become 'non-communicating', and are therefore not assessed by the FOT signal, occurring when airways excessively narrow or close (Nilsen et al., 2019). De-recruitment traces that contained error e.g. positive reactance measurements, sharp increases in reactance or deflections in trace that may represent leak or glottic closure were excluded. The mean of remaining DR1 and DR2 volume recordings were reported.

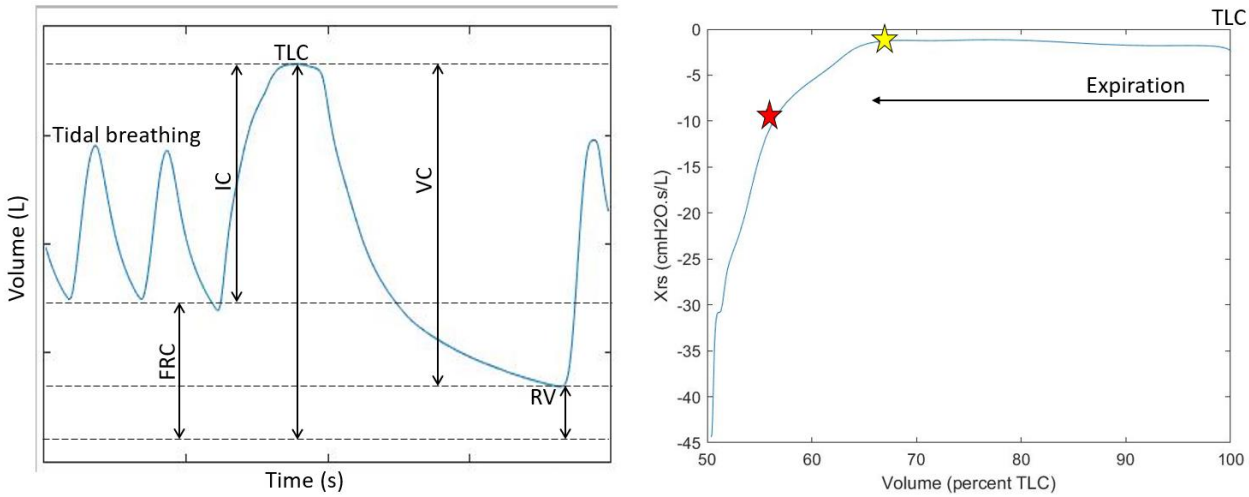

Figure 4.3. *Graphical display of the forced oscillation de-recruitment technique. Left – time volume trace displays a vital capacity (VC) manoeuvre completed by subject (blue trace), whilst attached to the loudspeaker which superimposes oscillations on gas flow which are used to measure reactance. Following tidal breathing, the subject inspires to total lung capacity (TLC) and expires completely at a comfortable pace to residual volume (RV). Inspiratory capacity (IC) from this manoeuvre and functional residual capacity (FRC) from multi-breath washout are used to calculate TLC volume, see text. Right – Reactance at 5Hz ($X_{rs\ 5Hz}$) plotted against percentage volume of TLC during expiration for a subject with asthma. The yellow star represents the start of reduction in X_{rs} ($DR1_{vol}$) and the red star is at the point of rapid reduction in X_{rs} ($DR2_{vol}$), reduction of X_{rs} on expiration is due to airway de-recruitment or closure (Nilsen et al., 2019).*

Multi breath nitrogen washout

The background information relating to multi-breath nitrogen washout, MBNW, is described in chapter 2. The device used for data collection in this study was the ndd EasyOne Pro LAB system (ndd Medical Technologies, Zurich, Switzerland). MBNW was performed according to current international guidelines (Robinson et al., 2013). Briefly, after achieving stable tidal breathing and FRC subjects inspired 100% oxygen in 1-litre breaths. The test continued until the nitrogen concentration of exhalate was <2.5% for ≥4 breaths, tests were performed in triplicate, and time between subsequent tests allowed for sufficient wash-in of ambient air so that lung gas concentration of nitrogen at baseline was ~79% (Robinson et al., 2013).

The derivation of markers of convection dependent (S_{cond}) and diffusive-convection dependent (S_{acin}) ventilation heterogeneity was completed using ndd EasyOne Pro LAB software according the published method (Stuart-Andrews et al., 2012). The reference values of Verbanck *et al.* (2012) were used to determine; upper limits of normal, percent of predicted mean, and Z-scores for S_{acin} and S_{cond} (Verbanck et al., 2012).

Spirometry

Spirometry measures flow and volume during a forced expiration from a position of TLC, as described in chapter 2. The same ndd EasyOne Pro LAB system used for MBNW was used to conduct spirometry. This device measures flow via two diagonally opposite ultrasonic flow transducers. The ultrasound transducers alternately send and receive ultrasonic waves, in the absence of any air flow, the transit time of the ultrasound waves is the same in both directions. As the subject breathes into the measuring device, the air flow generated inside the insert accelerates the waves in one direction and slows them down in the other, and the acceleration / deceleration is proportional to flow. The flow signal is integrated to give an indirect measure of volume.

Spirometry was performed according to current ATS/ERS guidelines (2019) (Graham et al., 2019) to obtain 3 technically acceptable results, and achieve recommended repeatability of the two largest FEV_1 and FVC results within 150mLs.

The absolute values were interpreted using each subject's; age, birth-sex, and height according to the Global Lung Initiative 2012 reference values (Quanjer et al., 2012) to provide a mean predicted normal value, and a grading of abnormality using Z-scores. Assessment of significant response to bronchodilator using spirometric parameters FEV_1 and FVC was according to the 2021 ATS/ERS interpretive strategy for lung function tests (Stanojevic et al., 2021).

Asthma Control Questionnaire

The Asthma Control Questionnaire (ACQ) (Juniper et al., 2006) was used with permission from Elizabeth Juniper. The ACQ assesses symptoms over 6 questions that score severity of impairment / burden from 0 (least) to 6 (worst), see appendix, and is scored overall as the average of all 6 questions. An ACQ score of >1.5 is considered as uncontrolled asthma (Jia et al., 2013).

4.3.3. MRI Ventilation Imaging

Specific ventilation imaging

The 3-T SVI protocol developed and described in chapter 3 was used for subject scanning. Safety screening was completed by a qualified radiographer. Subjects were prepared for SVI with application of an ECG for cardiac gating, and were fitted with the Hans Rudolph face mask (Kansas City, MO, USA, 8930 Series) (Geier et al., 2019) which was attached to oxygen tubing via an MR safe T-piece and connector for delivery of oxygen from the control room. During the scan, subjects voluntarily respiratory gated based on the noise generated by the scanner, by timing their breathing so that images were acquired at the end of an expiration (FRC), one breath per image (training provided prior). Successive images were obtained to a total of 220, with alternating blocks of inspired air FiO_2 0.21 and oxygen FiO_2 1.0. Switches occurred after every 20 images, apart from the initial oxygen block which consisted of 40 images. The analysis was completed as described in Chapter 3, figure 3.6.

Phase REsolved Functional Lung imaging

Phase REsolved Functional Lung imaging or PREFUL is an MR Imaging technique that uses Fourier decomposition to assess ventilation and perfusion (Klimeš et al., 2019) and which doesn't require the use of contrast agents. The analysis is based around the changes that occur in the lung MRI properties during normal breathing of air. This project included extensive physiological and imaging testing methods, the incorporation of work evaluating PREFUL was therefore a logical decision due to its minimal extra requirements for each subject. The practicalities of PREFUL make it a very attractive scan, other than the ability to

lie still inside the bore of the scanner there are no requirements for the subject. To complete the scan the subject lies still and breathes room air in a relaxed fashion. It is an entirely tracer free scan, so no contrast agents, special gases or associated equipment are required. It is quick to perform, taking only a few minutes to complete.

The PREFUL ventilation analysis outputs provide spatial and quantitative information. Mean regional ventilation and regional ventilation volume defect percent (VDP) quantify ventilation, whereas regional ventilation coefficient of variation and flow volume loop (FVL) correlation mean and coefficient of variation quantify ventilation heterogeneity. Spatial ventilation distribution is viewed in Regional Ventilation Maps and Flow-volume Loop correlation maps, of a single 15mm slice of coronal left and right lung ROI, see section *4.4.5. PREFUL results*.

Regional ventilation, RVent, calculation is based on the principle that the change in MR signal is proportional to change in volume, as was shown by Zapke and colleagues using a sponge soaked in silicon oil (Zapke et al., 2006). This principle is applied to lung tissue, whereby reduced MR signal during inspiration phase equates to lower density of lung parenchyma and therefore ventilation is assumed (Voskrebenzev et al., 2018).
RVent calculation:

$$RVent = \frac{V\ insp - V\ exp}{V\ mid} = \frac{S\ mid}{S\ insp} - \frac{S\ mid}{S\ exp} \qquad \text{(Klimeš et al., 2019)}$$

where V = volume, S = signal, units = a.u.

The ventilation defect percent, VDP, calculation, formulated to maintain a VDP<10% was defined as:

$$VDP\ = Median\ RVent\ -\ 1.75 * SD\ RVent \qquad \text{(Glandorf et al., 2020).}$$

Voxel specific flow volume loops, FVL, are generated. Along the x-axis RVent (a.u.) is used as a volume surrogate, and along the y-axis ΔRVent/Δtime (%/s) is used as a surrogate for flow. Healthy references voxels are identified as those that display normal flow to volume changes over the tidal breathing cycle, as well as a relatively high RVent (Moher Alsady et al., 2019). The average of the healthy FVLs is used as a reference, to which the FVL of voxels outside of the healthy regions are compared (Moher Alsady et al., 2019).

All scans were completed consecutively. Subjects were prepared for scanning as described in the next section (SVI), with the torso RF coil in position over the thorax ensuring coverage of lung apices. A fast-spoiled gradient echo sequence (FLASH) sequence was used to acquire 250 images of a 15mm iso central coronal slice (Voskrebenzev et al., 2018). Each subject generated 4 PREFUL datasets; baseline and post bronchodilator for two study visits. The 40 x250 DICOM image datasets were transferred to the developers at the Institute for Diagnostic and Interventional Radiology, Hannover, for analysis.

The analysis steps as outlined in the technical reference (Voskrebenzev et al., 2018) are:

1. Image registration: registration of all images to a mid-lung volume, figure 4.4, (selected as mid-way during a tidal breath in or out) to enable comparison of corresponding lung regions across different phases of breathing
2. Selection of ROI: coronal slice of left and right lung separated from chest wall, figure 4.4.
3. Filtration: low pass filter separates out signal changes due to in-flow blood leaving the respiratory cycle for analysis
4. Phase calculation: Fourier Transform is used to determine the phase of the respiratory cycle for each voxel and signal at the frequency of breathing targeted (Fourier decomposition)
5. Ventilation calculation: the relative changes in signal intensity are used to calculate the ventilation for each voxel and displayed in a map, figure 4.5.

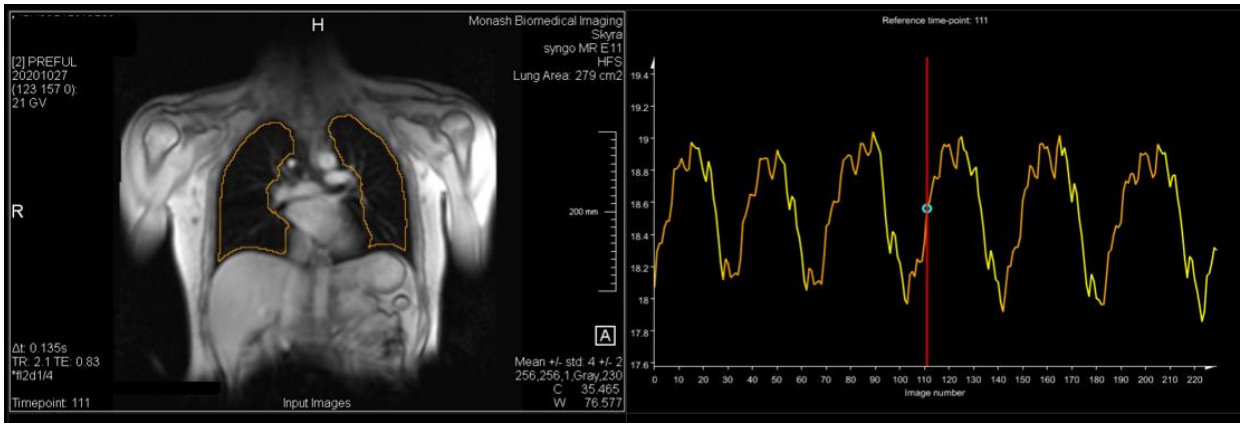

Figure 4.4. *Left) coronal slice of lungs visualized within chest wall, region of interest outlined in yellow, Right) tidal breathing trace across 225 consecutive images acquired (250 – 25 initial images to ensure steady state). Screen shot taken from PREFUL image analysis software: MR Lung Prototype v2.1.0 (Siemens Healthineers).*

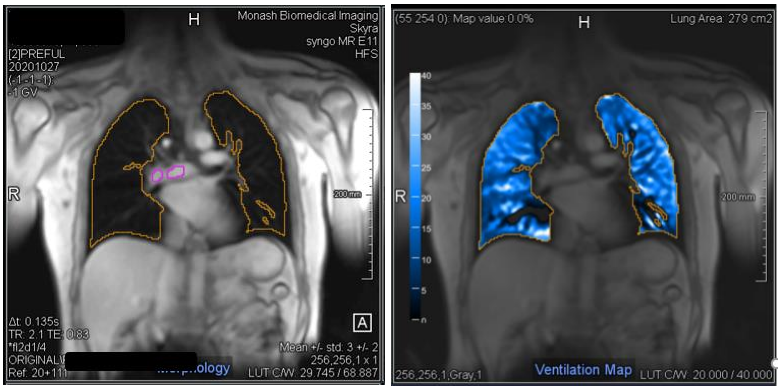

Figure 4.5. *Left) selection of region of interest depicted by yellow outline, Right) regional ventilation map. Screen shot taken from PREFUL image analysis software: MR Lung Prototype v2.1.0 (Siemens Healthineers).*

4.3.4. Targeting airway regions with bronchodilator

The single difference between study visits 1 and 2 for each participant was the aerosol particle size distribution of the bronchodilator administered, so that either the central or peripheral airways were targeted on each occasion. Monodisperse particle size distributions describe aerosol plumes of relatively uniform particle size, and use of such would be the optimum way to target inhaled drugs to airway regions according to particle size when controlling volume inhaled and flow.

Phipps *et al.* used gamma-scintigraphy of radiolabelled particles to demonstrate that particle size distributions of 2.6µm and 5.5µm MMAD (generated by nebulisers and inhaled during tidal breathing) deposited preferentially in the peripheral and central regions respectively (Phipps et al., 1989). Extensive research to identify nebulisers to produce aerosol particle size distributions similar to that of the Phipps study was undertaken. A leading expert in aerosol science Professor Jim Fink (Chief Scientific Officer at Aerogen Pharma Corp, California, USA) provided two nebulisers that met requirements. The two vibrating mesh nebulisers selected offered distinct particle size distribution profiles and are described below.

Large particle aerosol SABA

The large particle bronchodilator plume was administered via the Aerogen Solo vibrating mesh nebuliser. Vibrating mesh nebulisers produce aerosols as the solution passes through the mesh. They are superior to 'jet' style nebulisers due to the production of more consistent narrower particle size distributions and are effective in the aerosolisation of the entire drug solution. The specific Aerogen Solo device used had a Dv50 of 6.2µm and geometric standard deviation σ=0.09µm confirmed by laser diffraction (particle sizing experiments conducted by Aerogen Ltd. Galway), the particle size distribution is displayed in figure 4.6.

Small particle aerosol SABA

Traditional vibrating mesh nebulisers do not offer fine particle size distributions as dose delivery would be limited and impractically slow. However, the 'Aerogen PDAP' or Photo Defined Aperture Plate is engineered to contain around 20,000 apertures that produce fine particles <3µm at a pace similar to other vibrating mesh nebulisers (DiBlasi et al., 2021b). The specific Aerogen PDAP device used had a Dv50 of 2.6µm, σ=0.13 µm confirmed by laser diffraction (Aerogen Ltd. Galway), the particle size distribution is displayed in figure 4.6.

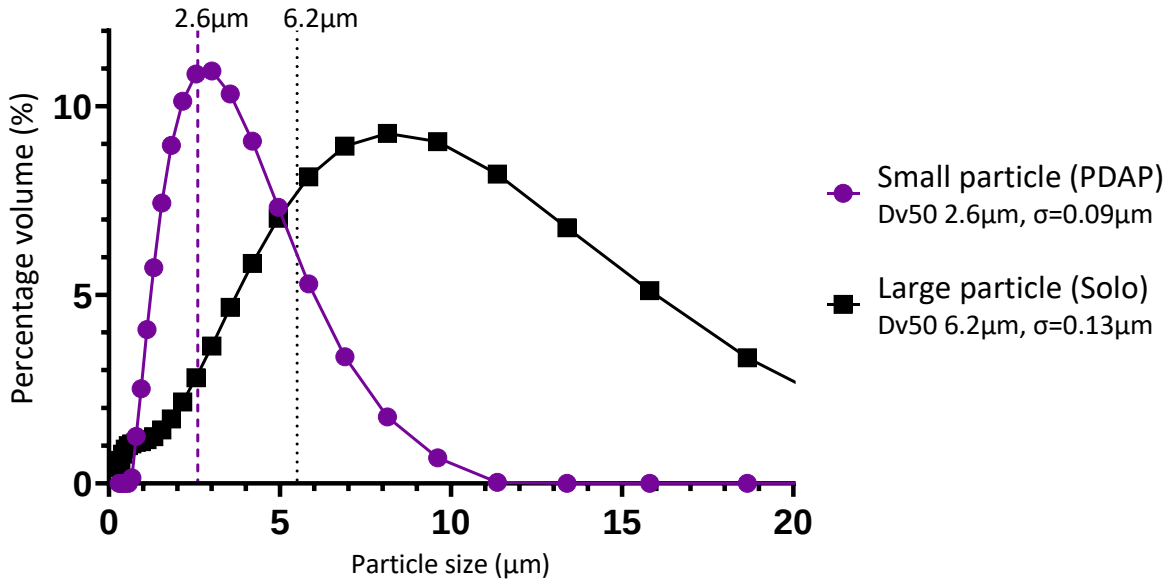

Figure 4.6. *Particle size distributions for the small particle aerosol (PDAP in purple circles) and the large particle aerosol (Solo in black squares). The vertical dotted line at 2.6µm represents the Dv50 of the PDAP aerosol which is the target median particle size for peripheral airway deposition. The volume of particles produced at size 2.6µm by the PDAP is >3x the volume produced by the Solo. Dv50 = median particle size by volume, σ = geometric standard deviation. The data displayed graphically was provided in tabular form from* Aerogen Ltd. Galway.

The narrower an aerosol particle size distribution the more precisely the aerosol can target a specific region. As shown in figure 4.6 the PDAP and Aerogen devices produce overlapping particle size distributions, yet they are distinct. Further, both small and large particle aerosols meet the criteria to be categorised as monodisperse with geometric standard deviation (GSD) <1.2µm (Zanen et al., 1994, Usmani et al., 2005). The particle size distributions of the nebulisers selected for this study offer narrower distributions compared to that reported in the other studies investigating the effect of inhaled medications of different particle sizes, described as MMAD/Dv50±GSD: PDAP=2.6±0.09 and Solo=6.2±0.13µm for small and large aerosols, compared with 4.9±2.5µm (Sa et al., 2015), 2.6±1.4µm and 5.5±1.7µm (Phipps et al., 1989).

The Solo produces a greater volume of larger sized particles, whereas the PDAP produces a greater volume of small particles. Particles of size 5.5µm are known to deposit in the central airways if inhaled during tidal breathing (Phipps et al., 1989), of which the Solo

produces a larger quantity relative the PDAP. Particles of size 2.6μm are known to deposit in the lung periphery with tidal breathing inhalation (Phipps et al., 1989), the PDAP produces a greater volume of particles size 2.6μm than the Solo, further, the difference in percentage volume produced at 2.6μm is more pronounced than the difference at 5.5μm between the two nebulisers.

In this study the site of aerosol deposition was not verified with radionuclide aerosol labelling and imaging. However, given the existing evidence that demonstrates preferential deposition in the central bronchial and peripheral regions with large and small particle aerosols respectively (Usmani et al., 2005, Phipps et al., 1989), it was assumed that use of the large particle aerosol producing nebuliser (Solo) would result in greater deposition of SABA aerosol in the central airways compared with the small particle aerosol producing nebuliser (PDAP). Conversely, it was expected that the PDAP would lead to significantly greater deposition of the SABA aerosol in the peripheral airways compared to the Solo.

4.3.5. Selection of bronchodilator and dose

The overlap in particle size distributions presented a challenge: the primarily 'large' particle plume contains some small particles, and vice versa. Therefore, in order to differentiate regional physiological responses to distinct yet overlapping particle size distributions, care must be taken to avoid the plateau of the dose response curve to prevent saturation of β-adrenoreceptors in the region not being targeted.

Short acting beta-2 agonists, SABAs, are an accepted form of drug for use in the assessment of in session bronchodilator response. Salbutamol or albuterol and terbutaline have superseded previous preparations of short-acting beta-2 agonists due to improved selectivity and greater potency (Anderson, 2018). Previously the recommended doses for inhalation were 200μg salbutamol and 500μg terbutaline (Anderson, 2018), however the current ATS/ERS international guidance for performing bronchodilator studies does not stipulate administration method, drug or dose (Stanojevic et al., 2021). Bronchodilator assessments vary greatly in clinical practice, for example salbutamol administered may be 200μg from a metered dose inhaler, or 2.5mg via a nebuliser.

Dose-response to salbutamol in asthma

The dose at which spirometric response to salbutamol plateaus varies in the literature. Some studies demonstrate a plateau prior to 1mg (Barnes and Pride, 1983, Douglas et al., 1986), whereas others have found continued improvement in FEV_1 with doses increasing from 200µg to 4mg (Lipworth et al., 1988). Pertinently, the steepest portion of the dose response curve has consistently been shown to occur below 100µg (Barnes and Pride, 1983, Fishwick et al., 2001, Lipworth et al., 1988) with a measurable response after 10µg for some subjects (Barnes and Pride, 1983). In one cohort the plateau in response measured by FEV_1 was achieved by 50µg with no further improvement observed at 100µg (Fishwick et al., 2001). Taken together the data in the literature suggests that a dose within the region of 10-50µg would be appropriate. These findings as well as consultation with experts in the field (Prof. Greg King & Prof. Jim Fink) resulted in selection of 30µg dose of salbutamol for nebulisation on both study visits.

Following baseline testing the 30µg dose of salbutamol contained in 1mL solution was administered, via the Aerogen Solo (large particle) or Aerogen PDAP (small particle). Each nebuliser was attached to an Aeroneb Solo Adapter (provided by Aerogen Ltd.) which acted as a holding chamber for the aerosol for inspiration, and also served to isolate the subject from the nebuliser, figure 4.7. Subjects were instructed to breath in relaxed fashion, whilst sitting upright to replicate the methodology of Phipps et al. (Phipps et al., 1989) to achieve distinct regional depositions of SABA aerosol for small particle versus large. Subjects continued to breathe tidally connected to the nebuliser adapter until the aerosolisation and inspiration of the 1mL solution was complete for full dose delivery.

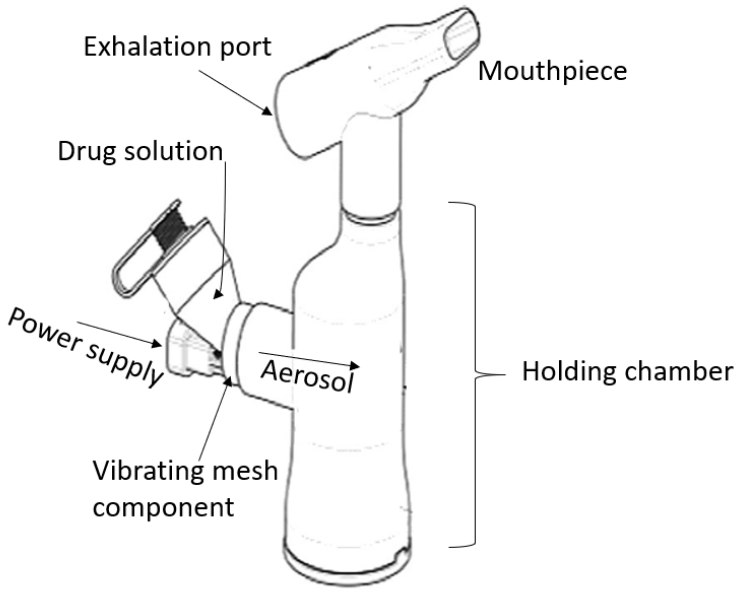

Figure 4.7. *Aerogen Solo adapter with vibrating nebuliser attached, annotated to demonstrate direction of drug solution, via vibrating mesh into holding chamber and to subject via mouthpiece. Adapted from (Ari et al., 2014).*

4.3.6. Statistics

Data handling was completed in excel, and statistical testing was completed in statistical software package GraphPad Prism (V.8.3.1). The Shapiro-Wilk test was used to assess data for normal / Gaussian distribution to determine distribution of data. Group data are expressed as mean ± SD for parametric data, and median (IQR) for non-parametric data. Between visit group comparisons for both baseline measurements and response to bronchodilator, and within visit subject response to bronchodilator were assessed with a paired t-test for parametric data, and Wilcoxon signed rank test for non-parametric data. Significance was defined as $p<0.05$.

Comparison of sub groups was completed using an unpaired t-test for parametric data and Mann-Whitney test for non-parametric data. Statistical significance was defined as $p<0.05$.

4.4. Results

4.4.1. Baseline characteristics

A total of 10 subjects were recruited and completed the 2 study visits. Participants were randomised to order of study visits. Half of the participants (n=5) completed the small particle visit first, and the other half vice versa. Participants were of age range 20 to 60 years old, 40% (n=4) were female, demographics are listed in table 4.2.

Table 4.2. Subject demographics	Median (IQR)
Subjects, n (F/M)	10 (4 / 6)
Age, years	44 (24)
Height, cm	164.5 (9.9)
Weight, kg	76.2 (17.0)
BMI, kg/m^2	27.6 (6.2)
GINA treatment step score	4 (1)
ACQ5	2.3 (2.4)
ACQ6	2 (2.1)

Data are displayed as median (IQR) unless otherwise stated.
BMI, body mass index; GINA, Global Initiative for Asthma; ACQ, asthma control questionnaire.

4.4.2. Physiological response to bronchodilator

The group average values for key physiological parameters at baseline and post salbutamol, for both the small particle and large particle visits are listed in table 4.3.

Response to large particle bronchodilator

There was a significant increase in FEV_1 following large particle bronchodilator, and the FEV_1/FVC ratio Z-score became less negative returning close to the lower limit of normal, table 4.3. The static lung volume functional residual capacity measured via multi-breath

nitrogen washout improved (reduced) post-bronchodilator. From oscillometry, respiratory system reactance measured during inspiration ($X_{rs\ 5Hz\ insp}$) became less negative indicating reduced elastance.

These results demonstrate a reduction in flow limitation, a reduction in gas trapping and a reduction in lung stiffness post large particle aerosol salbutamol. The difference in reactance was seen only in the inspiratory parameter of reactance, i.e. not in overall $X_{rs\ 5Hz}$ or $X_{rs\ 5Hz\ exp}$. As there is no dynamic airway collapse during inspiration (Dellacà et al., 2004), changes in inspiratory reactance reflect changes in lung compliance due to mechanisms relating to lung elastance, as opposed to lung de-recruitment that occurs secondary to airway closure (Dellaca et al., 2009). This suggests that the response is a reduction in lung stiffness, and could be due to relaxation of proximal bronchial smooth muscle (Berry and Fairshter, 1985).

Table 4.3. Physiological parameters; baseline and post salbutamol results for large (6.2µm) and small (2.6µm) particle aerosol visits.

		Large particle visit		Small particle visit		Response Large vs Small particle p value
		Baseline	Salbutamol	Baseline	Salbutamol	
Spirometry						
FEV_1	L	2.35 ± 0.78	2.49 ± 0.70†	2.21 ± 0.81	2.48 ± 0.71†	0.06
	% predicted	70.6 ± 20.0	75.1 ± 17.6	64.2 ± 28.3	70.8 ± 20.6†	0.06*
	Z-score	-2.14 ± 1.46	-1.82 ± 1.30	-2.43 ± 1.51	-1.82 ± 1.18†	0.05
FVC	L	3.52 ± 0.72	3.61 ± 0.67	3.38 ± 0.80	3.59 ± 0.61	0.2
	% predicted	87.0 ± 13.2	89.4 ± 11.6	81.0 ± 15.1	90.6 ± 9.2	0.1*
	Z-score	-1.00 ± 1.04	-0.82 ± 0.93	-1.28 ± 1.14	-0.83 ± 0.96	0.1
FEV_1/FVC	%	65.90 ± 14.10	68.65 ± 13.15†	64.26 ± 13.70	68.71 ± 12.68†	0.3
	Z-score	-2.06 ± 1.36	-1.76 ± 1.38	-2.29 ± 1.33	-1.76 ± 1.28†	0.2
FEF_{25-75}	$L.s^{-1}$	1.67 ± 1.10	1.90 ± 1.19	1.52 ± 0.96	1.85 ± 1.11†	0.4
PEF	$L.s^{-1}$	7.05 ± 2.28	7.28 ± 2.12	6.57 ± 2.37	7.43 ± 2.08†	0.1
MBNW						
FRC	L	3.42 ± 1.01	3.02 ± 0.91†	3.28 ± 0.91	3.01 ± 0.81†	0.2
S_{acin}	$L^{-}1$	0.196 ± 0.058	0.181 ± 0.062	0.205 ± 0.059	0.193 ± 0.067	0.4
	Z-score	3.46 ± 1.73	3.20 ± 2.01	4.01 ± 1.91	3.37 ± 2.03	0.4
S_{cond}	L^{-1}	0.025 ± 0.018	0.021 ± 0.015	0.023 ± 0.016	0.024 ± 0.020	0.8
	Z-score	-0.88 ± 1.53	-1.02 ± 1.19	-0.87 ± 1.23	-0.92 ± 1.57	0.7

FOT												
$R_{rs\ 5Hz}$	$cmH_2O.s.L^{-1}$	4.55		(2.73)	4.02		(1.41)	4.24		(2.09)	3.86 ± 1.83	0.3*
	% predicted	163.4		(79.7)	156.9		(57.5)	160.9		(75.4)	134.7 ± 38.1	0.5*
	Z-score	1.57		(1.69)	1.37		(0.80)	1.50		(1.43)	0.85 ± 1.03	0.3*
$Rrs_{\ 5Hz-19Hz}$	$cmH_2O.s.L^{-1}$	0.87		(2.03)	0.87 ± 0.82			1.40 ± 1.34			0.28 (0.77)†	0.53
$X_{rs\ 5Hz}$	$cmH_2O.s.L^{-1}$	-3.35 ± 2.47			-1.40		(1.21)	-3.97 ± 2.62			-1.44 1.23‡	0.5
	% predicted	230.1 ± 128.4			114.5		(72.2)	262.2 ± 142.7			131.6 ± 68.5‡	0.5
	Z-score	-1.42 ± 1.84			-0.16		(0.72)	-1.91 ± 1.60			-0.31 ± 0.61†	0.5
$X_{rs\ 5Hz\ insp}$	$cmH_2O.s.L^{-1}$	-2.19		(1.72)	-1.49		(1.23)†	-2.18		(3.22)	-1.90 ± 0.69‡	0.9
$X_{rs\ 5Hz\ exp}$	$cmH_2O.s.L^{-1}$	-1.77		(4.32)	-1.40		(1.12)	-2.09		(2.09)	-1.21 (1.33)‡	0.9
Ax	$cmH_2O.L^{-1}$	16.5		(50.0)	10.1		(14.8)	22.1		(60.2)	5.3 (15.0)‡	0.9
DR1	% of lung volume	70.9 ± 13.3			66.0 ± 9.0			72.8 ± 11.4			66.6 ± 9.8‡	0.4
DR2	% of lung volume	54.3 ± 11.7			51.4 ± 9.4			54.9 ± 7.7			52.5 ± 9.7‡	0.6

Abbreviation definitions: FEV_1, forced expired volume in 1s; FVC, forced vital capacity; FEF_{25-75}, forced expiratory flow during middle 50% volume of VC; PEF, peak expiratory flow, MBNW, multi-breath nitrogen washout; FRC, functional residual capacity; S_{acin} & S_{cond} ventilation heterogeneity in the acinar and conductive regions respectively; FOT, forced oscillation technique; R_{rs} and X_{rs}, resistance and reactance of the respiratory system measured at 5Hz respectively; $R_{rs\ 5Hz-19Hz}$, peripheral resistance; $X_{rs\ 5Hz\ insp}$ and $_{exp}$ reactance measured during inspiration and expiration respectively; DR1 and 2, closing volumes 1 and 2 (see text). Parametric data displayed mean ± SD, non-parametric data displayed as median (IQR). Parameters that are significantly different post bronchodilator vs baseline are shaded, symbols indicate level of significance: † = p value <0.05, ‡ = p value <0.01.
Right hand column gives analysis of difference in response to large particle aerosol bronchodilator vs response to small particle aerosol bronchodilator, p values from paired t-test, or Wilcoxon signed rank test* for non-parametric data.

Response to small particle bronchodilator

A greater number of physiological parameters were significantly different from baseline when measured post small particle bronchodilator, compared with the large particle visit (12 small vs 2 large).

Spirometry provided evidence of bronchodilation; on average there was a 12% increase in FEV_1 post bronchodilator table 4.3. Peak expiratory flow increased, the expiratory flow at mid volume (25-75% of FVC) increased, and impairment in the FEV_1/FVC Z-score a key marker of airflow obstruction reduced. The spirometric changes are all consistent with a reduction in expiratory flow limitation.

From multi-breath nitrogen washout there was an improvement (reduction) in functional residual capacity consistent with a reduction in gas trapping.

From oscillometry, there was a significant reduction in resistance measured at 5Hz minus that measured at 19Hz. Measures of respiratory impedance are dependent on the frequency of the input signal, whereby the low frequency component of oscillatory signal penetrates deeper into the respiratory system than high frequency oscillations. Therefore, the $R_{rs\ 5\text{-}19Hz}$ is taken as a marker of peripheral respiratory system resistance as resistance derived from higher frequency signal 19Hz, that does not penetrate the periphery, is removed, table 4.3. Total respiratory system reactance $X_{rs\ 5Hz}$ became less negative, and reactance area Ax reduced indicating a reduction in respiratory system stiffness.

Both the inspiratory and expiratory components of reactance improved, becoming less negative post-bronchodilator, which suggests a reduction in lung elastance attributable to multiple mechanisms; reduced lung stiffness due to relaxation of smooth muscle (Kelly et al., 2012) and due to a reduction in airway closure in the tidal breathing range (Dellacà et al., 2004).

There was an improvement in parameters of lung de-recruitment that was not seen with large particle aerosol salbutamol. The closing volumes DR1 and DR2 denoted as percentage

of TLC both reduced, table 4.3. This demonstrates a reduction in propensity for airway closure at higher lung volumes when assessed over the vital capacity range.

Patterns of those who responded according to spirometry guidelines

According to the ATS/ERS 2021 interpretive strategy, a positive response to bronchodilator measured with spirometry is defined as a volume increase in FEV_1 or FVC of ≥10% the mean predicted value (Stanojevic et al., 2021). In this study, only 50% of subjects met the criteria for a positive response to bronchodilator. To be classified as a responder, subjects were required to meet ATS/ERS criteria on at least one visit. For the following analyses the cohort were divided into 2 groups: responders and non-responders. Of those that responded, all 5 responded to small particle salbutamol, and only 1 responded to large particle salbutamol. The possible reasons for the lack of a response in the remaining cohort for either particle size are discussed later.

There was no difference in age, height, weight, ACQ score or GINA treatment step between the responder and non-responder groups (t-test or Mann-Whitney $p>0.05$). Compared with the non-responder group, the responder group had worse baseline spirometry; worse baseline respiratory system resistance; peripheral resistance; worse (greater) Ax_{5Hz} and inspiratory respiratory system reactance, Table 4.4.

Table 4.4. Baseline spirometry and oscillometry parameters of difference between responder and non-responder groups.

	Large particle visit							Small particle visit						
	Responders			Non-responders				Responders			Non-responders			
Spirometry	**Median**		**IQR**	**Median**		**IQR**	**p value**	**Median**		**IQR**	**Median**		**IQR**	**p value**
FEV_1 (Z-score)	-3.43	±	0.16	-0.89	±	1.85	0.01	-3.92	±	0.25	-1.37	±	2.20	0.02*
FVC (Z-score)	-1.77	±	0.14	-0.32	±	0.33	0.01	-2.04	±	0.31	-0.91	±	0.71	0.01
FEV_1/FVC	63.8	±	21.7	76.6	±	17.6	0.2	59.4	±	12.7	73.9	±	16.8	0.10
FOT														
Rrs_{5Hz} (Z-score)	2.39	±	2.53	0.51	±	0.58	0.04	2.05	±	1.70	0.48	±	1.15	0.02
$Rrs_{5\text{-}19Hz}$ ($cmH_2O.L.s^{-1}$)	2.19	±	3.23	0.22	±	0.14	0.056*	1.99	±	0.78	0.18	±	0.02	0.02*
Ax_{5Hz} ($cmH_2O.L.s^{-1}.Hz$)	57.4	±	85.8	4.63	±	3.69	0.03*	74.6	±	46.3	4.48	±	3.24	0.02*
$X_{rs\ 5Hz\ insp}$ ($cmH_2O.L.s^{-1}$)	-3.51	±	3.52	-1.70	±	0.25	0.045	-5.00	±	0.66	-1.60	±	0.43	0.01

Data as Median ± IQR. Abbreviation definitions: FEV_1, forced expired volume in 1s; FVC, forced vital capacity; FOT, forced oscillation technique; Rrs and Xrs insp, resistance and inspiratory reactance of the respiratory system measured at 5Hz respectively; Ax = area of reactance. *Mann-Whitney test for non-parametric data.

However, for the 5 ‘responder’ subjects, baseline physiology on the small particle visit was not different to baseline physiology on the large particle visit for any measure of pulmonary function (paired t-test p value>0.05).

The criteria for a significant response to bronchodilator assessed with oscillometry were published in the 2020 ERS standard: −40% in R_{rs5}, +50% in X_{rs5}, −80% in Ax (King et al., 2020). There are no published criteria for multi-breath nitrogen washout. For each parameter with an official definition of a significant response the number of responders on the small particle visit was equal to or greater than the number that responded on the large particle visit, table 4.5.

Table 4.5. Number of significant responders as defined by published criteria for each study visit

Criteria for significant response	Response SMALL particle (n out of total 10)	Response LARGE particle (n out of total 10)
Spirometry (FEV_1 and/or FVC) ATS/ERS 2021	5	1
Respiratory system resistance ERS 2020	1	1
Respiratory system reactance ERS 2020	4	3
Area of reactance ERS 2020	8	7

The number of subjects, out of total 10, who met the definition for a clinically significant response for each parameter with a published criterion are listed, for the small and large particle visits.

As well as FEV_1, the responders also had a greater response to the small particle SABA for; S_{acin} and $DR2_{volume}$, table 4.6. This means that for these subjects the small particle aerosol produced a greater reversal of airflow limitation, reduced peripheral ventilation heterogeneity to a greater degree and delayed significant airway closure to later in the expiratory manoeuvre, reducing the propensity of the small airways to close, compared to when they were treated with large particle SABA. At baseline the responder group all had an S_{acin} above the upper limit of normal (>0.120 L^{-1}) (Verbanck et al., 2012). Taken together, these results show that the responder group exhibit peripheral airway dysfunction as increased inhomogeneity of ventilation in the acinar region, and demonstrate a greater improvement in airway physiology when treated with small particle bronchodilator that targets the periphery, compared to large.

For those that did not meet published criteria for a significant response to bronchodilator on either visit there was no difference in response to small or large particle SABA, table 4.6.

Table 4.6. Responder vs Non-responder group physiological response to SABA

	Parameter	Response Small	Response Large	p value
Responders	Significant response ATS/ERS 2021 (n)	5	1	-
	ΔFEV_1 (mL)	510 ± 170	226 ± 151	0.01
	ΔS_{acin} (L^{-1})	-0.041 ± 0.007	0.013 ± 0.027	0.02
	ΔDR2 vol (% of total lung volume)	-7.6 ± 3.2	1.0 ± 5.3	0.01
Non-responders	Significant response ATS/ERS 2021 (n)	0	0	-
	ΔFEV_1 (mL)	42 ± 113	52 ± 104	0.88
	ΔSacin (L^{-1})	0.004 ± 0.034	-0.011 ± 0.019	0.57
	ΔDR2 vol (% of total lung volume)	-0.7 ± 5.9	-6.5 ± 9.0	0.36

The parameters that showed a significant difference (shaded) in response to small vs response to large particle bronchodilator for responder subjects are displayed (top) with non-responder group (bottom) for comparison. Expressed as mean ± SD. p value from paired t-test.

4.4.3. Graphical display of non-responders vs responders

The following figures demonstrate the response for all participants in respective 'non-responder' and 'responder' groups to both small and large particle short acting bronchodilator.

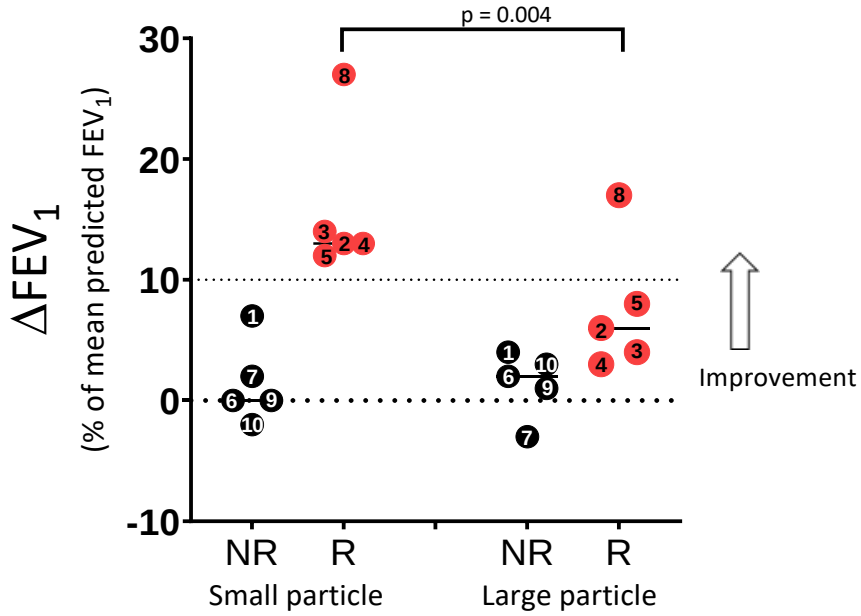

Figure 4.8. *Response to 30µg salbutamol in terms of FEV_1 as % of mean predicted value for small (left) and large (right) particle visits. NR = non-responder group displayed in black circles, R = responder group displayed as red circles. Individual subjects are numbered. The line at 10% marks the criteria for significance according to 2021 criteria, a priori all 'responder' subject sit above this line. The zero line equates to no response, the direction of improvement denoted by arrow. p value from paired t-test.*

Of the 5 'responders' only 1 subject also met the spirometric criteria for a significant response on the large particle visit, figure 4.8. All of the responder group demonstrated an improvement (reduction) in acinar ventilation heterogeneity in response to small particle bronchodilator, however 3 of those failed to respond on large particle visit, figure 4.9.

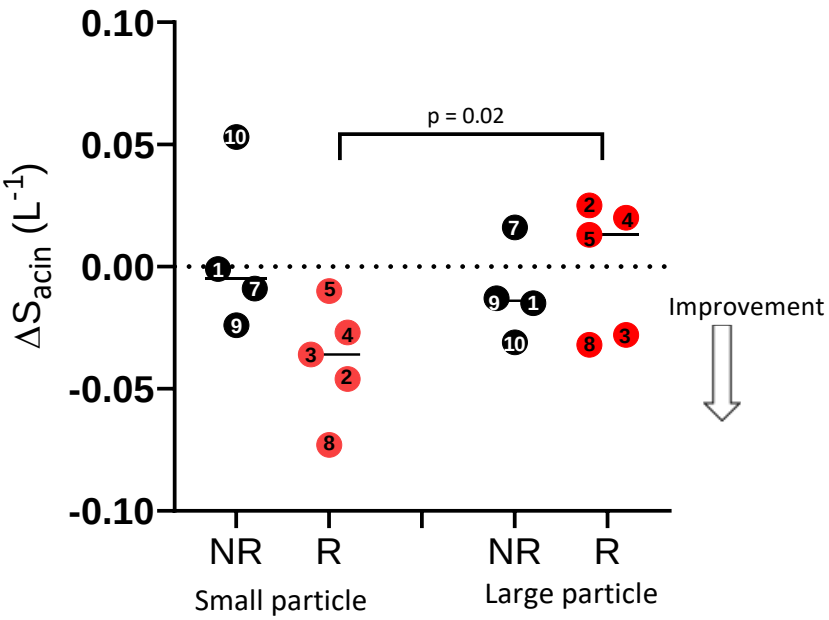

Figure 4.9. *Response to 30µg salbutamol in terms S_{acin} for small (left) and large (right) particle visits. NR = non-responder group displayed in black circles, R = responder group displayed as red circles. Individual subjects are numbered. The zero line equates to no response, the direction of improvement denoted by arrow. p value from paired t-test.*

$DR1_{volume}$ represents when airways begin to close during an expiration from total lung capacity, which coincides with an increase in magnitude of negative reactance as lung volume distal to the closing airways is 'de-recruited'. There was no difference in response to small vs large particle bronchodilator, although all subjects demonstrated an improvement (reduction in DR1 as % of TLC) in response to small particle, whereas there was a mixed response to large particle, figure 4.10 top.

$DR2_{volume}$ represents rapid reduction in reactance that coincides with rapid airway closure. All responder subjects demonstrated an improvement in DR2 with small particle, and this response was greater than that achieved by large particle bronchodilator, figure 4.10 bottom. Therefore, the small particle aerosol bronchodilator was superior in reducing airway closure to lower lung volumes, thereby increasing the ability of the airways to remain open which is beneficial for effective ventilation.

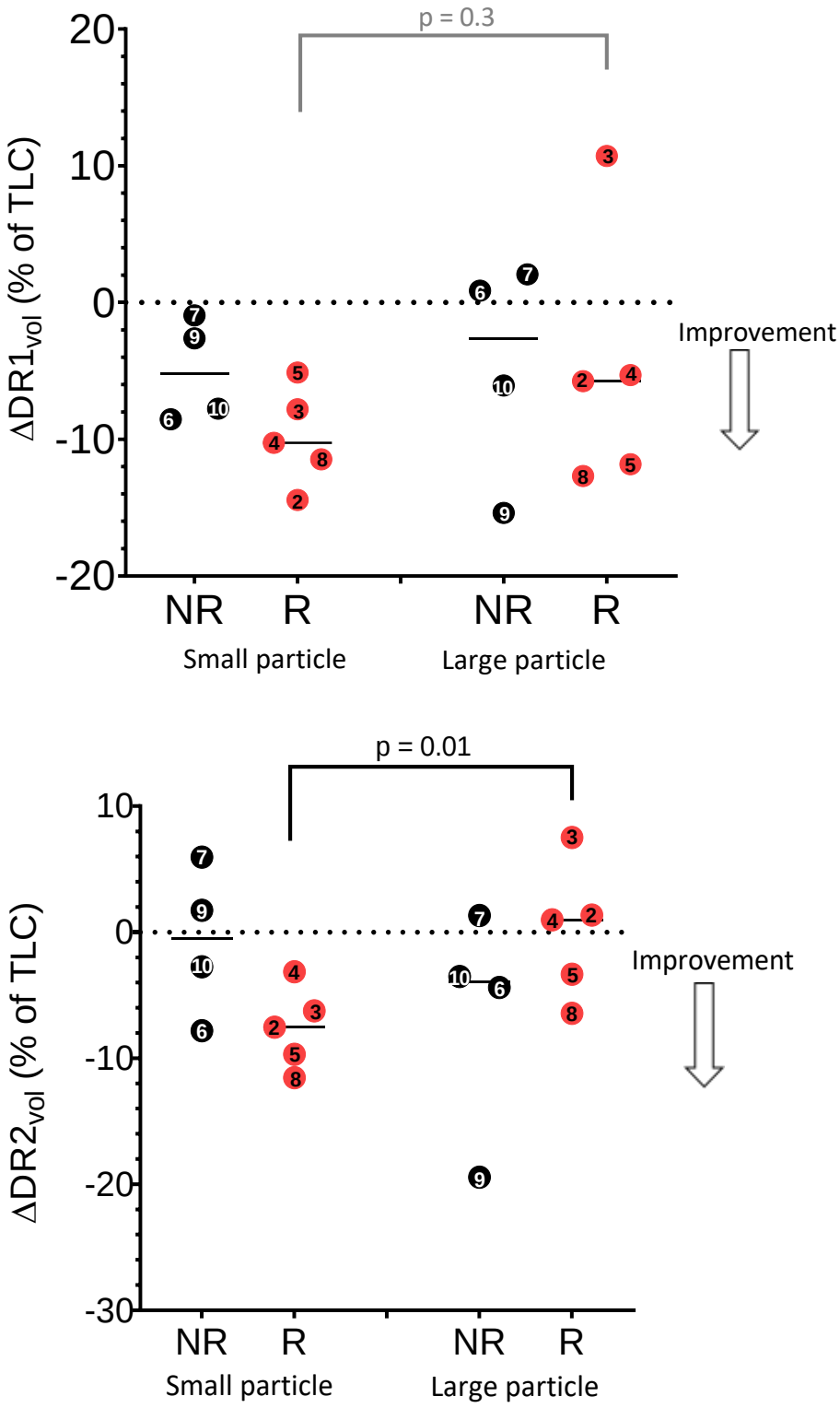

Figure 4.10. *Response to 30µg salbutamol for markers of airway closure DR1 volume (top) and DR2 volume (bottom) as % of total lung capacity, for small (left side of each graph) and large (right side of each graph) particle visits. NR = non-responder group displayed in black circles, R = responder group displayed as red circles. Individual subjects are numbered. The zero line equates to no response, the direction of improvement denoted by arrow. p value from paired t-test.*

4.4.4. Specific ventilation imaging

Specific ventilation maps

The specific ventilation (SV) maps for 8 of the 10 subjects are displayed in figure 4.11a and b. Datasets are missing for 2 subjects due to; poor respiratory gating resulting in inaccurate volume registration to FRC (subject 2), and failed cardiac gating (subject 6). The SV maps represent a single 15mm sagittal slice of right lung positioned approximately midway between the hilum and the lateral aspect of the lung.

Specific ventilation is the ratio of resting lung volume (FRC), to which the individual respiratory gates during the scan, and the volume of tidal breaths taken in between each image acquisition. Therefore, changes in both FRC and tidal volume affect the absolute value of SV. It is the range of SV within the lung that is the important parameter, the increasing range of SV indicates increasing ventilation heterogeneity, as regions of lung receive less fresh gas on inspiration compared to other compartments. To allow visualisation of the distribution of specific ventilation, as well as intra and inter subject SV map comparisons, the SV maps were normalised to the group mean SV measured at baseline on the large visit (0.237).

The pattern of increasing specific ventilation in the direction of gravity, is a normal physiological finding as the ratio of fresh gas to resident gas is lower in the non-dependent distended lung regions (Sa et al., 2010) and is most clearly visible in SV maps for subject 1, both at baseline and post-bronchodilator, (figure 4.11a top). Subject 1 exhibited no impairment in terms of physiological parameters including; FEV_1, FVC, S_{acin}, S_{cond}, R_{rs} and X_{rs} all of which were within normal limits at baseline and showed no significant response to bronchodilator. Therefore, the regional SV maps align with a pattern indicative of relatively normal lung function.

In contrast, the gravitational relationship in SV is not visible at baseline for subjects 4, 5, 7, 8, and 9, who also demonstrated a mild to moderate impairment in spirometry (4,5,8,9) or raised acinar ventilation heterogeneity (all) at baseline. Of these subjects the SV maps for

subjects 4, 5, 8 and 9 demonstrate an improvement post-bronchodilator on at least one visit: At baseline the SV maps for subject 4 show heterogeneity in SV throughout the whole sagittal ROI, and the post-bronchodilator SV maps display a gradient in SV increasing in the direction of gravity, this improvement is most pronounced in the response to small particle bronchodilator. Subject 4 also had a greater improvement in lung function with small particle bronchodilator; a larger increase in FEV_1, greater reduction in S_{acin} and DR_1 and DR_2 volumes, compared to the response to large particle.

The distribution of SV in the direction of gravity appears to be 'inverted' at baseline for subject 5 who has greater normalised SV values in the non-dependent lung region, which is consistent with regional bronchoconstriction in posterior lung (see figure 4.11a). The relationship was confirmed by height slope analysis (SV plotted against distance from dependent lung), slopes at baseline were both positive (small baseline slope = 43 and large baseline slope = 73). The post-bronchodilator SV maps for subject 5 display a more uniform distribution of SV post small and large particle bronchodilator, the analysed slopes for both small and large particle assessments are changed to negative orientation. A quantitative analysis of gravitational SV distribution, is described later and displayed in figure 4.12.

Subject 8 demonstrated the greatest response to bronchodilator in physiological measures, with the largest reduction in acinar ventilation heterogeneity (ΔS_{acin}) and improvement in forced expiratory flow (ΔFEV_1 as percentage of predicted value). The large particle visit SV maps also demonstrated an improvement post bronchodilator as distribution of SV changed from 'inverted' at baseline (non-dependent lung SV>dependent lung SV), to a more uniform distribution post-bronchodilator. On the small particle visit the patchy SV at baseline appears more evenly distributed post-bronchodilator. This is confirmed quantitatively; the change in the histogram width of SV distribution on a log scale was -0.53 post small particle bronchodilator and -0.23 post large particle bronchodilator, demonstrating a spatial reduction in ventilation heterogeneity in response to both size particle aerosol bronchodilator.

The post-bronchodilator SV maps for subject 9 also demonstrate an improvement compared to baseline. The post large particle bronchodilator SV map is more homogenous, with reduced areas of low SV, this is reflected in the SV histogram distribution width which reduces from 0.52 to 0.32. The expected vertical distribution of greater SV in the dependent lung is visible in the post bronchodilator maps for both visits for subject 9, but is most pronounced in the post small particle SV map.

A summary of key SVI changes for individual subjects for each visit are summarised in table 4.7.

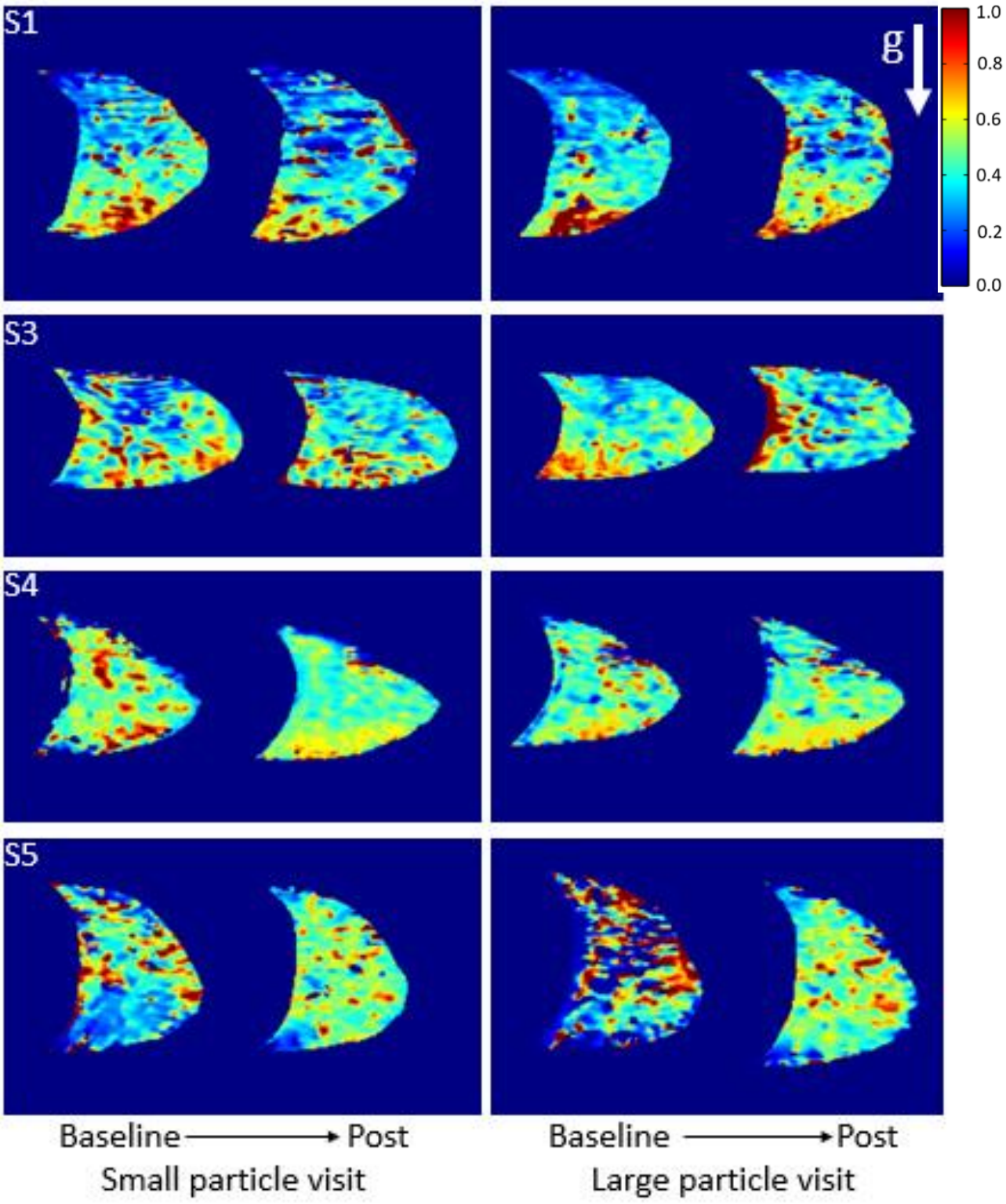

Figure 4.11a. *Normalised specific ventilation maps for subjects 1,3,4, and 5. Direction of gravity indicated by vector 'g'. Results from each individual are displayed across the row from left to right: small particle visit baseline → post bronchodilator → large particle visit baseline → post bronchodilator.*

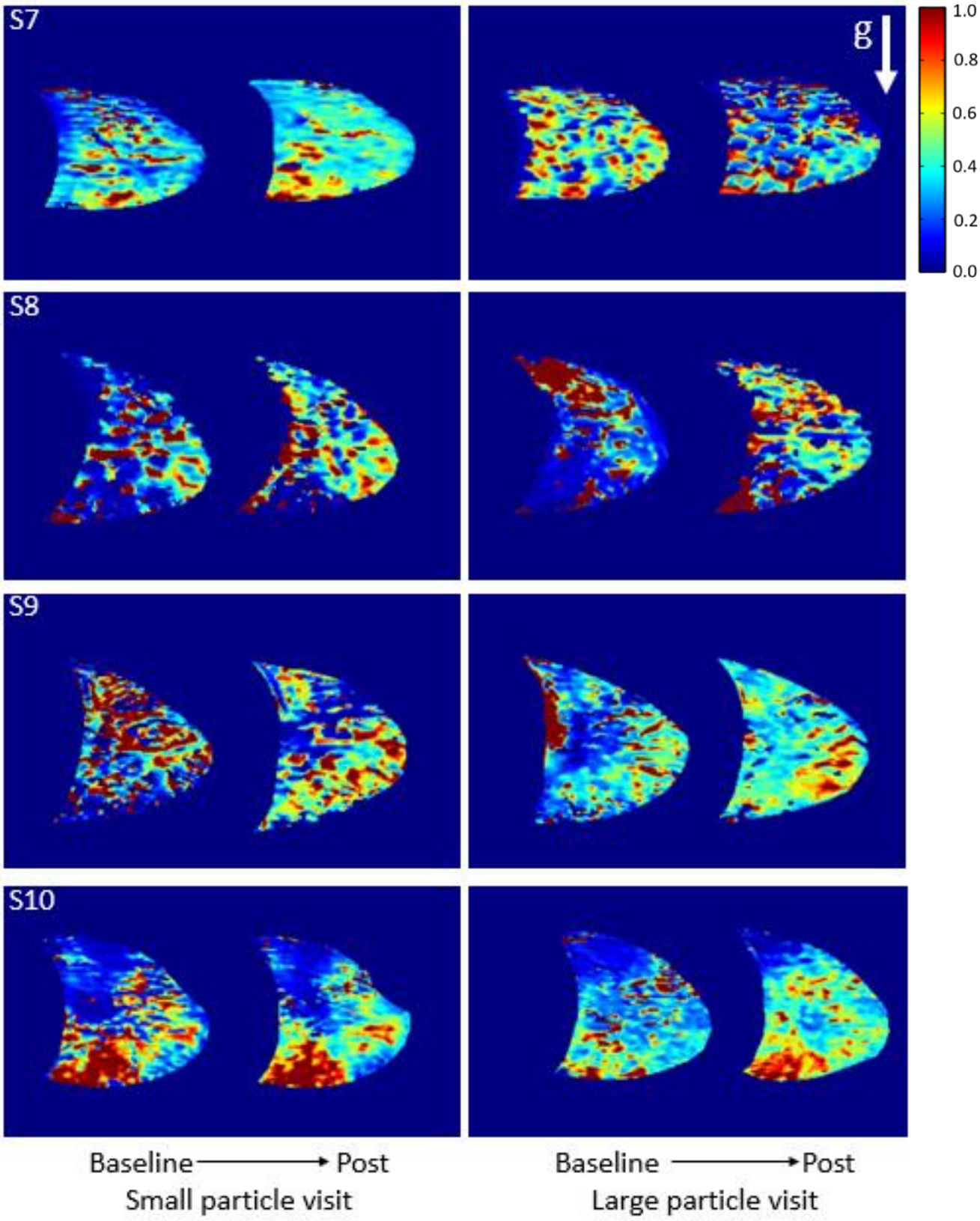

Figure 4.11b. *Normalised specific ventilation maps for subjects 7,8,9 and 10. Direction of gravity indicated by vector 'g'. Results from each individual are displayed across the row from left to right: small particle visit baseline → post bronchodilator → large particle visit baseline → post bronchodilator.*

Table 4.7. SVI markers of ventilation heterogeneity; individual subject responses. n=8

	Response large particle		Response small particle	
Subject	SV distribution width	ROI CoV	SV distribution width	ROI CoV
S1	↑	↓↓	↑	↑↑
S3	-	↑↑	↓	-
S4	-	-	↓	↓↓
S5	↓↓	↓↓	↓↓	↓↓
S7	↑	↑↑	↓↓	↓↓
S8	↓↓	↓↓	↓↓	↓↓
S9	↓↓	↓↓	↓↓	-
S10	↓	↓↓	↓↓	↓

ROI CoV, the coefficient of variation of SV within the sagittal slice region of interest.

Level of change indicated by symbols: - indicates post-bronchodilator difference of <0.05, ↓ or ↑ indicates difference ≥±0.05 and ↓↓ or ↑↑ indicates difference of ≥±0.09. Downward arrow indicates reduction in SV variability or improvement in ventilation heterogeneity (shaded).

Quantitative data for the cohort is displayed in Table 4.8. SV histogram distribution width, a measure of ventilation heterogeneity, shows a significant reduction for the small particle visit only. However, there was no difference in response to small vs large particle bronchodilator for the cohort as a whole, or for the responders vs non-responders.

Table 4.8. Whole cohort quantitative SVI. n=8

	Large particle visit		Small particle visit	
	Baseline	Salbutamol	Baseline	Salbutamol
Histogram parameters				
Amplitude	756.0 ± 324.8	794.1 ± 336.3	620.1 ± 269.5	907.3 ± 426.1
Centre	0.185 ± 0.113	0.211 ± 0.079	0.220 ± 0.116	0.222 ± 0.107
Width	0.511 ± 0.323	0.386 ± 0.247	0.567 ± 0.372	0.411 ± 0.250†
ROI SV parameters				
Mean SV	0.24 ± 0.12	0.25 ± 0.07	0.26 ± 0.12	0.24 ± 0.09
Coefficient of variation	0.88 ± 0.35	0.67 ± 0.26	0.85 ± 0.31	0.71 ± 0.30
Non-correlating voxels (n)	109 (192)	44 (65)	79 (308)	66 (69)

Data displayed as Mean±SD for parametric data, and median(IQR) for non-parametric data.
Baseline to post-salbutamol comparisons were conducted using a paired t test for parametric data and Wilcoxon Sign ranked test for non-parametric data.
† = paired students t-test p value = 0.03

The height plot slope previously described in Chapter 3 displays how specific ventilation changes for lung portions in the direction of gravity. In health, it is generally expected that there will be greater SV in the dependent lung compared with the non-dependent lung. Under the effects of gravity, the non-dependent lung (anterior aspect when supine) is more distended and receives less fresh gas on inspiration that the dependent lung (Sa et al., 2010). In this case, if average SV is plotted against the distance from dependent lung for ascending isogravitational sections the relationship will produce a negative slope, figure 4.12. In asthma SV is heterogeneously affected by poorly ventilated lung units (Lewis et al., 1978) due to bronchoconstriction, oedema, mucus plugging, thus the negative correlation between distance from dependent lung and SV may be reduced, or lost completely.

Treatment with bronchodilator may cause the height slope gradient, to return from an abnormal to normal (or more normal) orientation, therefore response in terms of change in height plot slope was analysed. The effect is most pronounced for the responder group on the large particle visit, but did not reach statistical significance.

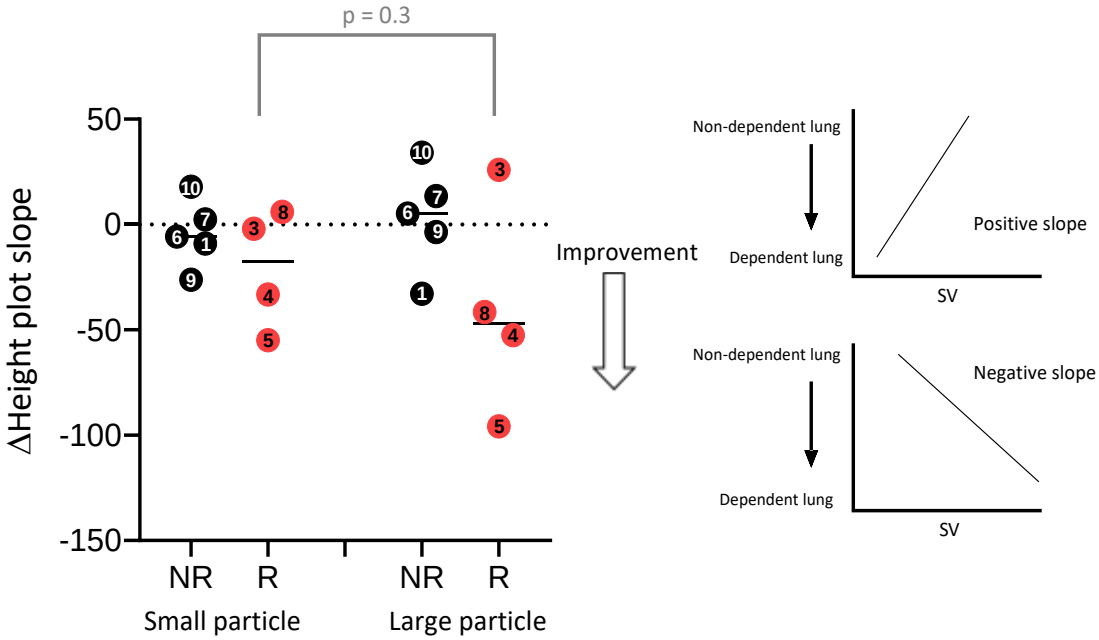

Figure 4.12. *The top right tile shows an abnormal gravitational variation in specific ventilation observed in asthma resulting in a positive slope, whereby the SV in the dependent lung < SV in the non-dependent lung. The bottom right-hand tile shows the expected distribution of SV from non-dependent (lower SV) to dependent (greater SV) lung. A reduction in height slope gradient will occur if the slope is changing from abnormal to more normal orientation.*

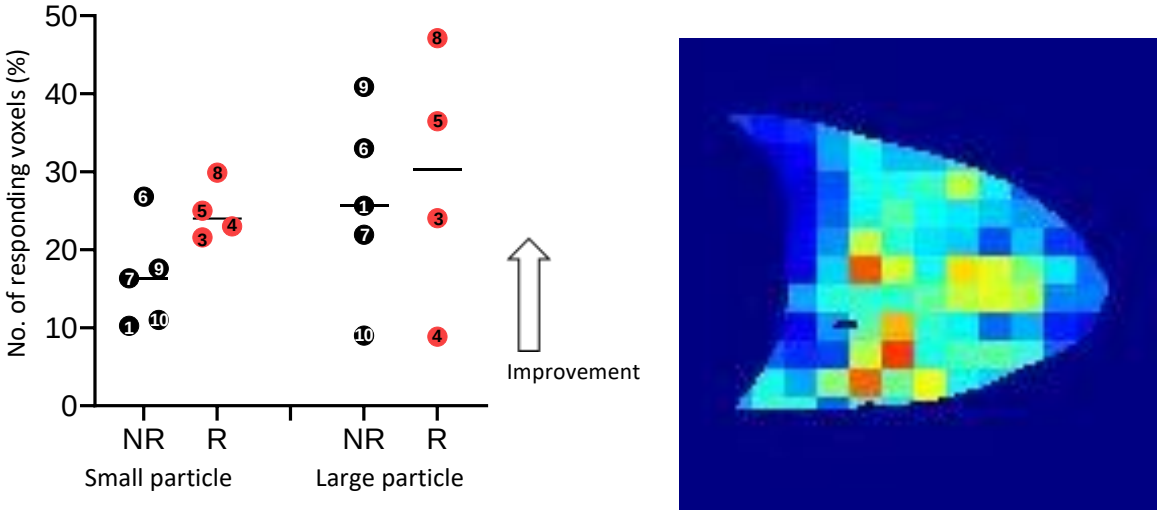

***Figure 4.13**. Left) Percentage of large voxels from the 12x12 grid that have a significant improvement in SV post bronchodilator, defined as a post-BD value >1.5x baseline value and >centre of normalised SV distribution. Right) example down-sampled SVI map*

To complete a spatial assessment of response to bronchodilator subject SV maps were down sampled by applying a 12x12 grid, corresponding large voxels SV values were compared; baseline versus post-bronchodilator. The criteria for a positive response to bronchodilator was met if the large voxel post-bronchodilator SV value was >1.5x the baseline value, and >centre value of the normalised SV distribution. To classify constriction Geier and colleagues used the criteria <0.5x baseline value and <centre value of the normalised SV distribution after administration of methacholine (Geier et al., 2018). The decision was made to increase criterion sensitivity for detecting dilation, by using fraction 1.5 rather than 2, as unlike the published study that used a pre-determined subject specific dose of methacholine to induce 'moderate bronchoconstriction', this study used a very small dose of salbutamol, therefore bronchodilation may be relatively mild.

All subjects had large voxels that showed significantly greater SV post bronchodilator demonstrating a spatial response to bronchodilator. There was no difference in how many large voxels responded between responder and non-responder groups, or between large and small visits. Subject 8 had the greatest percentage of large voxels that improved post

bronchodilator after both small and large particle bronchodilator, which corresponds with the physiological testing.

4.4.5. PREFUL results

Regional ventilation maps

Regional ventilation was calculated for each voxel within the region on interest (ROI) and displayed as regional ventilation maps for all 10 subjects, figure 4.14a and b. The implementation of PREFUL is in the coronal plane, therefore the regional ventilation maps present spatial relative ventilation for a single 15mm slice of coronal left and right lung.

On both baseline maps there is an area of low regional ventilation in the mid-lower section of right lung for subject 1, most pronounced on the small particle visit circled in figure 4.14a. This aspect improves demonstrating greater regional ventilation in this area on the post-bronchodilator maps. In contrast, global physiology measures for subject 1 demonstrated no impairment in spirometry, parameters of ventilation heterogeneity or resistance and reactance, further there was no response to bronchodilator for any of these variables. The only parameter evidencing any impairment from lung function techniques was Ax, which normalised after bronchodilator.

At baseline subjects 2, 3, 4 and 8 demonstrated the greatest impairment in spirometry with severely reduced FEV_1 (Z-scores <-3.5). Whilst subject 2 and 3 appear similar on spirometry their regional ventilation maps look very different. At baseline regional ventilation map for subject 2 is heterogenous, with contrasting 'dark' patches of low relative ventilation, most visible in the left lower lobe, marked in figure 4.14a. This area appears improved in the post small particle bronchodilator map, however there is no notable response to large particle bronchodilator. This mirrors the differences seen in response to small vs large particle salbutamol for subject 2 who had a greater increase in FEV_1, and a greater reduction in S_{acin} post small particle bronchodilator that was not seen post large particle bronchodilator.

In contrast, there are no obvious regions of low regional ventilation for subject 3 who produced regional ventilation maps that appear relatively normal. There is an area of low regional ventilation in the right middle lobe at baseline (arrows in figure 4.14a), most obvious on the small particle visit, which appears to resolve post bronchodilator. However, this is difficult to see and does not mimic the dramatic improvement seen for this subject in response to small particle bronchodilator (630mL increase in FEV_1). Neither do the quantitative values for regional ventilation for subject 3 reflect an improvement, mean regional ventilation decreased overall post small particle bronchodilator by -0.05.

Regional ventilation map for subject 4 is obscured, this subject had previously received a heart transplant, and their left lung coronal slice is largely obscured from view.

There is a region of low ventilation in the right lower lobe of subject 8 visible on both baseline regional ventilation maps, which displays increased regional ventilation post bronchodilator.

Baseline regional ventilation maps for subject 6 are striking with dark regions of very low relative regional ventilation in the right middle, right upper and left upper regions, circled in figure 4.14b. The area of low ventilation on the right lung is improved post bronchodilator with much more homogenous regional ventilation on both visits. The change in coefficient of variation of regional ventilation reflects this, CoV reduced on both visits by -0.25 in response to large particle and by -0.18 in response to small particle. In contrast subject 6 had lung function within normal limits (spirometry and oscillometry parameters), however they were unable to perform MBNW due to leak, and SVI data was not obtained due to poor cardiac gating.

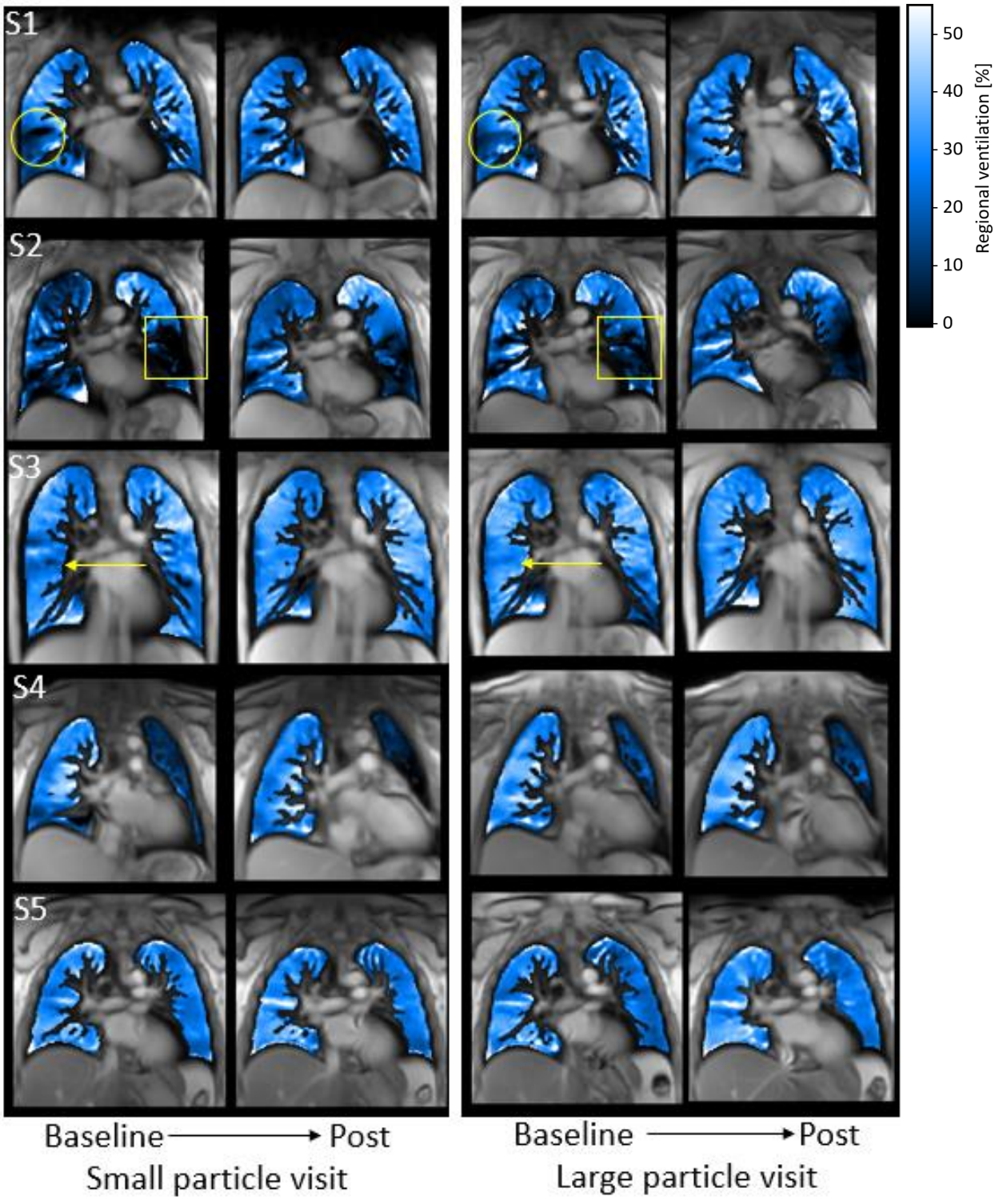

***Figure 4.14a**. Regional ventilation maps for 10 subjects. Results from each individual are displayed across the row from left to right: small particle visit baseline → post bronchodilator → large particle visit baseline → post bronchodilator. Yellow markers depict areas of low ventilation discussed in text.*

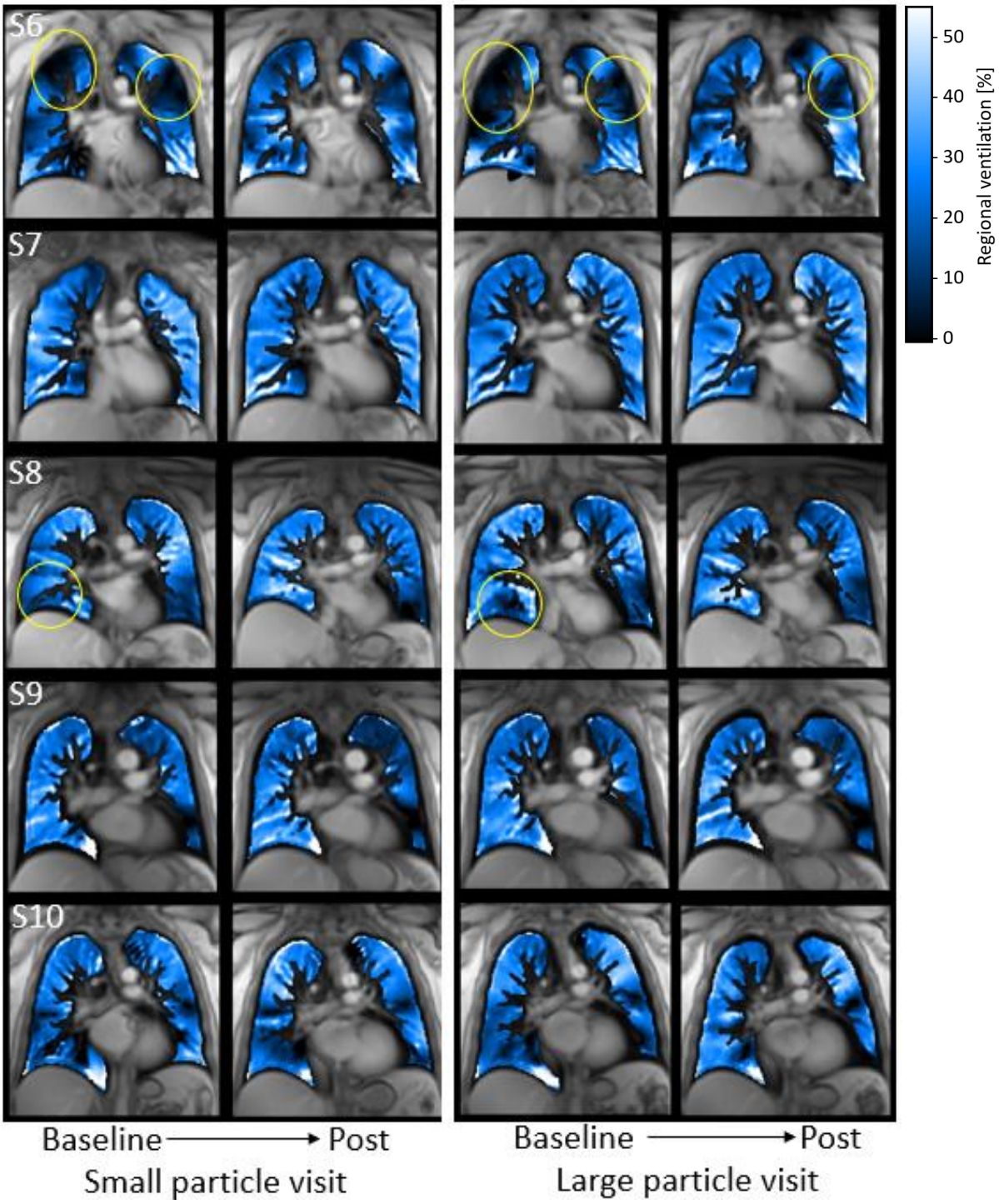

***Figure 4.14b**. Regional ventilation maps for 10 subjects. Results from each individual are displayed across the row from left to right: small particle visit baseline → post bronchodilator → large particle visit baseline → post bronchodilator. Yellow outlines depict areas of low ventilation discussed in text.*

FVL correlation maps

The analysis to generate flow-volume loop correlation maps was completed, as previously described (Moher Alsady et al., 2019). Briefly, healthy regions of lung parenchyma were identified as those with homogenous and relatively high fractional ventilation. For each voxel within the selected region the fractional ventilation and slope of fractional ventilation were used as surrogates for volume and flow respectively to generate voxel 'flow volume loops'. Cross correlation analysis of all voxels, using the healthy region as the reference, was completed, FVL correlation maps are displayed in figure 4.15a and b.

Overall, the FVL correlation maps follow the same pattern as regional ventilation maps. For each subject the areas that show poor correlation of voxel flow volume loops are the same regions that display low regional ventilation in figure 4.14.

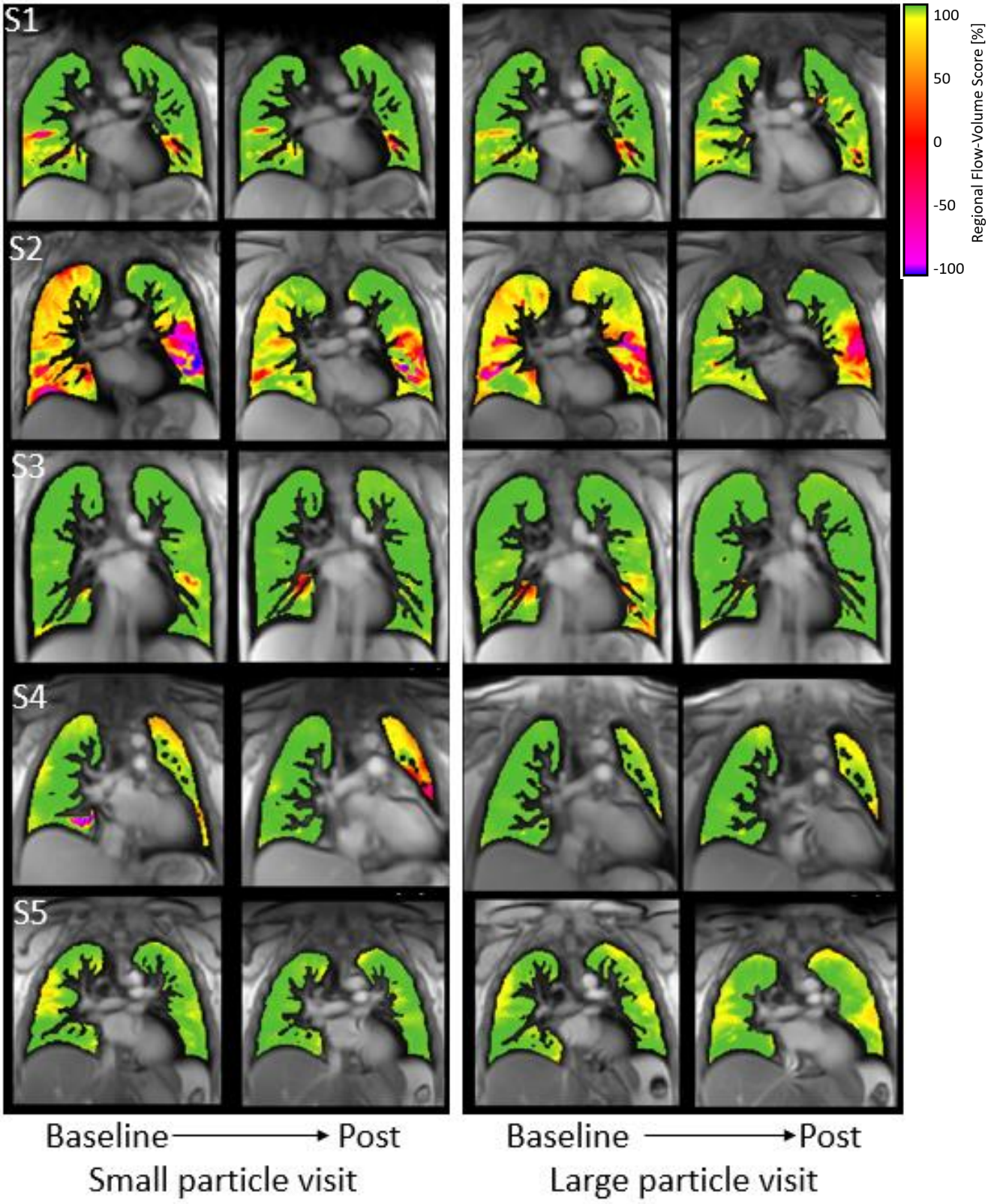

***Figure 4.15a**. FVL correlation maps for subjects 1,2,3,4 and 5. Results from each individual are displayed across the row from left to right: small particle visit baseline → post bronchodilator → large particle visit baseline → post bronchodilator.*

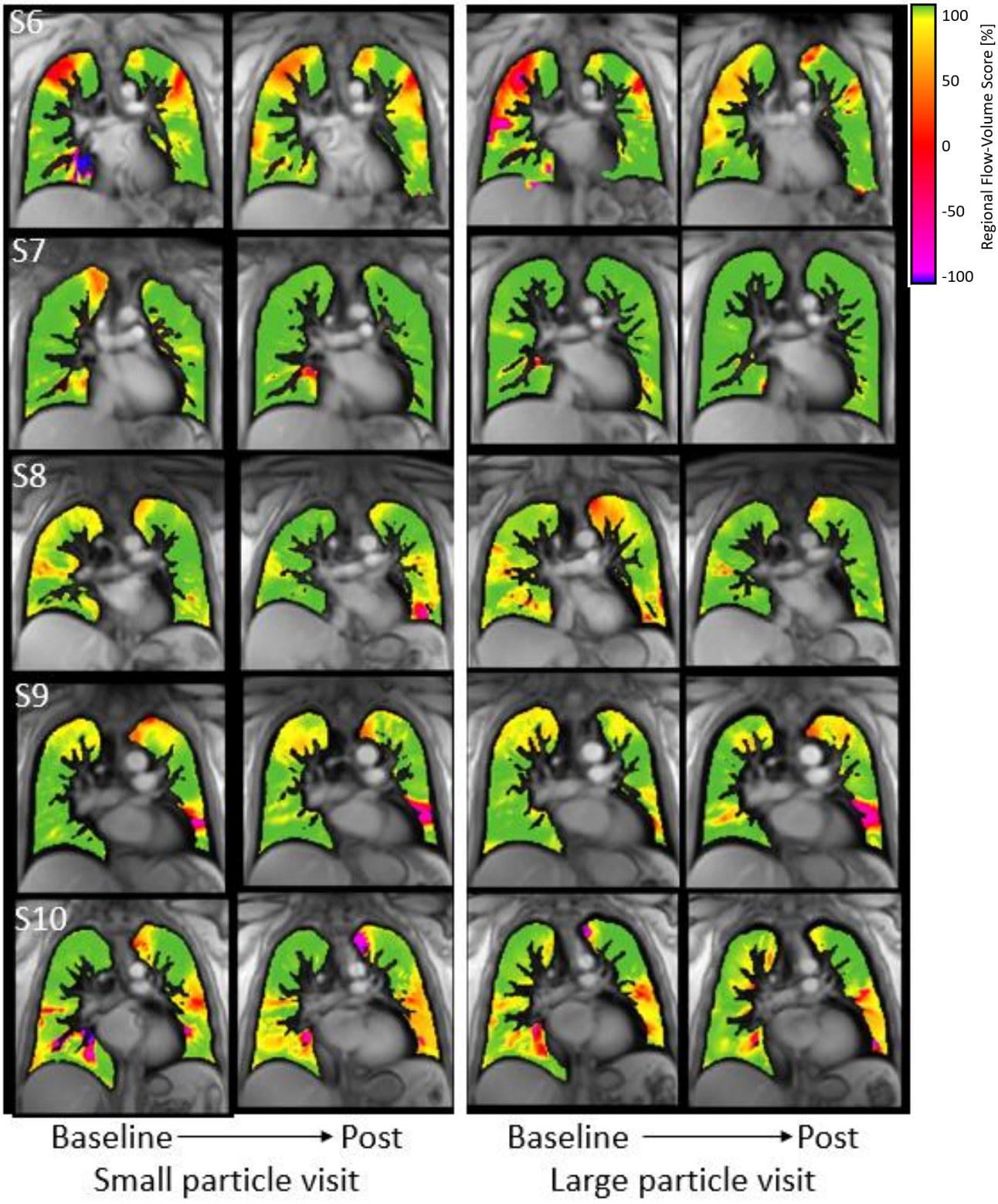

***Figure 4.15b**. FVL correlation maps for subjects 6,7,8,9 and 10. Results from each individual are displayed across the row from left to right: small particle visit baseline → post bronchodilator → large particle visit baseline → post bronchodilator.*

Table 4.9. PREFUL quantitative outputs from 1x 15mm coronal slice of left and right lung. n=10

	Large particle visit				Small particle visit			
	Baseline		Salbutamol		Baseline		Salbutamol	
RVent mean	0.256 ± 0.139		0.306 ± 0.106		0.251 ± 0.084		0.296 ± 0.099	
RVent CoV	0.538 ± 0.168		0.467 ± 0.151†		0.588 ± 1.814		0.673 ± 0.576	
Regional ventilation VDP	0.088 ± 0.112		0.040 ± 0.047		0.093 ± 0.100		0.055 ± 0.033	
FVL correlation mean	0.899 ± 0.095		0.932 ± 0.055		0.880 ± 0.116		0.914 ± 0.061	
FVL correlation CoV	0.212 ± 0.198		0.155 ± 0.139		0.298 ± 0.268		0.219 ± 0.125	
Lung Area Total (ml)	231.0 ± 49.7		219.1 ± 49.8		231.5 ± 52.1		217.0 ± 45.7†	

RVent = regional ventilation, CoV = coefficient of variation, VDP = volume defect percent. † = paired t-test p value<0.05

Table 4.9 details quantitative parameters for the whole cohort at baseline and post bronchodilator for both small and large particle visits. There was a significant difference post vs baseline for the coefficient of variation on the large particle visit only, suggesting a reduction in heterogeneity of RVent. In contrast to other measures of ventilation heterogeneity (SVI histogram width, Sacin) overall heterogeneity of RVent (CoV) increased on the small particle visit. When comparing the response of the whole group, no significant differences were found for any of the PREFUL parameters between large and small particle bronchodilator.

In general, total lung area reduced after administration of salbutamol, this reached significance on the small particle visit. Whist lung area is a mid-way volume, a reduction in lung area is consistent with the reduction in FRC as it equates to breathing at a lower lung volume, which suggests a reduction in gas trapping and airways resistance.

Within the responder group, there were no significant differences observed in any of the PREFUL parameters when comparing small response and large response subgroups. Therefore, the patterns observed in the measures of airway physiology seem not to translate to this ventilation scan.

4.5. Discussion

4.5.1. Whole cohort assessment of response to bronchodilator

In this cohort of subjects with asthma, the small particle bronchodilator achieved an improvement in a greater number of lung function parameters compared to large particle bronchodilator (13 vs 6). Notably, there were no parameters that showed a statistically significant response solely to the large particle bronchodilator, meaning the 6 parameters that demonstrated an improvement with the large particle bronchodilator also improved with the small particle bronchodilator. Further, of the parameters that have a published criterion defining a clinically significant response, for spirometry, the forced oscillation technique and multi-breath nitrogen washout, more subjects responded to small particle bronchodilator. Together these findings suggest that for this cohort, administration of fine particle inhaled bronchodilator resulted in a greater physiological response than the large particle bronchodilator, and the large particle bronchodilator offered no advantage over small particle in terms of reversing impairment in lung function.

One potential explanation for the superior effectiveness of a small particle bronchodilator in this cohort is the presence of peripheral airway dysfunction. Peripheral airway dysfunction was indicated by increased ventilation heterogeneity observed in the acinar region, group average S_{acin} was above the upper limit of normal (ULN) (Verbanck et al., 2012), whereas S_{cond} was within normal limits. Suggesting that this cohort fit an acinar-predominant phenotype within asthma.

The administration of a small particle short-acting β2 agonist (SABA) that primarily targets the peripheral regions (Phipps et al., 1989), increases levels of surfactant (Kumar et al., 2000), which in turn reduces surface tension and promotes airway stability (DiBlasi et al., 2021a). This mechanism that enhances peripheral airway stability could mitigate airway narrowing or closure, decrease susceptibility to airway closure cascade events, and improve homogeneity of ventilation (Venegas et al., 2005). These potential effects, reported in the literature, were observed in response to small particle bronchodilator in this cohort. The

improvements seen in respiratory system reactance (indicated by reduced lung stiffness, reflected by less negative X_{rs}), reduced airway closure at higher lung volumes, (evidenced by the decrease in both de-recruitment volumes 1 and 2), and reduced peripheral resistance (evidenced by a reduction in $R_{rs\ 5\text{-}19Hz}$). As these favourable outcomes were not observed with the administration of large particle SABA in this cohort, these results support the concept of phenotyping patients to inform personalised treatment approaches. Specifically, considerations of inhaled medication aerosol particle size may be tailored accordingly to individual patients.

4.5.2. 'Non-responders'

Despite confirmation of responsiveness to salbutamol measured with spirometry prior to recruitment into the study, 50% of this cohort did not achieve a significant response measured by spirometry on either visit. As highlighted in section 4.3.5 'Selection of bronchodilator dose', response to salbutamol according to dose, is hugely varied between individuals with asthma. Response has been measured with spirometry following administration of doses as small as 10µg (Barnes and Pride, 1983), and whilst the plateau in the dose response curve usually occurs under 100µg, some individuals have shown increasing response with doses up to 4mg (Lipworth et al., 1988). This cohort were recruited from an asthma clinic where the standard bronchodilator assessment involved administration of 400µg of salbutamol MDI via spacer, which was more than 13 times the dose used in this study. The lack of response observed in the 'non-responders' is therefore likely attributable to a relative tolerance to salbutamol. Whilst the study protocol dose used in this study was insufficient to elicit a response in some subjects during both study visits, it was necessary to opt for a conservative approach in dosing. Despite the aerosol particle plumes meeting the definition for 'monodisperse', indicating a narrow particle size distribution, there was still some overlap. Consequently, increasing the dose could have led to reaching the plateau of response in the airway region not specifically targeted on either visit, in turn masking the difference in response to small vs large particle that was observed in the responder group.

4.5.3. 'Responders'

Subgroup analysis of subjects who achieved the spirometric definition for a significant response provided further evidence supporting the superiority of small particle salbutamol for this cohort. Within this subgroup, FEV_1, S_{acin} and $DR_{2\ volume}$ displayed a greater response to small particle bronchodilator compared to large. This means that the 'responder' patients benefited from a greater reduction in expiratory airflow limitation, more homogenous ventilation in the acinar region and a reduction in rapid onset of airway closure with small particle bronchodilator, i.e. a greater reversal of physiological impairment due to asthma, with just 30µg salbutamol.

4.5.4. Specific ventilation imaging

SVI is an MR imaging technique that relies on a physiological 'wash in' of oxygen producing providing specific ventilation with spatial detail (Geier et al., 2018). Performing this technique requires specialist equipment, and the challenges presented are exacerbated at 3T relative to 1.5T.

The quantitative results obtained from SVI did not follow the patterns observed in traditional lung function measurements, which suggests that SVI provides unique, complementary information. A possible reason for this is that the resolution of the SVI sagittal slice is insufficient to capture the changes observed in peripheral airways. The changes detected in SVI parameters may reflect the response occurring in the larger airways. Further, the in-plane resolution is approximately 1cm, therefore this technique lacks the sensitivity to capture changes occurring at a smaller scale.

Interestingly, subject 8 exhibited the greatest physiological changes and responded to both small and large particle bronchodilator also demonstrated the greatest spatial response in SVI (reduction in histogram width). It is important to note that the SVI protocol used in this study assesses one slice of one lung only. Consequently, it offers a selective assessment

which may not represent the overall ventilation distribution within the entire lung, as assessed with lung function techniques.

PREFUL is an appealing test due to its relative ease of execution. However, the qualitative improvements observed in regional ventilation scans following bronchodilator administration are not evident in quantitative parameters. Previous studies have demonstrated a correlation between PREFUL parameters and long-term outcomes, such as post lung transplant survival (Moher Alsady et al., 2019). Nevertheless, in this study PREFUL parameters do not reflect the immediate improvement seen in lung function demonstrated with physiological techniques. An explanation for this disparity could be that the 3T PREFUL protocol used is limited to a single coronal slice, whereas physiological techniques assess global lung function.

4.5.5. Limitations

Due to unforeseen circumstances in the form of a global pandemic this study recruited a small number of patients (see Chapter 6), therefore correlations between imaging and physiological data, as well as overall conclusions are limited. Despite this, the study has demonstrated that particle size of inhaled bronchodilator does affect the elicited response.

For the whole cohort baseline lung function was worse on the small particle visit, this is noteworthy as baseline lung function is a key determinant of response, and might explain the greater number of significant responses to small particle aerosol. However, the prevalence of impairment in key lung function parameters at baseline remained consistent between both visits. 7 out of 10 subjects exhibited an abnormal FEV_1 Z-score, 8 out of 9 had S_{acin} values above the ULN, and 5 out of 10 demonstrated abnormal Z-scores for respiratory system resistance in both baseline visits. Further, there was no difference in baseline lung function for the responder group who did demonstrate a significantly a greater response to small particle vs large particle bronchodilator. This suggests that factors other than baseline lung function may contribute to the differential response between small and large bronchodilator aerosols.

Despite proximity (within 1 week) and same time of day testing, this study has not assumed a constant baseline, instead, baseline respiratory function in all domains was assessed on both occasions. Consequently, the measured response is specific to each visit, which represents a significant strength of this study.

4.6. Conclusion

This study has demonstrated that particle size is an important determinant of response. The subjects in this study were from the Alfred hospital asthma clinic and were categorised as severe or difficult cases. For the responder subjects, it would be pertinent to investigate a switch of their maintenance therapy (such as inhaled corticosteroids) to a fine particle preparation and evaluate their symptoms and airway function with objective measurements after a period of effective treatment.

Further investigation in a larger cohort is needed to confirm the result of this pilot study. Potentially by implementing sensitive tests in similar clinics and recruiting patients with peripheral dysfunction into the small particle treatment group.

Chapter 5. Conclusions and Future Work

This thesis integrated the traditionally distinct fields of medical physics and physiology to achieve a greater understanding of asthma pathophysiology. Collectively, this research has demonstrated the advantages of applying sophisticated physiological testing and imaging methods in an asthma cohort. These techniques have provided insights into the link between peripheral airway dysfunction and clinically important exacerbations, as well as proof of the concept of altering particle size to target bronchodilator therapy and generate different regional responses.

The work involved investigating differences in ventilation heterogeneity and respiratory mechanics in three different asthma groups (categorised according to their exacerbation history) to determine characteristics specific to those who are at risk of acute asthma events. To facilitate MRI ventilation scanning, a protocol for specific ventilation imaging, a technique that utilises the physiological wash-in of oxygen to generate contrast, was developed for use on a 3T scanner. In addition, the protocol and license for the free breathing ventilation scan PREFUL, phase resolved functional lung imaging, was obtained. Finally, response to small and large particle aerosol bronchodilator targeted at peripheral and central airways, was assessed with the combination of imaging and physiological methods to provide spatial and regional airway measures of ventilation heterogeneity.

The cross-sectional study described in Chapter 2 used multi-breath nitrogen washout and oscillometry as well as traditional spirometry to assess airway function in asthma patients who were; stable, exacerbation prone, and within 1 month of a treated acute exacerbation of asthma. Subjects with asthma who had had an exacerbation in the preceding year, and therefore at risk of further exacerbations, demonstrated worse peripheral airway function evidenced by more abnormal; S_{acin} from multi-breath nitrogen washout, and X_{rs} from oscillometry. Further, individuals who had recently received treatment for an asthma exacerbation demonstrated peripheral airway function similar to that of the stable group, which implies that the elevated dysfunction in the exacerbation group may be reversible.

These findings suggest that active dysfunction in the peripheral airways plays a significant role in the pathophysiology of asthma exacerbations. Prevention of asthma exacerbations must be achieved in order to prevent unnecessary deaths (Levy et al., 2014), and to accomplish the European Respiratory Society's aim of 'Asthma remission' (Dennis et al., 2022). The next step would be a large prospective study. Monitoring peripheral airway function in prospectively recruited patients in conjunction with recording exacerbations of asthma would assess the utility of markers such as S_{acin} and X_{rs} in predicting exacerbations, by capturing this data prior to exacerbations.

Chapter 3 focused on developing the SVI, specific ventilation imaging, 3T protocol and provided valuable insights into the challenges and limitations of specific ventilation measurements at different magnetic field strengths. We demonstrated that SVI imaging is feasible at 3T; however, it poses significant challenges compared to 1.5T. Despite extensive work to optimise both the protocol at the time of scanning and post-processing of MR images, 2 of 10 datasets were discarded due to insufficient quality. Consequently, for future SVI research, lower magnet field strengths are preferable.

In Chapter 4, the effectiveness of short-acting bronchodilator medication with two different particle sizes in subjects with asthma was evaluated. Comprehensive assessments of respiratory function were conducted using both physiological and MRI techniques on two separate occasions: one with a small particle bronchodilator targeting peripheral airways and another with a large particle bronchodilator targeting proximal airways. At baseline, the cohort displayed peripheral airway dysfunction with raised acinar ventilation heterogeneity (S_{acin}). Overall, subjects showed an improvement in a greater number of physiological parameters with the small particle bronchodilator compared to the large particle bronchodilator. The reversal of some aspects of airway dysfunction, including reduced lung stiffness (indicated by less negative X_{rs}), decreased airway closure at higher lung volumes (shown by lower de-recruitment volumes 1 and 2), and reduced peripheral resistance (seen in the decrease of R_{rs} 5-19Hz), were observed post small particle bronchodilator only. Further, of those who met the definition for a clinically significant response according to published criteria for spirometry (Stanojevic et al., 2021) and oscillometry (King et al., 2020),

reversal of airflow limitation (FEV_1), reduction in acinar ventilation heterogeneity (S_{acin}) and reduction in airway closure (DR2) was greater for small particle compared to large. These findings support the idea of phenotyping patients to guide personalised treatment strategies. Specifically, the choice of inhaled medication aerosol particle size could be customised for individual patients. For example, prescribing small particle aerosol inhaled therapies for patients that display peripheral airway dysfunction.

This pilot study has shown the feasibility of studies combing complex physiological testing and novel MR ventilation imaging techniques. Through the application of appropriately sensitive techniques, this work has proven the concept of targeting inhaled therapy to airway regions by altering the aerosol particle size and generating different responses. Moreover, the results have shown that for some subjects, it is possible to improve response to bronchodilator if the site of dysfunction is targeted. These findings have the potential for clinical impact by improving the management of asthma in the pursuit of personalised medicine.

The conclusions that are able to be drawn from the results of Chapter 4, as well as the applicability to the population with asthma are limited by small study sample size.
A larger study is required to establish the validity and reliability of the findings. In such a study there would be recommended alterations to the methodology, based off the lessons learnt here.

To address the 'non-response' rate, which was high (50%) in this study, an additional step in the recruitment process to include screening for reversibility at low doses of short-acting beta-agonist should be included. This screening step would help identify individuals who are more likely to respond to the intervention and exclude those who do not before MRI scanning.

As previously mentioned, the recommendation would be to perform the ventilation MR imaging component at 1.5T. Further, implementation of multi-slice SVI and 3 dimensional PREFUL would help correlate imaging findings with global physiology, and further our

understanding of how these imaging techniques relate to and augment the information from physiological methods.

Whole lung 3D PREFUL data gathered at 1.5T could be used to evaluate the ability of current PREFUL parameters in the identification of within-session response to bronchodilator. As the measured PREFUL parameters in Chapter 4 did not display differences between the pre- and post- bronchodilator data, identification of new PREFUL parameters that reflect the apparent qualitative differences seen in this study may be required.

Whilst there was a reduction in ventilation heterogeneity in response to small particle bronchodilator, evidenced by a reduction in SV distribution histogram width, there was no difference in response to small vs response to large particle. This may be due to insufficient resolution. The spatial resolution of SVI is limited to approximately $1cm^3$, which equates to about 6 acini (at functional residual capacity). Therefore, any effect smaller than that will not be seen (Sa et al., 2014) and it may be necessary to employ alternate imaging methods to capture minute changes or variations in ventilation at a more granular level.

A quicker path to clinical implementation could be an alternate study, still targeting treatment but with inhaled corticosteroids +/- long-acting bronchodilator, over an efficacious period. The studies investigating the efficacy of different particle sizes in terms of exacerbations and respiratory function are outdated by 10 years. The use of the small particle producing PDAP (photo defined aperture plate) technology is relatively new. It would be beneficial to conduct a study using inhaled corticosteroids (ICS) via PDAP, comparing it to the conventional ICS delivery method, with the hypothesis that the PDAP generates a greater treatment effect in those with peripheral airway dysfunction, in terms of symptoms, exacerbations and objective measures of airway function. A randomised trial could be conducted whereby participants are assessed at baseline and then randomised to treatment groups, both receiving ICS therapy via a nebuliser, with the delivery method being blinded:

Group 1: ICS via the conventional solo equivalent method.

Group 2: ICS via the PDAP equivalent method.

Post-assessment would evaluate the outcomes and compare the efficacy between the two groups. The results of the bronchodilator study demonstrated efficacy with doses fractional to that used clinically. If a similar effect was found with ICS this would allow treatment at lower doses, which would be beneficial in reducing the negative side effects associated with inhaled corticosteroids.

Through implementing more specialised tests, it is possible to create a clearer picture of how regional airway function relates to the clinical picture of asthma, to identify potential treatment target sites, and to ensure that the benefits and the risks of altering inhaled drug particle size are accurately assessed. By adopting a more personalised approach to asthma management, clinicians may be better equipped to identify at risk patients, and the specific areas of the respiratory system that require treatment, which could lead to improved clinical outcomes.

Chapter 6. The Impact of COVID-19

It would be remiss of me to submit this thesis, completed in the era of COVID-19, without including a statement detailing some of the impacts the global pandemic had on the completion of this work. This is my personal reflection.

Following successful registration as a Clinical and Respiratory Sleep Scientist my desire to delve deeper into the field of respiratory science presented the opportunity of research under The Alfred Hospital and Monash University affiliation, Melbourne, thanks to Professor Bruce Thompson. Prior to the first year of undertaking my PhD I had completed various challenges, including enrolling the PhD at Newcastle University, UK, obtaining a VISA with working rights for Australia, and moving to Melbourne. Then, following an unforeseen complication with availability of respiratory patient cohorts, I began developing my research project within asthma and succeeded in completing protocol development and gaining ethical approval in 2019.

March 2020

Like most people, I was thrown into a life of extremely limited in person interactions, both personal and professional meetings were exclusively taking place via conferencing software. I felt guilt as my ex-colleagues within the NHS were redeployed to front-line in-patient care whilst I sat working from home, but unable to conduct the research project I had set up. All whilst worrying about loved ones back in England, who I would be unable to see for 3 years all up. Of course, there were many positives, as well as lessons learned from the lockdown period. However, the relentless and repetitive nature of lockdowns in Melbourne, which made it amongst the most locked down cities in the world by October 2021 (262 days over 6 separate lock downs) left me languishing, and took a toll on my mental health and wellbeing. The recovery from this was not instantaneous upon the reopening of the state.

Project logistics

Conducting any non-essential research was prohibited during each lockdown period, therefore collection of prospective data was impossible at this time. The specifics of the

project that I had devised, including lung function testing and use of aerosol producing nebulisers, ranked it highly on the forbidden list. Not only must a face mask be removed for subjects to perform lung function, thereby removing a personal protective barrier to virus transmission, but lung function itself was identified as an aerosol generating procedure (Ikin et al., 2021). Further, the respiratory manoeuvres involved in lung function testing also often cause cough, in turn increasing the spread of potentially virus containing droplets. Even in the clinical setting there was a dramatic reduction in respiratory lung function testing aimed at reducing the spread of COVID-19 (McGowan et al., 2022), this was despite potentially disastrous consequences for those who had their diagnostic tests postponed or cancelled, and for those with chronic respiratory disease who were left unmonitored.
On a positive note, the COVID-19 pandemic has drawn worldwide attention to the importance of aerosols, particulates and deposition, as scientists around the world worked to understand the behaviour of respiratory droplets and aerosols to develop strategies to limit the transmission of respiratory illnesses like COVID-19.

The working model of the asthma clinic, from which I recruited subjects, transformed in response to the pandemic, which had a negative impact on recruitment. The most effective recruitment process involved: 1) the respiratory scientists conducting spirometry for patients attending for their asthma review screened potential participants for eligibility; 2) me, on hand to explain and discuss the study to anyone who might be interested; and 3) the consultant physician conducting the asthma clinic review who was informed and aware of the research. With the move to telehealth and the reduction in objective lung function monitoring of patients with chronic respiratory disease such as asthma, additional unavoidable obstacles to prospective data collection were created, even when research was permitted.

Work on the COVID-ward 2 East

Around 18months into the pandemic the Victorian population vaccination rates were increasing and the state government communicated a commitment to remaining ‘open’. During spring and summer 2021 the spread of the COVID virus was high, and infection rates resulted in saturated COVID wards in hospitals, and unprecedented pressures on in-patient

services. At the Alfred the non-invasive ventilation service, who were supporting the respiratory COVID ward put out a request for help. In response to this I took a 3 month break from research to work on the respiratory patient COVID ward caring for COVID positive patients who required; high-flow oxygen, continuous positive airway pressure (CPAP) or non-invasive ventilation.

My time on ward 2-East was a unique experience. Working to optimise oxygenation of patients with COVID-19 pneumonia I implemented clinical skills; titrating supplemental oxygen therapy to meet target saturations, initiating CPAP to recruit airspaces, and guiding positional therapy to aid ventilation and perfusion matching. The role also challenged me to exercise skills beyond what I was used to practicing clinically. This included discussing with patients the severity of their condition, or how upholding cultural or religious beliefs would be to the detriment of their prognosis, e.g. refusal to remove facial hair thereby preventing effective CPAP therapy due to insufficient mask seal.

The break from the often-solitary nature of completing a PhD, particularly in the lockdown era, was welcomed and I appreciated the camaraderie and team work. However, the work drained me in other ways. Prior to this role my clinical experience had been based mainly within out-patient diagnostic services, therefore I had limited experience with in-patient wards, and even less so with death.

Many of the patients from 2-East will remain in my memory, some of whom went home, some of whom did not. One lady admitted to 2-East presented with the high clinical risk combination of brittle asthma and COVID. She was not for escalation to ICU, therefore despite being too breathless to speak more than one word, and plummeting oxygen saturations, treatment options were limited to the ward resources described. In her final days I held her hand as well as the screen via which she had some of her last conversations with her family. This case served as a first-hand experience and reminder of the importance of research such as this, working to increase understanding of asthma pathophysiology and towards improvements in asthma care.

Publications to date

O'Sullivan C.F., Nilsen K., Borg B., *et al.* (2022) 'Small airways dysfunction is associated with increased exacerbations in patients with asthma.' *Journal of Applied Physiology*, 133:3, p. 629-636.

O'Sullivan C.F., Nilsen K., Prisk G.K, *et al.* (2021). 'Commentaries on Viewpoint: Small airways vs. large airways in asthma: time for a new perspective.' *Journal of Applied Physiology*, 131(6): p. 1842-1848.

Presented abstracts

O'Sullivan C., Prisk G.K, Nilsen K. *et al.* Feasibility of Specific Ventilation Imaging on a 3T MRI scanner. *ERS International Congress, September 2022 (Barcelona).* **Poster presentation.**

O'Sullivan C., Prisk G.K, Nilsen K. *et al.* Targeting peripheral airway dysfunction with small particle bronchodilator in asthma. *ANZSRS annual scientific meeting, April 2022 (virtual).* **Oral presentation.**

O'Sullivan C., Prisk G.K, Nilsen K. *et al.* Targeting peripheral airway dysfunction with small particle bronchodilator in asthma. *The Thoracic Society of Australia & New Zealand, annual scientific meeting, April 2022 (virtual)*. **Oral presentation.**

O'Sullivan C., Prisk G.K, Nilsen K. *et al.* Spatial response to small and large bronchodilator in subject with asthma. *ERS International Congress, September 2*021 (virtual). **Poster presentation.**

O'Sullivan C., Nilsen K., Borg B., e*t al.* Assessment of ventilation heterogeneity and respiratory mechanics in stable and refractory asthma. *The Thoracic Society of Australia &*

New Zealand, annual scientific meeting, May 2021 (postponed from 2020) (virtual). **Poster presentation.**

O'Sullivan C., Nilsen K., Borg B., e*t al.* Assessment of ventilation heterogeneity and respiratory mechanics in stable and refractory asthma. ANZSRS annual scientific meeting, *May 2021 (postponed from 2020) (virtual)*. **Oral presentation.**

Invited talk

The peripheral airways in Asthma: significance, assessment, and targeted treatment. Monash Biomedical Imaging, Clayton, Melbourne. *Webinar series. Online September 2022.*

Awards

The Thoracic Society of Australia & New Zealand, ASM, Asthma and Allergy SIG Award: Winner of best oral presentation. April 2022.

International Partnership seed funding for comparison MR ventilation scanning (Chapter 3).

References

AGUSTI, A., BEL, E., THOMAS, M., VOGELMEIER, C., BRUSSELLE, G., HOLGATE, S., HUMBERT, M., JONES, P., GIBSON, P. G., VESTBO, J., BEASLEY, R. & PAVORD, I. D. 2016. Treatable traits: toward precision medicine of chronic airway diseases. *European Respiratory Journal,* 47**,** 410.

AGUSTI, A. & PAVORD, I. D. 2018. Do we really need a new classification of airway diseases? *The Lancet Respiratory Medicine,* 6**,** 891-893.

ANDERSON, S. D. 2018. Repurposing drugs as inhaled therapies in asthma. *Adv Drug Deliv Rev,* 133**,** 19-33.

ANNESI-MAESANO, I. & FORASTIERE, F. 2019. Doubts about the adverse effects of air pollution on asthma? *European Respiratory Journal,* 54**,** 1901900.

ARAI, T. J., HORN, F. C., SÁ, R. C., RAO, M. R., COLLIER, G. J., THEILMANN, R. J., PRISK, G. K. & WILD, J. M. 2018. Comparison of quantitative multiple-breath specific ventilation imaging using colocalized 2D oxygen-enhanced MRI and hyperpolarized 3He MRI. *Journal of Applied Physiology,* 125**,** 1526-1535.

ARAI, T. J., VILLONGCO, C. T., VILLONGCO, M. T., HOPKINS, S. R. & THEILMANN, R. J. 2012. Affine transformation registers small scale lung deformation. *Annu Int Conf IEEE Eng Med Biol Soc,* 2012**,** 5298-301.

ARI, A., DE ANDRADE, A. D., SHEARD, M., ALHAMAD, B. & FINK, J. B. 2014. Performance Comparisons of Jet and Mesh Nebulizers Using Different Interfaces in Simulated Spontaneously Breathing Adults and Children. *Journal of Aerosol Medicine and Pulmonary Drug Delivery,* 28**,** 281-289.

BALZAR, S., CHU, H. W., STRAND, M. & WENZEL, S. 2005. Relationship of small airway chymase-positive mast cells and lung function in severe asthma. *Am J Respir Crit Care Med,* 171**,** 431-9.

BARNES, P. J. & PRIDE, N. B. 1983. Dose-response curves to inhaled beta-adrenoceptor agonists in normal and asthmatic subjects. *Br J Clin Pharmacol,* 15**,** 677-82.

BATEMAN, E., KARPEL, J., CASALE, T., WENZEL, S. & BANERJI, D. 2006. Ciclesonide reduces the need for oral steroid use in adult patients with severe, persistent asthma. *Chest,* 129**,** 1176-87.

BATES, J. H. & LUTCHEN, K. R. 2005. The interface between measurement and modeling of peripheral lung mechanics. *Respir Physiol Neurobiol,* 148**,** 153-64.

BERRY, R. B. & FAIRSHTER, R. D. 1985. Partial and maximal expiratory flow-volume curves in normal and asthmatic subjects before and after inhalation of metaproterenol. *Chest,* 88**,** 697-702.

BLEECKER, E. R., FITZGERALD, J. M., CHANEZ, P., PAPI, A., WEINSTEIN, S. F., BARKER, P., SPROULE, S., GILMARTIN, G., AURIVILLIUS, M., WERKSTRÖM, V. & GOLDMAN, M. 2016. Efficacy and safety of benralizumab for patients with severe asthma uncontrolled with high-dosage inhaled corticosteroids and long-acting β(2)-agonists (SIROCCO): a randomised, multicentre, placebo-controlled phase 3 trial. *Lancet,* 388**,** 2115-2127.

BLOOM, C. I., PALMER, T., FEARY, J., QUINT, J. K. & CULLINAN, P. 2019. Exacerbation Patterns in Adults with Asthma in England. A Population-based Study. *Am J Respir Crit Care Med,* 199**,** 446-453.

BOURDIN, A., PAGANIN, F., PRÉFAUT, C., KIESELER, D., GODARD, P. & CHANEZ, P. 2006. Nitrogen washout slope in poorly controlled asthma. *Allergy,* 61**,** 85-9.

BROWN, N. J., SALOME, C. M., BEREND, N., THORPE, C. W. & KING, G. G. 2007. Airway distensibility in adults with asthma and healthy adults, measured by forced oscillation technique. *Am J Respir Crit Care Med,* 176**,** 129-37.

BURNS, G. P. & GIBSON, G. J. 2002. A novel hypothesis to explain the bronchconstrictor effect of deep inspiration in asthma. *Thorax,* 57**,** 116-9.

BUSH, A. & SAGLANI, S. 2018. Structurally Unsound? Why Airways Become Asthmatic. *Am J Respir Cell Mol Biol,* 59**,** 405-406.

BUSSE, W. W. 2019. Biological treatments for severe asthma: A major advance in asthma care. *Allergol Int,* 68**,** 158-166.

CASTRO-RODRIGUEZ, J. A., SAGLANI, S., RODRIGUEZ-MARTINEZ, C. E., OYARZUN, M. A., FLEMING, L. & BUSH, A. 2018. The relationship between inflammation and remodeling in childhood asthma: A systematic review. *Pediatr Pulmonol,* 53**,** 824-835.

CASTRO, M., ZANGRILLI, J., WECHSLER, M. E., BATEMAN, E. D., BRUSSELLE, G. G., BARDIN, P., MURPHY, K., MASPERO, J. F., O'BRIEN, C. & KORN, S. 2015. Reslizumab for inadequately controlled asthma with elevated blood eosinophil counts: results from two multicentre, parallel, double-blind, randomised, placebo-controlled, phase 3 trials. *Lancet Respir Med,* 3**,** 355-66.

CHAPMAN, D. G., BEREND, N., KING, G. G. & SALOME, C. M. 2011. Effect of deep inspiration avoidance on ventilation heterogeneity and airway responsiveness in healthy adults. *Journal of Applied Physiology,* 110**,** 1400-1405.

CHUNG, K. F., WENZEL, S. E., BROZEK, J. L., BUSH, A., CASTRO, M., STERK, P. J., ADCOCK, I. M., BATEMAN, E. D., BEL, E. H., BLEECKER, E. R., BOULET, L.-P., BRIGHTLING, C., CHANEZ, P., DAHLEN, S.-E., DJUKANOVIC, R., FREY, U., GAGA, M., GIBSON, P., HAMID, Q., JAJOUR, N. N., MAUAD, T., SORKNESS, R. L. & TEAGUE, W. G. 2014. International ERS/ATS guidelines on definition, evaluation and treatment of severe asthma. *European Respiratory Journal,* 43**,** 343.

CLAY, M. M., PAVIA, D. & CLARKE, S. W. 1986. Effect of aerosol particle size on bronchodilatation with nebulised terbutaline in asthmatic subjects. *Thorax,* 41**,** 364-8.

COOK, F. R., GEIER, E. T., ASADI, A. K., SÁ, R. C. & PRISK, G. K. 2015. Rapid Prototyping of Inspired Gas Delivery System for Pulmonary MRI Research. *3D Print Addit Manuf,* 2**,** 196-203.

CUSTOVIC, A., AINSWORTH, J., ARSHAD, H., BISHOP, C., BUCHAN, I., CULLINAN, P., DEVEREUX, G., HENDERSON, J., HOLLOWAY, J., ROBERTS, G., TURNER, S., WOODCOCK, A. & SIMPSON, A. 2015. The Study Team for Early Life Asthma Research (STELAR) consortium 'Asthma e-lab': team science bringing data, methods and investigators together. *Thorax,* 70**,** 799.

DARQUENNE, C. 2012. Aerosol deposition in health and disease. *Journal of aerosol medicine and pulmonary drug delivery,* 25**,** 140-147.

DARQUENNE, C., PAIVA, M. & PRISK, G. K. 2000. Effect of gravity on aerosol dispersion and deposition in the human lung after periods of breath holding. *J Appl Physiol (1985),* 89**,** 1787-92.

DELLACA, R. L., ANDERSSON OLERUD, M., ZANNIN, E., KOSTIC, P., POMPILIO, P. P., HEDENSTIERNA, G., PEDOTTI, A. & FRYKHOLM, P. 2009. Lung recruitment assessed by total respiratory system input reactance. *Intensive Care Med,* 35**,** 2164-72.

DELLACÀ, R. L., DUFFY, N., POMPILIO, P. P., ALIVERTI, A., KOULOURIS, N. G., PEDOTTI, A. & CALVERLEY, P. M. 2007. Expiratory flow limitation detected by forced oscillation and negative expiratory pressure. *Eur Respir J,* 29**,** 363-74.

DELLACÀ, R. L., SANTUS, P., ALIVERTI, A., STEVENSON, N., CENTANNI, S., MACKLEM, P. T., PEDOTTI, A. & CALVERLEY, P. M. 2004. Detection of expiratory flow limitation in COPD using the forced oscillation technique. *Eur Respir J,* 23**,** 232-40.

DENLINGER, L. C., PHILLIPS, B. R., RAMRATNAM, S., ROSS, K., BHAKTA, N. R., CARDET, J. C., CASTRO, M., PETERS, S. P., PHIPATANAKUL, W., AUJLA, S., BACHARIER, L. B., BLEECKER, E. R., COMHAIR, S. A., COVERSTONE, A., DEBOER, M., ERZURUM, S. C., FAIN, S. B., FAJT, M., FITZPATRICK, A. M., GAFFIN, J., GASTON, B., HASTIE, A. T., HAWKINS, G. A., HOLGUIN, F., IRANI, A. M., ISRAEL, E., LEVY, B. D., LY, N., MEYERS, D. A., MOORE, W. C., MYERS, R., OPINA, M. T., PETERS, M. C., SCHIEBLER, M. L., SORKNESS, R. L., TEAGUE, W. G., WENZEL, S. E., WOODRUFF, P. G., MAUGER, D. T., FAHY, J. V. & JARJOUR, N. N. 2017. Inflammatory and Comorbid Features of Patients with Severe Asthma and Frequent Exacerbations. *Am J Respir Crit Care Med,* 195**,** 302-313.

DENNIS, T., VANESSA, M. M., IAN, D. P. & PETER, G. G. 2022. Asthma remission- what is it and how can it be achieved? *European Respiratory Journal***,** 2102583.

DIBLASI, R. M., KAJIMOTO, M., POLI, J. A., DEUTSCH, G., PFEIFFER, J., ZIMMERMAN, J., CROTWELL, D. N., MALONE, P., FINK, J. B., RINGER, C., UTHAMANTHIL, R., LEDEE, D. & PORTMAN, M. A. 2021a. Breath-Synchronized Nebulized Surfactant in a Porcine Model of Acute Respiratory Distress Syndrome. *Crit Care Explor,* 3**,** e0338.

DIBLASI, R. M., MICHELETTI, K. J., ZIMMERMAN, J. D., POLI, J. A., FINK, J. B. & KAJIMOTO, M. 2021b. Physiologic Effects of Instilled and Aerosolized Surfactant Using a Breath-Synchronized Nebulizer on Surfactant-Deficient Rabbits. *Pharmaceutics,* 13.

DIETRICH, O., REISER, M. F. & SCHOENBERG, S. O. 2008. Artifacts in 3-T MRI: physical background and reduction strategies. *Eur J Radiol,* 65**,** 29-35.

DOLOVICH, M. A. 2000. Influence of inspiratory flow rate, particle size, and airway caliber on aerosolized drug delivery to the lung. *Respir Care,* 45**,** 597-608.

DONOVAN, G. M. & NOBLE, P. B. 2021a. Small airways vs large airways in asthma: time for a new perspective. *J Appl Physiol (1985),* 131**,** 1839-1841.

DONOVAN, G. M. & NOBLE, P. B. 2021b. Small airways vs large airways in asthma: time for a new perspective. *Journal of Applied Physiology,* 131**,** 1839-1841.

DOUGLAS, J. G., LESLIE, M. J., CROMPTON, G. K. & GRANT, I. W. 1986. A comparative study of two doses of salbutamol nebulized at 4 and 8 litres per minute in patients with chronic asthma. *Br J Dis Chest,* 80**,** 55-8.

DOWNIE, S. R., SALOME, C. M., VERBANCK, S., THOMPSON, B., BEREND, N. & KING, G. G. 2007. Ventilation heterogeneity is a major determinant of airway hyperresponsiveness in asthma, independent of airway inflammation. *Thorax,* 62**,** 684-9.

DOWNIE, S. R., SALOME, C. M., VERBANCK, S., THOMPSON, B. R., BEREND, N. & KING, G. G. 2013. Effect of methacholine on peripheral lung mechanics and ventilation heterogeneity in asthma. *J Appl Physiol (1985),* 114**,** 770-7.

EDELMAN, R. R., HATABU, H., TADAMURA, E., LI, W. & PRASAD, P. V. 1996. Noninvasive assessment of regional ventilation in the human lung using oxygen-enhanced magnetic resonance imaging. *Nat Med,* 2**,** 1236-9.

EL BAOU, C., DI SANTOSTEFANO, R. L., ALFONSO-CRISTANCHO, R., SUAREZ, E. A., STEMPEL, D., EVERARD, M. L. & BARNES, N. 2017. Effect of inhaled corticosteroid particle size on asthma efficacy and safety outcomes: a systematic literature review and meta-analysis. *BMC Pulmonary Medicine,* 17**,** 31.

ERZURUM, S. C. & GASTON, B. M. 2012. Biomarkers in asthma: a real hope to better manage asthma. *Clin Chest Med,* 33**,** 459-71.

FAIN, S. B., GONZALEZ-FERNANDEZ, G., PETERSON, E. T., EVANS, M. D., SORKNESS, R. L., JARJOUR, N. N., BUSSE, W. W. & KUHLMAN, J. E. 2008. Evaluation of structure-function relationships in asthma using multidetector CT and hyperpolarized He-3 MRI. *Acad Radiol,* 15**,** 753-62.

FARAH, C. S., KING, G. G., BROWN, N. J., DOWNIE, S. R., KERMODE, J. A., HARDAKER, K. M., PETERS, M. J., BEREND, N. & SALOME, C. M. 2012a. The role of the small airways in the clinical expression of asthma in adults. *J Allergy Clin Immunol,* 129**,** 381-7, 387.e1.

FARAH, C. S., KING, G. G., BROWN, N. J., PETERS, M. J., BEREND, N. & SALOME, C. M. 2012b. Ventilation heterogeneity predicts asthma control in adults following inhaled corticosteroid dose titration. *J Allergy Clin Immunol,* 130**,** 61-8.

FARROW, C. E., SALOME, C. M., HARRIS, B. E., BAILEY, D. L., BAILEY, E., BEREND, N., YOUNG, I. H. & KING, G. G. 2012. Airway closure on imaging relates to airway hyperresponsiveness and peripheral airway disease in asthma. *J Appl Physiol (1985),* 113**,** 958-66.

FARROW, C. E., SALOME, C. M., HARRIS, B. E., BAILEY, D. L., BEREND, N. & KING, G. G. 2017. Peripheral ventilation heterogeneity determines the extent of bronchoconstriction in asthma. *J Appl Physiol (1985),* 123**,** 1188-1194.

FERRON, G. A., HORNIK, S., KREYLING, W. G. & HAIDER, B. 1985. Comparison of experimental and calculated data for the total and regional deposition in the human lung. *Journal of Aerosol Science,* 16**,** 133-143.

FISHWICK, D., BRADSHAW, L., MACDONALD, C., BEASLEY, R., GASH, D., BENGTSSON, T., BONDESSON, E. & BORGSTRÖM, L. 2001. Cumulative and single-dose design to assess the bronchodilator effects of beta2-agonists in individuals with asthma. *Am J Respir Crit Care Med,* 163**,** 474-7.

FITZPATRICK, A. M. & MOORE, W. C. 2017. Severe Asthma Phenotypes - How Should They Guide Evaluation and Treatment? *J Allergy Clin Immunol Pract,* 5**,** 901-908.

GARNER, O., RAMEY, J. S. & HANANIA, N. A. 2022. Management of Life-Threatening Asthma: Severe Asthma Series. *Chest*.

GEIER, E. T., KUBO, K., THEILMANN, R. J., PRISK, G. K. & SA, R. C. 2018. The spatial pattern of methacholine bronchoconstriction recurs when supine, independently of posture during provocation, but does not recur between postures. *J Appl Physiol (1985)*.

GEIER, E. T., THEILMANN, R. J., DARQUENNE, C., PRISK, G. K. & SA, R. C. 2019. Quantitative Mapping of Specific Ventilation in the Human Lung using Proton Magnetic Resonance Imaging and Oxygen as a Contrast Agent. *J Vis Exp*.

GELB, A. F., YAMAMOTO, A., VERBEKEN, E. K. & NADEL, J. A. 2015. Unraveling the Pathophysiology of the Asthma-COPD Overlap Syndrome: Unsuspected Mild Centrilobular Emphysema Is Responsible for Loss of Lung Elastic Recoil in Never

Smokers With Asthma With Persistent Expiratory Airflow Limitation. *Chest,* 148**,** 313-320.

GILLIS, H. L. & LUTCHEN, K. R. 1999. Airway remodeling in asthma amplifies heterogeneities in smooth muscle shortening causing hyperresponsiveness. *J Appl Physiol (1985),* 86**,** 2001-12.

GLANDORF, J., KLIMEŠ, F., VOSKREBENZEV, A., GUTBERLET, M., BEHRENDT, L., CRISOSTO, C., WACKER, F., CIET, P., WILD, J. M. & VOGEL-CLAUSSEN, J. 2020. Comparison of phase-resolved functional lung (PREFUL) MRI derived perfusion and ventilation parameters at 1.5T and 3T in healthy volunteers. *PLoS One,* 15**,** e0244638.

GOLDIN, J. G., TASHKIN, D. P., KLEERUP, E. C., GREASER, L. E., HAYWOOD, U. M., SAYRE, J. W., SIMMONS, M. D., SUTTORP, M., COLICE, G. L., VANDEN BURGT, J. A. & ABERLE, D. R. 1999. Comparative effects of hydrofluoroalkane and chlorofluorocarbon beclomethasone dipropionate inhalation on small airways: assessment with functional helical thin-section computed tomography. *J Allergy Clin Immunol,* 104**,** S258-67.

GOLDMAN, H. I. & BECKLAKE, M. R. 1959. Respiratory function tests; normal values at median altitudes and the prediction of normal results. *Am Rev Tuberc,* 79**,** 457-67.

GRAHAM, B. L., STEENBRUGGEN, I., MILLER, M. R., BARJAKTAREVIC, I. Z., COOPER, B. G., HALL, G. L., HALLSTRAND, T. S., KAMINSKY, D. A., MCCARTHY, K., MCCORMACK, M. C., OROPEZ, C. E., ROSENFELD, M., STANOJEVIC, S., SWANNEY, M. P. & THOMPSON, B. R. 2019. Standardization of Spirometry 2019 Update. An Official American Thoracic Society and European Respiratory Society Technical Statement. *American Journal of Respiratory and Critical Care Medicine,* 200**,** e70-e88.

GULOTTA, C., SUKI, B., BRUSASCO, V., PELLEGRINO, R., GOBBI, A., PEDOTTI, A. & DELLACÀ, R. L. 2012. Monitoring the Temporal Changes of Respiratory Resistance: A Novel Test for the Management of Asthma. *American Journal of Respiratory and Critical Care Medicine,* 185**,** 1330-1331.

HAUBER, H. P., GOTFRIED, M., NEWMAN, K., DANDA, R., SERVI, R. J., CHRISTODOULOPOULOS, P. & HAMID, Q. 2003. Effect of HFA-flunisolide on peripheral lung inflammation in asthma. *J Allergy Clin Immunol,* 112**,** 58-63.

HEYDER, J., GEBHART, J., RUDOLF, G., SCHILLER, C. F. & STAHLHOFEN, W. 1986. Deposition of particles in the human respiratory tract in the size range 0.005–15 µm. *Journal of Aerosol Science,* 17**,** 811-825.

HODGSON, D., ANDERSON, J., REYNOLDS, C., MEAKIN, G., BAILEY, H., PAVORD, I., SHAW, D. & HARRISON, T. 2015. A randomised controlled trial of small particle inhaled steroids in refractory eosinophilic asthma (SPIRA). *Thorax,* 70**,** 559.

HOLGATE, S. T. 1998. The inflammation-repair cycle in asthma: the pivotal role of the airway epithelium. *Clin Exp Allergy,* 28 Suppl 5**,** 97-103.

HOPKINS, S. R., HENDERSON, A. C., LEVIN, D. L., YAMADA, K., ARAI, T., BUXTON, R. B. & PRISK, G. K. 2007. Vertical gradients in regional lung density and perfusion in the supine human lung: the Slinky effect. *Journal of Applied Physiology,* 103**,** 240-248.

HOSHINO, M. 2010. Comparison of effectiveness in ciclesonide and fluticasone propionate on small airway function in mild asthma. *Allergol Int,* 59**,** 59-66.

HULTQUIST, C., WOLLMER, P., EKLUNDH, G. & JONSON, B. 1992. Effect of inhaled terbutaline sulphate in relation to its deposition in the lungs. *Pulm Pharmacol,* 5**,** 127-32.

IKIN, J., CARROLL, M. T. C., WALKER, J., BORG, B., BROWN, D., COPE, M., DEL MONACO, A., DENNEKAMP, M., DIMITRIADIS, C., GAO, C. X., GUO, Y., JOHNSTON, F., LIEW, D., MAYBERY, D., THOMPSON, B., SIM, M. & ABRAMSON, M. J. 2021. Cohort Profile: The Hazelwood Health Study Adult Cohort. *Int J Epidemiol,* 49**,** 1777-1778.

IVANCSÓ, I., BÖCSKEI, R., MÜLLER, V. & TAMÁSI, L. 2013. Extrafine inhaled corticosteroid therapy in the control of asthma. *J Asthma Allergy,* 6**,** 69-80.

JAMES, A. L., DONOVAN, G. M., GREEN, F. H. Y., MAUAD, T., ABRAMSON, M. J., CAIRNCROSS, A., NOBLE, P. B. & ELLIOT, J. G. 2023. Heterogeneity of Airway Smooth Muscle Remodeling in Asthma. *Am J Respir Crit Care Med,* 207**,** 452-460.

JAMES, A. L., PARÉ, P. D. & HOGG, J. C. 1989. The mechanics of airway narrowing in asthma. *Am Rev Respir Dis,* 139**,** 242-6.

JAMES, A. L. & WENZEL, S. 2007. Clinical relevance of airway remodelling in airway diseases. *European Respiratory Journal,* 30**,** 134.

JIA, C. E., ZHANG, H. P., LV, Y., LIANG, R., JIANG, Y. Q., POWELL, H., FU, J. J., WANG, L., GIBSON, P. G. & WANG, G. 2013. The Asthma Control Test and Asthma Control Questionnaire for assessing asthma control: Systematic review and meta-analysis. *J Allergy Clin Immunol,* 131**,** 695-703.

JOHNSON, M. A., NEWMAN, S. P., BLOOM, R., TALAEE, N. & CLARKE, S. W. 1989. Delivery of albuterol and ipratropium bromide from two nebulizer systems in chronic stable asthma. Efficacy and pulmonary deposition. *Chest,* 96**,** 6-10.

JUNIPER, E. F., BOUSQUET, J., ABETZ, L. & BATEMAN, E. D. 2006. Identifying 'well-controlled' and 'not well-controlled' asthma using the Asthma Control Questionnaire. *Respir Med,* 100**,** 616-21.

KELLY, V. J., BROWN, N. J., SANDS, S. A., BORG, B. M., KING, G. G. & THOMPSON, B. R. 2012. Effect of airway smooth muscle tone on airway distensibility measured by the forced oscillation technique in adults with asthma. *J Appl Physiol (1985),* 112**,** 1494-503.

KELLY, V. J., SANDS, S. A., HARRIS, R. S., VENEGAS, J. G., BROWN, N. J., STUART-ANDREWS, C. R., KING, G. G. & THOMPSON, B. R. 2013. Respiratory system reactance is an independent determinant of asthma control. *J Appl Physiol (1985),* 115**,** 1360-9.

KERR, P. J., BRENNAN, V., MAC HALE, E., DOYLE, F. & COSTELLO, R. W. 2022. Improving Medication Adherence in Asthma. *Semin Respir Crit Care Med,* 43**,** 675-683.

KHREIS, H., CIRACH, M., MUELLER, N., DE HOOGH, K., HOEK, G., NIEUWENHUIJSEN, M. J. & ROJAS-RUEDA, D. 2019. Outdoor air pollution and the burden of childhood asthma across Europe. *European Respiratory Journal,* 54**,** 1802194.

KING, G. G., BATES, J., BERGER, K. I., CALVERLEY, P., DE MELO, P. L., DELLACÀ, R. L., FARRÉ, R., HALL, G. L., IOAN, I., IRVIN, C. G., KACZKA, D. W., KAMINSKY, D. A., KUROSAWA, H., LOMBARDI, E., MAKSYM, G. N., MARCHAL, F., OPPENHEIMER, B. W., SIMPSON, S. J., THAMRIN, C., VAN DEN BERGE, M. & OOSTVEEN, E. 2020. Technical standards for respiratory oscillometry. *Eur Respir J,* 55.

KING, G. G., JAMES, A., HARKNESS, L. & WARK, P. A. B. 2018. Pathophysiology of severe asthma: We've only just started. *Respirology,* 23**,** 262-271.

KLIMEŠ, F., VOSKREBENZEV, A., GUTBERLET, M., KERN, A., BEHRENDT, L., KAIREIT, T. F., CZERNER, C., RENNE, J., WACKER, F. & VOGEL-CLAUSSEN, J. 2019. Free-breathing quantification of regional ventilation derived by phase-resolved functional lung (PREFUL) MRI. *NMR Biomed,* 32**,** e4088.

KRAFT, M., RICHARDSON, M., HALLMARK, B., BILLHEIMER, D., VAN DEN BERGE, M., FABBRI, L. M., VAN DER MOLEN, T., NICOLINI, G., PAPI, A., RABE, K. F., SINGH, D.,

BRIGHTLING, C. & SIDDIQUI, S. 2022. The role of small airway dysfunction in asthma control and exacerbations: a longitudinal, observational analysis using data from the ATLANTIS study. *Lancet Respir Med,* 10**,** 661-668.

KRAMER, S., ROTTIER, B. L., SCHOLTEN, R. J. & BOLUYT, N. 2013. Ciclesonide versus other inhaled corticosteroids for chronic asthma in children. *Cochrane Database Syst Rev***,** Cd010352.

KUETHE, D., CAPRIHAN, A., GACH, H., LOWE, I. & FUKUSHIMA, E. 2000. Imaging obstructed ventilation with NMR using inert fluorinated gases. *Journal of applied physiology (Bethesda, Md. : 1985),* 88**,** 2279-86.

KUMAR, V. H., CHRISTIAN, C. & KRESCH, M. J. 2000. Effects of salmeterol on secretion of phosphatidylcholine by alveolar type II cells. *Life Sci,* 66**,** 1639-46.

KUWANO, K., BOSKEN, C. H., PARE, P. D., BAI, T. R., WIGGS, B. R. & HOGG, J. C. 1993. Small airways dimensions in asthma and in chronic obstructive pulmonary disease. *Am Rev Respir Dis,* 148**,** 1220-5.

LAMBERT, R. K., WIGGS, B. R., KUWANO, K., HOGG, J. C. & PARÉ, P. D. 1993. Functional significance of increased airway smooth muscle in asthma and COPD. *J Appl Physiol (1985),* 74**,** 2771-81.

LAUBE, B. L., JANSSENS, H. M., DE JONGH, F. H., DEVADASON, S. G., DHAND, R., DIOT, P., EVERARD, M. L., HORVATH, I., NAVALESI, P., VOSHAAR, T. & CHRYSTYN, H. 2011. What the pulmonary specialist should know about the new inhalation therapies. *Eur Respir J,* 37**,** 1308-31.

LEVY, M. L. 2015. The national review of asthma deaths: what did we learn and what needs to change? *Breathe (Sheff),* 11**,** 14-24.

LEVY, M. L., ANDREWS, R., BUCKINGHAM, R., EVANS, H., FRANCIS, C., HOUSTON, R., LOWE, D., NASSER, S., PATON, J., PURI, N., STEWART, K. & THOMAS, M. 2014. Why asthma still kills. *The National review of asthma deaths.* Royal College of Physicians.

LEWIS, S. M., EVANS, J. W. & JALOWAYSKI, A. A. 1978. Continuous distributions of specific ventilation recovered from inert gas washout. *Journal of Applied Physiology,* 44**,** 416-423.

LIPPMANN, M., YEATES, D. B. & ALBERT, R. E. 1980. Deposition, retention, and clearance of inhaled particles. *Br J Ind Med,* 37**,** 337-62.

LIPWORTH, B. J., CLARK, R. A., DHILLON, D. P., BROWN, R. A. & MCDEVITT, D. G. 1988. Beta-adrenoceptor responses to high doses of inhaled salbutamol in patients with bronchial asthma. *Br J Clin Pharmacol,* 26**,** 527-33.

LOFTUS, P. A. & WISE, S. K. 2015. Epidemiology and economic burden of asthma. *Int Forum Allergy Rhinol,* 5 Suppl 1**,** S7-10.

LÖTVALL, J., AKDIS, C. A., BACHARIER, L. B., BJERMER, L., CASALE, T. B., CUSTOVIC, A., LEMANSKE, R. F., JR., WARDLAW, A. J., WENZEL, S. E. & GREENBERGER, P. A. 2011. Asthma endotypes: a new approach to classification of disease entities within the asthma syndrome. *J Allergy Clin Immunol,* 127**,** 355-60.

MACKLEM, P. T. & MEAD, J. 1967. Resistance of central and peripheral airways measured by a retrograde catheter. *J Appl Physiol,* 22**,** 395-401.

MAI, V. M., LIU, B., LI, W., POLZIN, J., KURUCAY, S., CHEN, Q. & EDELMAN, R. R. 2002. Influence of oxygen flow rate on signal and T1 changes in oxygen-enhanced ventilation imaging. *Journal of Magnetic Resonance Imaging,* 16**,** 37-41.

MARTIN, R. F. 2000. General Deming Regression for Estimating Systematic Bias and Its Confidence Interval in Method-Comparison Studies. *Clinical Chemistry,* 46**,** 100-104.

MAUAD, T., SILVA, L. F., SANTOS, M. A., GRINBERG, L., BERNARDI, F. D., MARTINS, M. A., SALDIVA, P. H. & DOLHNIKOFF, M. 2004. Abnormal alveolar attachments with decreased elastic fiber content in distal lung in fatal asthma. *Am J Respir Crit Care Med,* 170**,** 857-62.

MCDONALD, V. M., CLARK, V. L., CORDOVA-RIVERA, L., WARK, P. A. B., BAINES, K. J. & GIBSON, P. G. 2020. Targeting treatable traits in severe asthma: a randomised controlled trial. *European Respiratory Journal,* 55**,** 1901509.

MCDONALD, V. M., FINGLETON, J., AGUSTI, A., HILES, S. A., CLARK, V. L., HOLLAND, A. E., MARKS, G. B., BARDIN, P. P., BEASLEY, R., PAVORD, I. D., WARK, P. A. B. & GIBSON, P. G. 2019. Treatable traits: a new paradigm for 21st century management of chronic airway diseases: Treatable Traits Down Under International Workshop report. *European Respiratory Journal,* 53**,** 1802058.

MCGOWAN, A., LAVENEZIANA, P., BAYAT, S., BEYDON, N., BOROS, P. W., BURGOS, F., FLEŽAR, M., FRANCZUK, M., GALARZA, M. A., KENDRICK, A. H., LOMBARDI, E., MAKONGA-BRAAKSMA, J., MCCORMACK, M. C., PLANTIER, L., STANOJEVIC, S., STEENBRUGGEN, I., THOMPSON, B., COATES, A. L., WANGER, J., COCKCROFT, D. W., CULVER, B., SYLVESTER, K. & DE JONGH, F. 2022. International consensus on lung function testing during the COVID-19 pandemic and beyond. *ERJ Open Res,* 8.

MCNULTY, W. & USMANI, O. S. 2014. Techniques of assessing small airways dysfunction. *Eur Clin Respir J,* 1.

MILANESE, M., CRIMI, E., SCORDAMAGLIA, A., RICCIO, A., PELLEGRINO, R., CANONICA, G. W. & BRUSASCO, V. 2001. On the functional consequences of bronchial basement membrane thickening. *J Appl Physiol (1985),* 91**,** 1035-40.

MILLER, M. K., LEE, J. H., MILLER, D. P. & WENZEL, S. E. 2007. Recent asthma exacerbations: A key predictor of future exacerbations. *Respiratory Medicine,* 101**,** 481-489.

MILLER, M. R., HANKINSON, J., BRUSASCO, V., BURGOS, F., CASABURI, R., COATES, A., CRAPO, R., ENRIGHT, P., VAN DER GRINTEN, C. P., GUSTAFSSON, P., JENSEN, R., JOHNSON, D. C., MACINTYRE, N., MCKAY, R., NAVAJAS, D., PEDERSEN, O. F., PELLEGRINO, R., VIEGI, G. & WANGER, J. 2005. Standardisation of spirometry. *Eur Respir J,* 26**,** 319-38.

MINSHALL, E. M., HOGG, J. C. & HAMID, Q. A. 1998. Cytokine mRNA expression in asthma is not restricted to the large airways. *J Allergy Clin Immunol,* 101**,** 386-90.

MITCHELL, D. M., SOLOMON, M. A., TOLFREE, S. E., SHORT, M. & SPIRO, S. G. 1987. Effect of particle size of bronchodilator aerosols on lung distribution and pulmonary function in patients with chronic asthma. *Thorax,* 42**,** 457-61.

MOHER ALSADY, T., VOSKREBENZEV, A., GREER, M., BECKER, L., KAIREIT, T. F., WELTE, T., WACKER, F., GOTTLIEB, J. & VOGEL-CLAUSSEN, J. 2019. MRI-derived regional flow-volume loop parameters detect early-stage chronic lung allograft dysfunction. *J Magn Reson Imaging,* 50**,** 1873-1882.

MOLIMARD, M., MARTINAT, Y., ROGEAUX, Y., MOYSE, D., PELLO, J. Y. & GIRAUD, V. 2005. Improvement of asthma control with beclomethasone extrafine aerosol compared to fluticasone and budesonide. *Respir Med,* 99**,** 770-8.

MOORE, W. C., MEYERS, D. A., WENZEL, S. E., TEAGUE, W. G., LI, H., LI, X., D'AGOSTINO, R., JR., CASTRO, M., CURRAN-EVERETT, D., FITZPATRICK, A. M., GASTON, B., JARJOUR, N. N., SORKNESS, R., CALHOUN, W. J., CHUNG, K. F., COMHAIR, S. A., DWEIK, R. A., ISRAEL, E., PETERS, S. P., BUSSE, W. W., ERZURUM, S. C. & BLEECKER, E. R. 2010.

Identification of asthma phenotypes using cluster analysis in the Severe Asthma Research Program. *Am J Respir Crit Care Med,* 181**,** 315-23.
NEWMAN, S. P. 2000. Can lung deposition data act as a surrogate for the clinical response to inhaled asthma drugs? *Br J Clin Pharmacol,* 49**,** 529-37.
NIHLBERG, K., ANDERSSON-SJÖLAND, A., TUFVESSON, E., ERJEFÄLT, J. S., BJERMER, L. & WESTERGREN-THORSSON, G. 2010. Altered matrix production in the distal airways of individuals with asthma. *Thorax,* 65**,** 670.
NILSEN, K., THIEN, F., THAMRIN, C., ELLIS, M. J., PRISK, G. K., KING, G. G. & THOMPSON, B. R. 2019. Early onset of airway derecruitment assessed using the forced oscillation technique in subjects with asthma. *Journal of Applied Physiology,* 126**,** 1399-1408.
NILSEN, K., THOMPSON, B. R., ZAJAKOVSKI, N., KEAN, M., HARRIS, B., COWIN, G., ROBINSON, P., PRISK, G. K. & THIEN, F. 2021. Airway closure is the predominant physiological mechanism of low ventilation seen on hyperpolarized helium-3 MRI lung scans. *J Appl Physiol (1985),* 130**,** 781-791.
NWARU, B. I., EKSTROM, M., HASVOLD, P., WIKLUND, F., TELG, G. & JANSON, C. 2020. Overuse of short-acting beta2-agonists in asthma is associated with increased risk of exacerbation and mortality: a nationwide cohort study of the global SABINA programme. *Eur Respir J,* 55.
O'SULLIVAN, C. F., NILSEN, K., BORG, B., ELLIS, M., MATSAS, P., THIEN, F., DOUGLASS, J. A., STUART-ANDREWS, C., KING, G. G., PRISK, G. K. & THOMPSON, B. R. 2022. Small airways dysfunction is associated with increased exacerbations in patients with asthma. *J Appl Physiol (1985),* 133**,** 629-636.
O'SULLIVAN, C. F., NILSEN, K., BORG, B., ELLIS, M., MATSAS, P., THIEN, F., DOUGLASS, J. A., STUART-ANDREWS, C., KING, G. G., PRISK, G. K. & THOMPSON, B. R. 2022. Small airways dysfunction is associated with increased exacerbations in patients with asthma. *Journal of Applied Physiology,* 133**,** 629-636.
OHBAYASHI, H. 2007. One-year evaluation of the preventative effect of hydrofluoroalkane-beclomethasone dipropionate on eosinophilic inflammation of asthmatic peripheral airways. *Respiration,* 74**,** 146-53.
OHNO, Y. & HATABU, H. 2007. Basics concepts and clinical applications of oxygen-enhanced MR imaging. *Eur J Radiol,* 64**,** 320-8.
OOSTVEEN, E., BODA, K., VAN DER GRINTEN, C. P., JAMES, A. L., YOUNG, S., NIELAND, H. & HANTOS, Z. 2013. Respiratory impedance in healthy subjects: baseline values and bronchodilator response. *Eur Respir J,* 42**,** 1513-23.
OOSTVEEN, E., MACLEOD, D., LORINO, H., FARRE, R., HANTOS, Z., DESAGER, K. & MARCHAL, F. 2003. The forced oscillation technique in clinical practice: methodology, recommendations and future developments. *Eur Respir J,* 22**,** 1026-41.
PATEL, P., MUKAI, D. & WILSON, A. F. 1990. Dose-response effects of two sizes of monodisperse isoproterenol in mild asthma. *Am Rev Respir Dis,* 141**,** 357-60.
PAVORD, I. D., KORN, S., HOWARTH, P., BLEECKER, E. R., BUHL, R., KEENE, O. N., ORTEGA, H. & CHANEZ, P. 2012. Mepolizumab for severe eosinophilic asthma (DREAM): a multicentre, double-blind, placebo-controlled trial. *Lancet,* 380**,** 651-9.
PELLEGRINO, R., VIEGI, G., BRUSASCO, V., CRAPO, R. O., BURGOS, F., CASABURI, R., COATES, A., VAN DER GRINTEN, C. P., GUSTAFSSON, P., HANKINSON, J., JENSEN, R., JOHNSON, D. C., MACINTYRE, N., MCKAY, R., MILLER, M. R., NAVAJAS, D., PEDERSEN, O. F. & WANGER, J. 2005. Interpretative strategies for lung function tests. *Eur Respir J,* 26**,** 948-68.

PHIPPS, P. R., GONDA, I., BAILEY, D. L., BORHAM, P., BAUTOVICH, G. & ANDERSON, S. D. 1989. Comparisons of planar and tomographic gamma scintigraphy to measure the penetration index of inhaled aerosols. *Am Rev Respir Dis,* 139**,** 1516-23.

POPOV, T. A., PETROVA, D., KRALIMARKOVA, T. Z., IVANOV, Y., POPOVA, T., PENEVA, M., ODZHAKOVA, T., ILIEVA, Y., YAKOVLIEV, P., LAZAROVA, T., GEORGIEV, O., HODZHEV, V., HODZHEVA, E., STAEVSKA, M. T. & DIMITROV, V. D. 2013. Real life clinical study design supporting the effectiveness of extra-fine inhaled beclomethasone/formoterol at the level of small airways of asthmatics. *Pulmonary Pharmacology & Therapeutics,* 26**,** 624-629.

POSTMA, D. S., BRIGHTLING, C., BALDI, S., VAN DEN BERGE, M., FABBRI, L. M., GAGNATELLI, A., PAPI, A., VAN DER MOLEN, T., RABE, K. F., SIDDIQUI, S., SINGH, D., NICOLINI, G. & KRAFT, M. 2019. Exploring the relevance and extent of small airways dysfunction in asthma (ATLANTIS): baseline data from a prospective cohort study. *Lancet Respir Med,* 7**,** 402-416.

PRATT, W. K. 2007. *Digital Image Processing*, John Wiley & Sons, Inc., Hoboken, New Jersey.

PRISK, G. K. & SÁ, R. C. 2014. It's about numbers, not pictures. *J Appl Physiol (1985),* 116**,** 127-8.

QUANJER, P. H., STANOJEVIC, S., COLE, T. J., BAUR, X., HALL, G. L., CULVER, B. H., ENRIGHT, P. L., HANKINSON, J. L., IP, M. S. M., ZHENG, J. & STOCKS, J. 2012. Multi-ethnic reference values for spirometry for the 3–95-yr age range: the global lung function 2012 equations. *European Respiratory Journal,* 40**,** 1324.

RABE, K. F., NAIR, P., BRUSSELLE, G., MASPERO, J. F., CASTRO, M., SHER, L., ZHU, H., HAMILTON, J. D., SWANSON, B. N., KHAN, A., CHAO, J., STAUDINGER, H., PIROZZI, G., ANTONI, C., AMIN, N., RUDDY, M., AKINLADE, B., GRAHAM, N. M. H., STAHL, N., YANCOPOULOS, G. D. & TEPER, A. 2018. Efficacy and Safety of Dupilumab in Glucocorticoid-Dependent Severe Asthma. *N Engl J Med,* 378**,** 2475-2485.

REDDEL, H. K., FITZGERALD, J. M., BATEMAN, E. D., BACHARIER, L. B., BECKER, A., BRUSSELLE, G., BUHL, R., CRUZ, A. A., FLEMING, L., INOUE, H., KO, F. W.-S., KRISHNAN, J. A., LEVY, M. L., LIN, J., PEDERSEN, S. E., SHEIKH, A., YORGANCIOGLU, A. & BOULET, L.-P. 2019. GINA 2019: a fundamental change in asthma management. *European Respiratory Journal,* 53**,** 1901046.

REDDEL, H. K., TAYLOR, D. R., BATEMAN, E. D., BOULET, L. P., BOUSHEY, H. A., BUSSE, W. W., CASALE, T. B., CHANEZ, P., ENRIGHT, P. L., GIBSON, P. G., DE JONGSTE, J. C., KERSTJENS, H. A., LAZARUS, S. C., LEVY, M. L., O'BYRNE, P. M., PARTRIDGE, M. R., PAVORD, I. D., SEARS, M. R., STERK, P. J., STOLOFF, S. W., SULLIVAN, S. D., SZEFLER, S. J., THOMAS, M. D. & WENZEL, S. E. 2009. An official American Thoracic Society/European Respiratory Society statement: asthma control and exacerbations: standardizing endpoints for clinical asthma trials and clinical practice. *Am J Respir Crit Care Med,* 180**,** 59-99.

ROBINSON, P. D., GOLDMAN, M. D. & GUSTAFSSON, P. M. 2009. Inert Gas Washout: Theoretical Background and Clinical Utility in Respiratory Disease. *Respiration,* 78**,** 339-355.

ROBINSON, P. D., LATZIN, P., VERBANCK, S., HALL, G. L., HORSLEY, A., GAPPA, M., THAMRIN, C., ARETS, H. G., AURORA, P., FUCHS, S. I., KING, G. G., LUM, S., MACLEOD, K., PAIVA, M., PILLOW, J. J., RANGANATHAN, S., RATJEN, F., SINGER, F., SONNAPPA, S., STOCKS, J., SUBBARAO, P., THOMPSON, B. R. & GUSTAFSSON, P. M. 2013. Consensus

statement for inert gas washout measurement using multiple- and single- breath tests. *Eur Respir J,* 41**,** 507-22.
RUFFIN, R. E., DOLOVICH, M. B., OLDENBURG, F. A., JR. & NEWHOUSE, M. T. 1981. The preferential deposition of inhaled isoproterenol and propranolol in asthmatic patients. *Chest,* 80**,** 904-7.
SA, R. C., ASADI, A. K., THEILMANN, R. J., HOPKINS, S. R., PRISK, G. K. & DARQUENNE, C. 2014. Validating the distribution of specific ventilation in healthy humans measured using proton MR imaging. *J Appl Physiol (1985),* 116**,** 1048-56.
SA, R. C., CRONIN, M. V., HENDERSON, A. C., HOLVERDA, S., THEILMANN, R. J., ARAI, T. J., DUBOWITZ, D. J., HOPKINS, S. R., BUXTON, R. B. & PRISK, G. K. 2010. Vertical distribution of specific ventilation in normal supine humans measured by oxygen-enhanced proton MRI. *J Appl Physiol (1985),* 109**,** 1950-9.
SA, R. C., ZEMAN, K. L., BENNETT, W. D., PRISK, G. K. & DARQUENNE, C. 2015. Effect of Posture on Regional Deposition of Coarse Particles in the Healthy Human Lung. *J Aerosol Med Pulm Drug Deliv,* 28**,** 423-31.
SALOME, C. M., THORPE, C. W., DIBA, C., BROWN, N. J., BEREND, N. & KING, G. G. 2003. Airway re-narrowing following deep inspiration in asthmatic and nonasthmatic subjects. *Eur Respir J,* 22**,** 62-8.
SAMEE, S., ALTES, T., POWERS, P., DE LANGE, E. E., KNIGHT-SCOTT, J., RAKES, G., MUGLER, J. P., 3RD, CIAMBOTTI, J. M., ALFORD, B. A., BROOKEMAN, J. R. & PLATTS-MILLS, T. A. 2003. Imaging the lungs in asthmatic patients by using hyperpolarized helium-3 magnetic resonance: assessment of response to methacholine and exercise challenge. *J Allergy Clin Immunol,* 111**,** 1205-11.
SCICHILONE, N., BATTAGLIA, S., SORINO, C., PAGLINO, G., MARTINO, L., PATERNO, A., SANTAGATA, R., SPATAFORA, M., NICOLINI, G. & BELLIA, V. 2010. Effects of extra-fine inhaled beclomethasone/formoterol on both large and small airways in asthma. *Allergy,* 65**,** 897-902.
STANISZ, G. J., ODROBINA, E. E., PUN, J., ESCARAVAGE, M., GRAHAM, S. J., BRONSKILL, M. J. & HENKELMAN, R. M. 2005. T1, T2 relaxation and magnetization transfer in tissue at 3T. *Magn Reson Med,* 54**,** 507-12.
STANOJEVIC, S., KAMINSKY, D. A., MILLER, M., THOMPSON, B., ALIVERTI, A., BARJAKTAREVIC, I., COOPER, B. G., CULVER, B., DEROM, E., HALL, G. L., HALLSTRAND, T. S., LEUPPI, J. D., MACINTYRE, N., MCCORMACK, M., ROSENFELD, M. & SWENSON, E. R. 2021. ERS/ATS technical standard on interpretive strategies for routine lung function tests. *European Respiratory Journal***,** 2101499.
STUART-ANDREWS, C. R., KELLY, V. J., SANDS, S. A., LEWIS, A. J., ELLIS, M. J. & THOMPSON, B. R. 2012. Automated detection of the phase III slope during inert gas washout testing. *J Appl Physiol (1985),* 112**,** 1073-81.
SULAIMAN, I. & COSTELLO, R. W. 2021. Adherence to Asthma Treatments: An Audit of a Warehouse of Data. *Chest,* 159**,** 891-892.
SVENNINGSEN, S., KIRBY, M., STARR, D., LEARY, D., WHEATLEY, A., MAKSYM, G. N., MCCORMACK, D. G. & PARRAGA, G. 2013. Hyperpolarized (3) He and (129) Xe MRI: differences in asthma before bronchodilation. *J Magn Reson Imaging,* 38**,** 1521-30.
TANG, F. S. M., RUTTING, S., FARROW, C. E., TONGA, K. O., WATTS, J., DAME-CARROL, J. R., BERTOLIN, A., KING, G. G., THAMRIN, C. & CHAPMAN, D. G. 2020. Ventilation heterogeneity and oscillometry predict asthma control improvement following step-up inhaled therapy in uncontrolled asthma. *Respirology,* 25**,** 827-835.

THIEME, S. F., DIETRICH, O., MAXIEN, D., NIKOLAOU, K., SCHOENBERG, S. O., REISER, M. & FINK, C. 2011. Oxygen-enhanced MRI of the lungs: intraindividual comparison between 1.5 and 3 tesla. *Rofo,* 183**,** 358-64.

THIEN, F. & THOMPSON, B. R. 2018. Precision Medicine in Asthma: Integrating Imaging and Inflammatory Biomarkers. *Am J Respir Crit Care Med,* 197**,** 845-846.

THOMPSON, B. R., DOUGLASS, J. A., ELLIS, M. J., KELLY, V. J., O'HEHIR, R. E., KING, G. G. & VERBANCK, S. 2013. Peripheral lung function in patients with stable and unstable asthma. *Journal of Allergy and Clinical Immunology,* 131**,** 1322-1328.

USMANI, O. S. 2012. Treating the small airways. *Respiration,* 84**,** 441-53.

USMANI, O. S., BIDDISCOMBE, M. F. & BARNES, P. J. 2005. Regional lung deposition and bronchodilator response as a function of beta2-agonist particle size. *Am J Respir Crit Care Med,* 172**,** 1497-504.

USMANI, O. S., BIDDISCOMBE, M. F., NIGHTINGALE, J. A., UNDERWOOD, S. R. & BARNES, P. J. 2003. Effects of bronchodilator particle size in asthmatic patients using monodisperse aerosols. *J Appl Physiol (1985),* 95**,** 2106-12.

VENEGAS, J. G., WINKLER, T., MUSCH, G., VIDAL MELO, M. F., LAYFIELD, D., TGAVALEKOS, N., FISCHMAN, A. J., CALLAHAN, R. J., BELLANI, G. & SCOTT HARRIS, R. 2005. Self-organized patchiness in asthma as a prelude to catastrophic shifts. *Nature,* 434**,** 777-782.

VERBANCK, S. & PAIVA, M. 2011. Gas mixing in the airways and airspaces. *Compr Physiol,* 1**,** 809-34.

VERBANCK, S., SCHUERMANS, D., PAIVA, M. & VINCKEN, W. 2006. The functional benefit of anti-inflammatory aerosols in the lung periphery. *J Allergy Clin Immunol,* 118**,** 340-6.

VERBANCK, S., SCHUERMANS, D., VAN MUYLEM, A., PAIVA, M., NOPPEN, M. & VINCKEN, W. 1997. Ventilation distribution during histamine provocation. *J Appl Physiol (1985),* 83**,** 1907-16.

VERBANCK, S., THOMPSON, B. R., SCHUERMANS, D., KALSI, H., BIDDISCOMBE, M., STUART-ANDREWS, C., HANON, S., VAN MUYLEM, A., PAIVA, M., VINCKEN, W. & USMANI, O. 2012. Ventilation heterogeneity in the acinar and conductive zones of the normal ageing lung. *Thorax,* 67**,** 789-95.

VOSKREBENZEV, A., GUTBERLET, M., KLIMES, F., KAIREIT, T. F., SCHONFELD, C., ROTARMEL, A., WACKER, F. & VOGEL-CLAUSSEN, J. 2018. Feasibility of quantitative regional ventilation and perfusion mapping with phase-resolved functional lung (PREFUL) MRI in healthy volunteers and COPD, CTEPH, and CF patients. *Magn Reson Med,* 79**,** 2306-2314.

WAGNER, E. M., BLEECKER, E. R., PERMUTT, S. & LIU, M. C. 1998. Direct assessment of small airways reactivity in human subjects. *Am J Respir Crit Care Med,* 157**,** 447-52.

WANGER, J., CLAUSEN, J. L., COATES, A., PEDERSEN, O. F., BRUSASCO, V., BURGOS, F., CASABURI, R., CRAPO, R., ENRIGHT, P., VAN DER GRINTEN, C. P. M., GUSTAFSSON, P., HANKINSON, J., JENSEN, R., JOHNSON, D., MACINTYRE, N., MCKAY, R., MILLER, M. R., NAVAJAS, D., PELLEGRINO, R. & VIEGI, G. 2005. Standardisation of the measurement of lung volumes. *European Respiratory Journal,* 26**,** 511.

WARD, C., PAIS, M., BISH, R., REID, D., FELTIS, B., JOHNS, D. & WALTERS, E. H. 2002. Airway inflammation, basement membrane thickening and bronchial hyperresponsiveness in asthma. *Thorax,* 57**,** 309-16.

WEIBEL, E. R. 1963. Principles and methods for the morphometric study of the lung and other organs. *Lab Invest,* 12**,** 131-55.

WEIBEL, E. R. & GOMEZ, D. M. 1962. Architecture of the human lung. Use of quantitative methods establishes fundamental relations between size and number of lung structures. *Science,* 137**,** 577-85.

WESTBROOK, C. & TALBOT, J. 2018. *MRI in Practice,* Newark, UNITED KINGDOM, John Wiley & Sons, Incorporated.

WILLIAMSON, J. P., MCLAUGHLIN, R. A., NOFFSINGER, W. J., JAMES, A. L., BAKER, V. A., CURATOLO, A., ARMSTRONG, J. J., REGLI, A., SHEPHERD, K. L., MARKS, G. B., SAMPSON, D. D., HILLMAN, D. R. & EASTWOOD, P. R. 2011. Elastic Properties of the Central Airways in Obstructive Lung Diseases Measured Using Anatomical Optical Coherence Tomography. *American Journal of Respiratory and Critical Care Medicine,* 183**,** 612-619.

ZAINUDIN, B. M., BIDDISCOMBE, M., TOLFREE, S. E., SHORT, M. & SPIRO, S. G. 1990. Comparison of bronchodilator responses and deposition patterns of salbutamol inhaled from a pressurised metered dose inhaler, as a dry powder, and as a nebulised solution. *Thorax,* 45**,** 469-73.

ZANEN, P., GO, L. T. & LAMMERS, J.-W. J. 1994. The optimal particle size for β-adrenergic aerosols in mild asthmatics. *International Journal of Pharmaceutics,* 107**,** 211-217.

ZAPKE, M., TOPF, H. G., ZENKER, M., KUTH, R., DEIMLING, M., KREISLER, P., RAUH, M., CHEFD'HOTEL, C., GEIGER, B. & RUPPRECHT, T. 2006. Magnetic resonance lung function--a breakthrough for lung imaging and functional assessment? A phantom study and clinical trial. *Respir Res,* 7**,** 106.

ZEDAN, M. M., LAIMON, W. N., OSMAN, A. M. & ZEDAN, M. M. 2015. Clinical asthma phenotyping: A trial for bridging gaps in asthma management. *World J Clin Pediatr,* 4**,** 13-8.

ZIMMERMANN, S. C., HUVANANDANA, J., NGUYEN, C. D., BERTOLIN, A., WATTS, J. C., GOBBI, A., FARAH, C. S., PETERS, M. J., DELLACÀ, R. L., KING, G. G. & THAMRIN, C. 2020. Day-to-day variability of forced oscillatory mechanics for early detection of acute exacerbations in COPD. *European Respiratory Journal,* 56**,** 1901739.